การประยุกต์เพื่อการศึกษาเซลล์เดี่ยว: การปรับปรุงการรอดชีวิตของเซลล์ในชุดทดลองและการออกแบบอุปกรณ์ปล่อยเซลล์เดี่ยว

นายธรรมวิทย์ สุวรรณพันธุ์

วิทยานิพนธ์นี้เป็นส่วนหนึ่งของการศึกษาตามหลักสูตรปริญญาวิศวกรรมศาสตรมหาบัณฑิต
สาขาวิชาวิศวกรรมเครื่องกล ภาควิชาวิศวกรรมเครื่องกล
คณะวิศวกรรมศาสตร์ จุฬาลงกรณ์มหาวิทยาลัย
ปีการศึกษา 2558

Applications For A Single-Cell Study: Improving Cell Viability In Experimental Setups And Designing of A Single Cell Releasing Device

Mr. Thammawit Suwannaphan

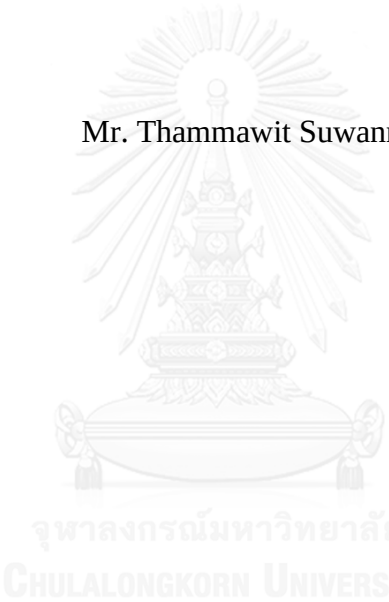

A Thesis Submitted in Partial Fulfillment of the Requirements
for the Degree of Master of Engineering Program in Mechanical Engineering
Department of Mechanical Engineering
Faculty of Engineering
Chulalongkorn University
Academic Year 2015

Thesis Title	Applications For A Single-Cell Study: Improving Cell Viability In Experimental Setups And Designing of A Single Cell Releasing Device
By	Mr. Thammawit Suwannaphan
Field of Study	Mechanical Engineering
Thesis Advisor	Assistant Professor Alongkorn Pimpin, Ph.D.
Thesis Co-Advisor	Prapruddee Piyaviriyakul, Ph.D.
	Wutthinan Jeamsaksiri, Ph.D.

Accepted by the Faculty of Engineering, Chulalongkorn University in Partial Fulfillment of the Requirements for the Master's Degree

.....Dean of the Faculty of Engineering
(Associate Professor Supot Teachavorasinskun, D.Eng.)

THESIS COMMITTEE

.....Chairman
(Assistant Professor Werayut Srituravanich, Ph.D.)

.....Thesis Advisor
(Assistant Professor Alongkorn Pimpin, Ph.D.)

.....Thesis Co-Advisor
(Prapruddee Piyaviriyakul, Ph.D.)

.....Thesis Co-Advisor
(Wutthinan Jeamsaksiri, Ph.D.)

.....Examiner
(Saran Salakij, Ph.D.)

.....External Examiner
(Mayuree Chanasakulniyom, Ph.D.)

ธรรมวิทย์ สุวรรณพันธุ์ : การประยุกต์เพื่อการศึกษาเซลล์เดี่ยว: การปรับปรุงการรอดชีวิตของเซลล์ในชุดทดลองและการออกแบบอุปกรณ์ปล่อยเซลล์เดี่ยว (Applications For A Single-Cell Study: Improving Cell Viability In Experimental Setups And Designing of A Single Cell Releasing Device) อ.ที่ปรึกษาวิทยานิพนธ์หลัก: ผศ. ดร. อลงกรณ์ พิมพ์พิณ, อ.ที่ปรึกษาวิทยานิพนธ์ร่วม: อ. น.สพ ดร. ประพฤติดี ปิยะวิริยะกุล, ดร. วุฒินันท์ เจียมศักดิ์ศิริ, 106 หน้า.

ในส่วนแรกเป็นการศึกษาเพื่อสังเกตการมีชีวิตอยู่ของเซลล์เม็ดเลือดขาวระหว่างกระบวนการแยกเซลล์ด้วยอุปกรณ์ท่อขดเกลียวด้วยการทดสอบสามเทคนิค ได้แก่ การย้อมสีทริพแพนบลู กล้องจุลทรรศน์อิเล็กตรอนแบบส่องกราดและการย้อมสีแบบไรท์ หลังจากนำเซลล์ไปฉีดผ่านชุดทดลอง พบว่าความเค้นเฉือนและความเค้นดึงภายในระบบฉีดซึ่งประกอบด้วย หลอดฉีดยาและเข็มฉีดยานั้น ไม่มีผลต่อการตายของเซลล์ แต่เซลล์กลับเกิดการเสียรูปร่างในกรณีการฉีดผ่านเข็มฉีดยาขนาด 5 มิลลิลิตร ที่ 8 มิลลิลิตรต่อนาที ซึ่งเป็นกรณีที่มีความเค้นสูงสุดในการทดลอง โดยการตรวจสอบด้วยกล้องจุลทรรศน์อิเล็กตรอนแบบส่องกราด แสดงให้เห็นว่าเซลล์รูปร่างปกติลดลงไปประมาณ 12% ส่วนเทคนิคของการย้อมสีแบบไรท์ แสดงให้เห็นว่าเซลล์ปกติลดลงไปประมาณ 16% สำหรับการทดสอบการมีชีวิตรอดของเซลล์หลังผ่านทั้งระบบอุปกรณ์ท่อขดเกลียวด้วยเทคนิคทริพแพนบลู แสดงให้เห็นว่าประมาณ 70% ของเซลล์ทั้งหมดมีชีวิตรอดหลังจากทดสอบด้วยหลอดฉีด 1 มิลลิลิตร ด้วยอัตราการไหล 1 มิลลิลิตรต่อนาที ผลการทดลองทั้งหมดบ่งชี้ว่าเซลล์ส่วนมากตายในอุปกรณ์คัดแยกไม่ใช่จากระบบฉีด งานที่สองเป็นการศึกษาอุปกรณ์ปล่อยเซลล์เดี่ยวซึ่งประกอบด้วยท่อหลักอยู่บนหลุมดักจับและท่อรองอยู่ใต้หลุมดักจับอนุภาค หลักการคือของไหลในท่อหลักจะถูกปล่อยด้วยอัตราการไหลที่ต่ำกว่าอัตราการไหลในท่อรองเพื่อตรึงเซลล์ให้ลอยอยู่กลางหลุม ในส่วนของการปล่อยเซลล์นั้น ของไหลในท่อหลักจะถูกปล่อยอย่างช้าๆ ในขณะที่อัตราการไหลในท่อรองจะเพิ่มมากขึ้นเพื่อผลักอนุภาคให้หลุดออกมา ผลจากแบบจำลองคณิตศาสตร์แสดงให้เห็นว่า เมื่อขนาดของเซลล์เพิ่มขึ้นอัตราการไหลของของไหลที่สามารถตรึงอนุภาคให้ลอยอยู่กลางหลุมก็เพิ่มขึ้นด้วย และอัตราการไหลจะเพิ่มขึ้นตามขนาดของอนุภาคจนถึงขนาด 14 ไมโครเมตร ซึ่งจะต้องใช้อัตราการไหลที่ 1.2 นาโนลิตรต่อชั่วโมง และถ้าขนาดของอนุภาคใหญ่กว่า 14 ไมโครเมตร อัตราการไหลของของไหลมีแนวโน้มลดลง

ภาควิชา วิศวกรรมเครื่องกล	ลายมือชื่อนิสิต .....
สาขาวิชา วิศวกรรมเครื่องกล	ลายมือชื่อ อ.ที่ปรึกษาหลัก .....
ปีการศึกษา 2558	ลายมือชื่อ อ.ที่ปรึกษาร่วม .....
	ลายมือชื่อ อ.ที่ปรึกษาร่วม .....

5770197521 : MAJOR MECHANICAL ENGINEERING
KEYWORDS: MICROFLUIDICS / SINGLE CELL / CANCER / SHEAR STRESS / EXTENSIONAL STRESS / CELL VIABILITY / CELL RELEASING

THAMMAWIT SUWANNAPHAN: Applications For A Single-Cell Study: Improving Cell Viability In Experimental Setups And Designing of A Single Cell Releasing Device. ADVISOR: ASST. PROF. ALONGKORN PIMPIN, Ph.D., CO-ADVISOR: PRAPRUDDEE PIYAVIRIYAKUL, Ph.D., WUTTHINAN JEAMSAKSIRI, Ph.D., 106 pp.

In the first phase, it was about an investigation of cell viability of white blood cells during the sorting process in a spiral microchannel with three methods including Trypan Blue staining, Scanning Electron Microscopy (SEM) and Wright's staining. After the white blood cells were injected through the setup, the outcome showed that in a feeding system, between a syringe and needle, despite of high shear and extensional stresses induced in fluid stream, no effects of these stresses on cell viability was found. Despite of that, cells were more likely to be deformed in the case with maximum stresses, in which flow passing through 5 ml syringe at 8 ml/min. Normal cells was decreased about 12% under SEM and about 16% with Wright's stain testing. Finally, a whole setup of spiral microchannel was also experimented using Trypan Blue staining. About 70% of cells could survive after passing through a whole setup with a 1 ml syringe at 1 ml/min. This suggested that majority of cell death occurred in the spiral channel not in the feeding system. For the second phase, it was about designing of a releasing device which is used to discharge a specific cell for a further biological testing. The idea is that the releasing device is designed as the main channel located over the wells and the second channels (buffer channels) located at the bottom of the wells. During immobilization, the fluid in the main channel will flow over the wells, while the fluid from buffer channels will slowly be injected to keep the cells floating. In the releasing process, the fluid flow in the main channel will be slowed down. Meanwhile, the stronger fluid flow is injected from the buffer channels to push the cells out of the wells. Using computational software, the results showed that when the cell size was increased, the required flow rate was increased as well until the cell size of around 14 μm. At this size, the required flow rate was around 1.2 nl/hr. For the cell size bigger than 14 μm, the required flow rate gradually reduced.

Department:	Mechanical Engineering	Student's Signature .....
Field of Study:	Mechanical Engineering	Advisor's Signature .....
Academic Year:	2015	Co-Advisor's Signature .....
		Co-Advisor's Signature .....

ACKNOWLEDGEMENTS

In this thesis, I would like to take this opportunity to thank all people who have supported and helped me in the field of Engineering and Biology research, especially Professor Alongkorn Pimpin, who always taught, motivated and made me enthusiastic about doing research in the field of Microfluidics. Furthermore, I also thank to his guidances, valuable inputs, good suggestions, tremendous help and computer facilities. Without his guidance and persistent, this dissertation would not have been possible.

I would like to acknowledge to Professor Werayut Srituravanich who taught and gave good suggestions for Microfabrication and thank for great opportunities to allow me to present and practice verbally my work in English during the program in monthly meeting.

I would like to express my gratitude towards Professor Prapruddee Piyaviriyakul who allowed me to use facilities: laboratory, biology lab equipment and supplies. I also would like to thank to Professor Achariya Sailasuta who provided a lively research groups of Microfluidic meeting and I would like to express the deepest appreciation to my mentor and partner— Dr. Dettachai Ketpun and Dr. Sudchaya Bhanpattanakul who always helped me with experimental preparation, suggestions and friendship and I am also grateful to Dr. Wutthinan Jeamsaksiri of Thailand Microelectronic Center for introducing me to the scholarship— Thailand Graduate Institute of Science and Technology (TGIST).

I would like to express my gratitude towards Professor Mayuree Chanasakulniyom for her suggestions and guidance on the research and also appreciate to Professor Saran Salakij who gave valuable comments on computational simulation and reading a draft of the thesis. I am also thankful to Professor Theerayuth Kaewamatawong for guidance on a light microscope and good suggestions for cell structures.

In addition, a thank to the scholarships: the Ratchadaphiseksomphot Endowment Fund of Chulalongkorn University for the first year and Thailand Graduate Institute of Science and Technology (TGIST) for the second year of the program for supporting financially including free tuition, materials, salary and great opportunities of valuable conferences.

Personally, I would like to thank my friends and family. I am grateful to Miss Maria Clara Naranjo and Miss Lena Hamvas who helped me with writing the scholarship paper, patiently revised and corrected my thesis in English and thank for our true friendship over the years. Furthermore, I am grateful to Barnick and Taylor's family for hosting and supporting me along the way in particular Mrs. Sujittra Barnick and Mrs. Siriporn Taylor. Finally, my greatest gratitude goes to my parents for their support and encouragement, especially Mrs. Daranee Attachoo who supported and loved me the most. Without her, I may never have gotten to where I am today.

CONTENTS

Page

Page

Page

List of Figures

List of Tables

Chapter 1
Introduction

1.1 Importance and Rationale

Cancer is one of the most lethal and vicious diseases. Cancer affects humans and animals alike, and the some of diseases are incurable. As reported by the Ministry of Public Health, the statistics of cancer in Thailand over the past ten years has been increasing. Statistics indicates that cancer is the leading cause of death in Thailand, and 60,000 patients die every year. In addition, the number of deaths around the world due to cancer was about 8.2 millions in 2012 [1, 2]. Because of the biology of cancer, the cancer cells change all the time, and this makes it difficult to obtain accurate data on cancer cell behavior resulting of a difficulty in diagnosis. For this reason, we cannot make clear conclusions or provide precise diagnostic technique of an individual patient. Therefore, alternative methods in the field to improve comprehension of cancer behavior in the biological study of cancer cells have been studied.

The analysis of biological cancer cells is gathered by collecting samples of tissue cells. The tissue samples contain several cells. Based on the behavior of the cellular heterogeneity, this conventional technique could result in various outcomes. To resolve this, a single cell study is necessary in order to clearly analyze cancer cell behavior, and could provide a better outcome from a study. Microfluidic system is among various techniques that was recently developed to meet requirements from medical diagnosis. This technology allows us to analyze a single cell more clearly compared to the conventional methods, and appears to be more popular in other fields besides in biological study.

In our group, researchers from The Faculty of Veterinary Science at Chulalongkorn University has been researching the causes of cancer in animals as well as developing the techniques of cancer cell analysis. Working together with doctors from The Faculty of Veterinary Science and researchers from Thailand Micro Electronics Center (TMEC), engineers from The Faculty of Engineering at Chulalongkorn University willingly cooperate in this research by designing and developing advanced technological devices that can help analyzing cancer cells in a single cell manner. In the current developed system, there are three main processes in a single-cancer-cell biochip, i.e. sorting, trapping, and releasing, which will be discussed in details in the next section.

However, the current system has some limitations in terms of cell viability. From the previous experiment, it already confirmed that cancer cells were dead after the process of cell separation. There were about 50 percent of cells survival and the rest of them were dead and deformed due to hydrodynamic shear stress and extensional stress. Theoretically, the majority of cell death occurs between syringe and needle which probably damages cell severely. In addition, the flow inside the sorting device may also create high shear stress and damage the cells as well. For this reason, it is necessary to find protocols of experiment as well as to design the system

in order to increase cell viability as much as possible. For the releasing device, it is needed to develop and establish together with trapping and sorting technique for selectively study biological properties for an individual cell.

In this study, we divide this research into two phases. The first phase is about investigating and improving cell viability in the setup of spiral microchannel. This includes syringe, silicone tube, needle, spiral microchannel, straight channel and outlets by using computational simulation and actual experiments in different conditions. The second phase is to design the releasing device by using computational simulation. The flowing fluid mediated detachment is chosen as the releasing method because it does not require external forces which may affect the cell biology and its property.

1.2 Objectives of Study

The first phase is to improve cell viability in the setup of spiral microchannel device by finding the way to reduce a risk of cell death in the devices, including the syringe, silicone tube, needle, spiral microchannel, straight channel and outlets.

The second phase is to design and simulate the releasing device using flowing-fluid mediated detachment for a solid particle in order to find the appropriate flow rate and total forces to immobilize and release particle out of well.

1.3 Research Methodology

1.3.1 The First Phase

-Researching and studying of the improving cell viability and important parameters in the setup of spiral microchannel.

-Investigating the effects of shear stress and extensional stress on the cell death in the setup by using computational simulation to design the setup including the syringe, silicone tube, needle, spiral microchannel device, straight channel and outlets.

-Investigating cell viability with the actual cells by using different suspension media, varying the volume of the syringe 1, 2.5 and 5 ml, needle, connected and disconnected with a the tube, spiral microchannel, and flow rates in order to find the percentage of cells that could survive in the setup.

-Comparing both experiments of cell viability and computational simulation of flow streeses to explain the behavior and phenomenon in the setup.

-Analyzing and explaining possible ways to reduce cell death in the setup.

1.3.2 The Second Phase

-Flowing-fluid mediated detachment was chosen because it does not require external forces which may affect the cell biological properties.

-This releasing device was designed as the main channel located over the wells and the second channels (buffer channels) located at the bottom of the wells.

-Using computational software with an empty well to see the streamline and physical effects on the empty well with varying flow rates and well's sizes.

-Using computational software again, in which cells were modeled as solid particles—5 to 20 μm was employed in order to help examine the flow behavior—pressure and velocity distributions—as well as to examine the devices' feasibility for trapping and releasing mode.

1.4 Benefits

1. The investigation could help analyzing the improvement of cell viability in the setup of sorting device as well as finding the potential ways to increase cell viability.

2. Whenever this new releasing design is done, this design could pave the way to integrate three main techniques into a single biochip for analyzing either human or animal single-cancer cell study. It will become a new fully integrated technique for various applications including stem cell study, drug delivery and biological analysis.

1.5 Research Plan

Protocols	Year 1						Year 2					
	Aug -Sep	Oct-Nov	Dec	Jan-Fab	Mar -Apr	May	Aug -Sep	Oct-Nov	Dec	Jan-Fab	Mar -Apr	May
Literature Review	←	—	→									
Microfluidics-device Design		←	—	→								
Simulation			←	—	—	—	—	→				
Device Fabrication								←	—	→		
Examination										←	—	→
Data Analysis for Improvement										←	—	→

Chapter 2

Literature Review

Microfluidics is a multi-disciplinary technology because it involves with a well-rounded education and wide spectrum of knowledge including physics, chemistry, biology, engineering and nanotechnology**.** Microfluidics provides several advantages such as inexpensiveness, small sample size, high throughput, sensitivity, short time sample preparation, and simplicity to various analysis in chemical and biological studies [3, 4].

In order to analyze a single cell and its behavior, researchers need to separate cells and grow them under controlled conditions by using microfluidic devices that can integrate many experimental processes into a small device [5] known as Lab-on-a-Chip (LOC). Studying a single cell in Lab-on-a-Chip devices could provide us with an insight of cell behavior without the impact of environmental perturbations. This helps further analyze as well as understand either cell-to-cell variability or an individual cell behavior [3]. Moreover, a single cell can be monitored as it migrates or as it divides inside a microchip. Cell division is crucial in the field of cancer cell analysis. For these reasons, microfluidics is one of the most interesting innovative methods to help us understand the behavior of cancer cells as well as diagnose other lethally-vicious diseases.

As the above mentioned reasons, microfluidic systems help further research as well as bring the test conveniently and immediately in the usage of Point-of-Care (POC). There are three main processes including sorting, trapping and releasing which are integrated into one device in our studies. Each part consecutively operates in different ways in order to analyze a single cell. The sorting technique is the first technique which separates cells of different sizes. The trapping technique is used to trap a single cell in reservoirs or wells. Finally, the releasing technique is the last step which allows us to retrieve selected cells to the streamline for post processing.

2.1 Cell and Particle Sorting

Generally, the sorting technique has two principles— passive and active techniques— which can be performed using the unique characteristics in microfluidics. The first one is called “passive” which relies on the behavior of particle and hydrodynamic forces from a laminar flow such as pinched flow fractionation, deterministic lateral displacement, inertial separation, filters and micro vortex manipulation [4, 6]. Another is called “active” which is based on external force fields— acoustophoresis, dielectrophoresis, magnetic and optical [4]. In the next section, working principles, advantages and disadvantages of these techniques will be discussed.

2.1.1 Pinched Flow Fraction (PFF)

This technique is one of the passive sorting techniques depending on size of particles in a microchannel by flowing fluid as a laminar flow. The fluid flows the particles moving in the channel. The microchannel has an area which is called "Pinched segment" where particles are allowed to align towards one of the sidewalls as shown in Figure 2.1. The motion of particles is controlled by the flow rate of two fluids. In the flow, the particles tend to flow along the streamline passing through its center of mass. The mixture of fluid and the particles are separated and passing through the area of the pinched segment. The idea of this technique is to separate the particles by using the spreading streamlines based on the particle size. This technique can be applied to separate various kinds and numbers of particles [4].

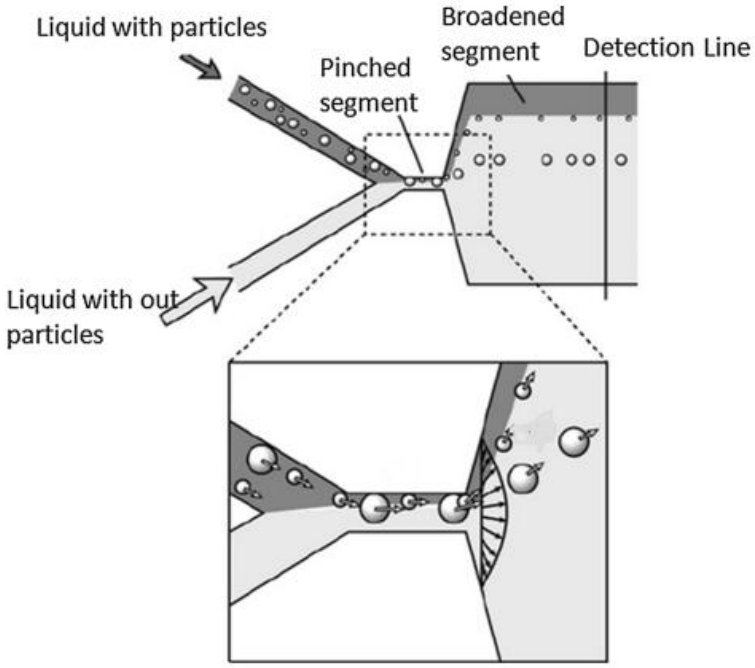

Figure 2.1 The illustration of pinched flow fractionation (PFF) [4]

2.1.2 Deterministic Lateral Displacement

Deterministic lateral displacement is a passive technique which works well with flow as laminar. The idea is to add obstacles in the course of the particle and release particles to follow along the streamline if the size of the particles is smaller than a given size (critical size). In contrast, if the size of the particles is bigger than a critical size, it will collide into obstacles as presented in Figure 2.2. As a result, these particles will be responsible for a streamline switch and changes its direction. With this technique, the different size of particles is able to be separated laterally by the shift in the arrays [6].

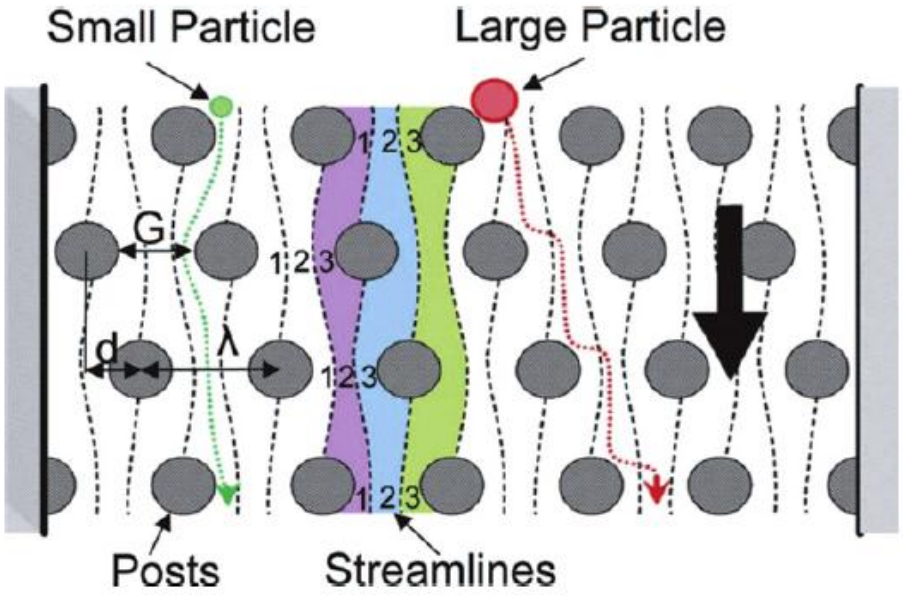

Figure 2.2 Deterministic lateral displacement: an array of microposts with a row shift fraction of one-third is used to sort small particles (green dotted line) from large ones (red dotted line) [6]

2.1.3 Inertial Lift Force and Drag Force

Inertial lift force and Dean drag force technique is one of the most commonly used techniques because it provides several advantages such as high throughput, easy fabrication, non-invasive manipulation and no need of external forces [7].

2.1.3.1 Spiral Microchannel

One of this technique has been used as a sorting device which is called spiral microchannel as exhibited in Figure 2.3. This technique uses the balance of hydrodynamic forces—Inertial lift force and Dean drag force. Inertial lift forces acting on cells in a channel, this can be explained by the result of the net force of a shear-induced inertial lift force and a wall-induced inertial lift force in a straight channel. This net force generally drives particles toward the outer sidewall [8], while Deans drag force is caused by the Dean vortex induced inside a curve of a microchannel [9] as demonstrated in Figure 2.4. The counter rotating vortices in the top and bottom half of the microchannel are generated due to spiral microchannel geometry [10]. With the equilibrium between the two forces, particles will be focused and moved at a specific distance from the inner wall, and the particle with different size will be focused at the different distance [10-12].

However, some reports demonstrate that Dean flow-based technique has a limitation of focusing small particles (less than 5 micrometers in diameter) [8]. For full information of important parameters in a spiral microchannel technique, see Appendix C.

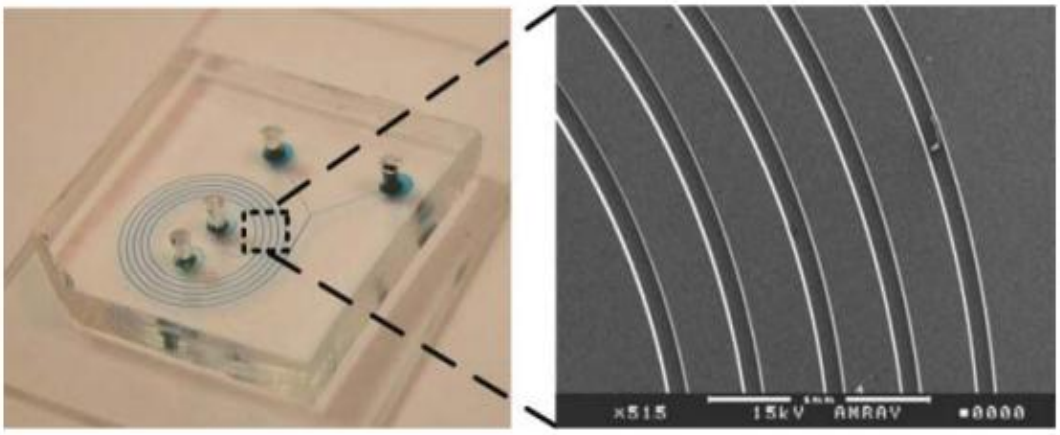

Figure 2.3 Picture of the spiral microchannels [11].

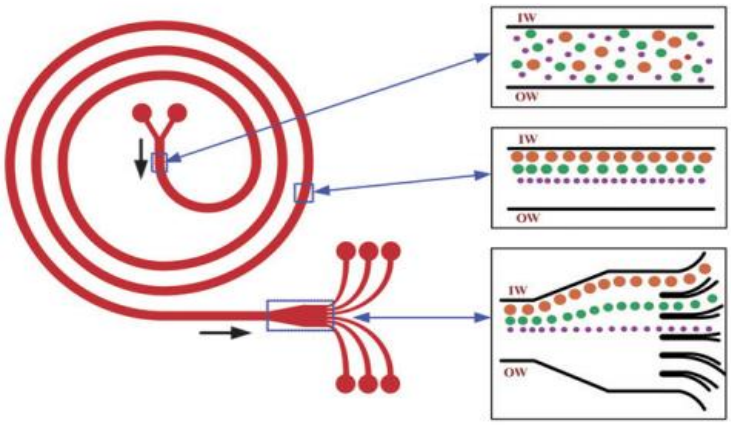

(a)

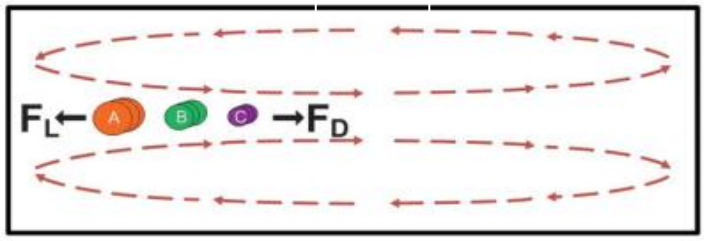

(b)

Figure 2.4 The picture of the direction of inertial lift force and Dean drag force acting on a particle (a) the spiral and straight channel and (b) cross sectional area [12]

2.1.3.2 Expansion and Contraction

This technique relies on size-based differential equilibrium positions of the particles perpendicular to the flow. Due to Zhang experiment, it illustrates that the expansion-contraction array channel can work well with high concentrated bio-particle sample [13]. This technique provides two main forces; inertial lift forces—shear and wall induced inertial lift forces—and Dean drag force which is similar to the technique of spiral microchannel but the Dean drag force is generated in different ways.

Similarly, the group of Lee conducted an experiment in a contraction and expansion array microchannel to separate different sizes of particles. This study uses polystyrene beads of 4 and 10 μm as experimental particles [14]. The main reason of using this technique is that this technique provides high throughput without requiring any external forces that may affect cell biological property. The working principle is that when the fluid moving in the straight microchannel, shear induced inertial lift force will be generated by shear gradient from the velocity profile that migrates a particle away from the centerline toward the sidewall. Whereas, when the particle is moving toward and being close to the sidewall, there will be the wall induced inertial lift force moving particles away from the wall to the center of the channel. These two forces will move particle to the equilibrium position where the net force becomes zero. However, the equilibrium positions of particles cannot be separated from each other widely enough. In order to separate widely, secondary force is needed to separate streamline focusing from each other. This force is known as Dean drag force. The abrupt change of the cross sectional area creates Dean vortices in both sides (upper half and lower half of the channel) in the direction of two counters rotating clockwise. In other words, the abrupt change of cross section can curve fluid streams as exhibited in Figure 2.5. When the fluid is entering the contraction region, the velocity of fluid will be accelerated due to the decrease of cross section which produces Dean drag force. In contrast, when the fluid is entering the expansion region, the Dean drag force will be diminished due to the increase of cross section. The Dean vortices help particles move to a new equilibrium position. Additionally, without the influence of Dean drag force, the particles are still in the equilibrium position at 0.2 of hydraulic diameter from sidewall [14]. However, under the influence of Dean drag force, a new equilibrium position will be greater than 0.2 of hydraulic diameter. This indicates how Dean drag force works and help stream focusing separate from each other widely.

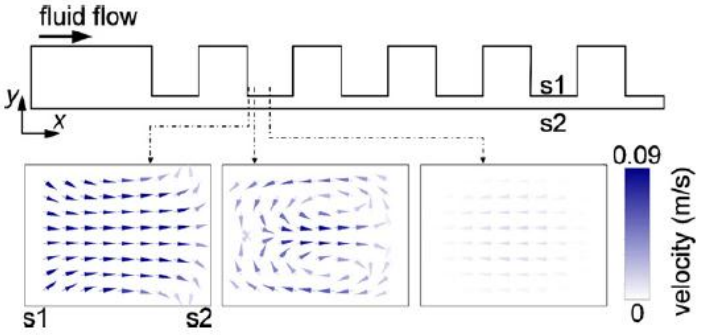

Figure 2.5 Schematic picture of the side view of expansion and contraction device and the picture of dean vortices in the upper half and lower half at the cross section in the second contraction region [14].

After knowing the working principle of this technique, the group of Lee designs the inertial separation in a contraction and expansion array microchannel with one-sided rectangular structures to fix the direction of inducing dean flow sustaining which the flow rates are varied from 3-22 ml/hr. The main channel is 350 μm width and 38 μm depth. As for the contraction region, it is 50 μm in width and 300 μm long in length. On the other hand, the expansion region with the length and width are 300 μm and 300 μm, respectively as demonstrated in Figure 2.6. Furthermore, there is an observation window after every sixth rectangular structures and the total number of rectangular structures are 30. The observation window is used to measure the inertial separation of particles and allows us to see of what happen to the streamline focusing inside the device.

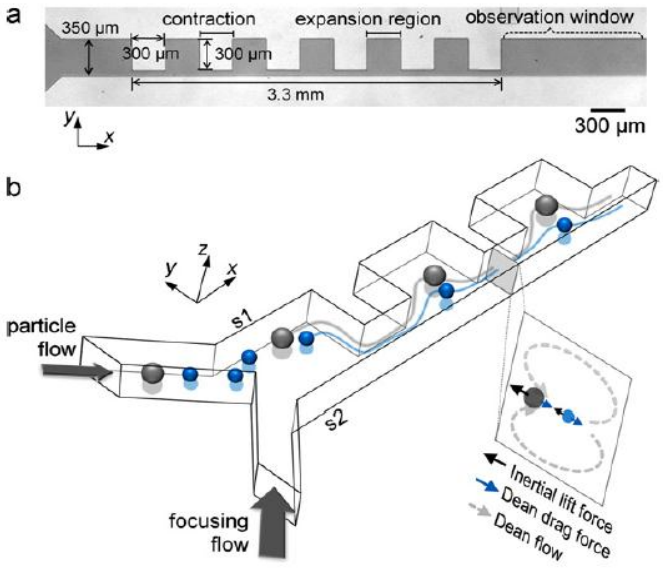

Figure 2.6 Schematic picture of the design of expansion and contraction device and the direction of inertial lift force, Dean drag force and Dean flow [14].

The conclusion is made that two sizes of particles of 4 μm and 10 μm can separate from each other after passing the sixth contraction region but they cannot separate after passing twelfth and eighteenth contractions. However, the particle of 10 and 15 μm occupies a similar equilibrium position. Therefore, there is no effect of separation on the particle of 10 and 15 μm. The results can conclude that the critical size of the particle is about 6-7 μm. Under the critical size, the particles tend to move toward the sidewall 2 while the above critical size occupies the equilibrium position near to sidewall 1 as seen in Figure 2.7 [14].

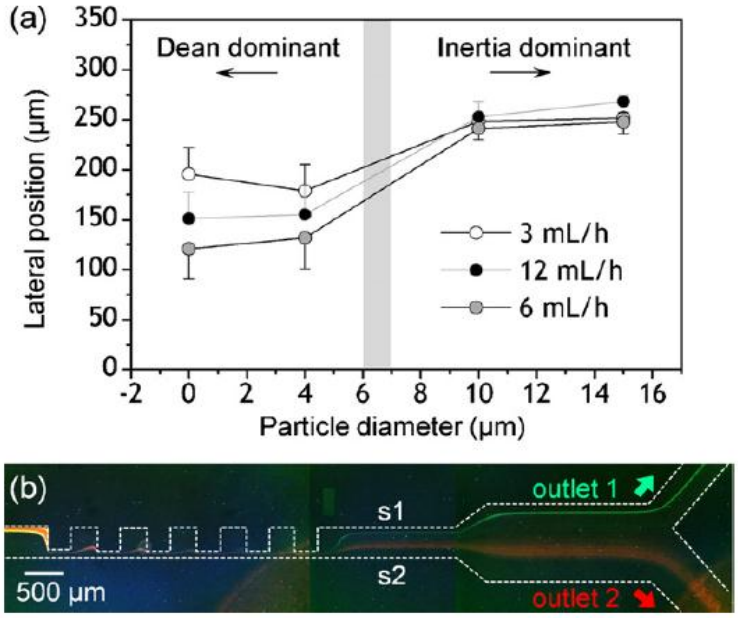

Figure 2.7 The positions of particle streamlines (a) lateral position versus particle diameter varying total flow rates (b) Fluorescence micrograph image of the streamline at a total flow rate of 14.5 ml/hr [14].

2.1.4 Filters

Filtration-based cell sorting is one of the most common technique in microfluidics. The developed microfabircation protocols provide a great resolution, high precise control and reproducibility of the design. The working principle of this technique is to have membrane pores as filters. This technique has several types of filtration such as weir-type, pillars, pillar-type and cross-flow as depicted in Figure 2.8. [6, 15]. The drawback of these filtration techniques are that clogging may occur during separation. This problem may be solved by using cross-flow or modifying the pillar geometry. Due to the development of filtration method, this technique has been flourishing in the areas of microfluidics which provides more efficiency and cost effectiveness [16]. Zhang and teams report the technique of filtration. They state that this technique focuses on large particles and removes the large particles from the mixture particles. Due to small particles, the high purity of separation is about (90%-100%). However, some of the small particles enter the reservoirs with undesirable purity (~20%) of large particle collection [13].

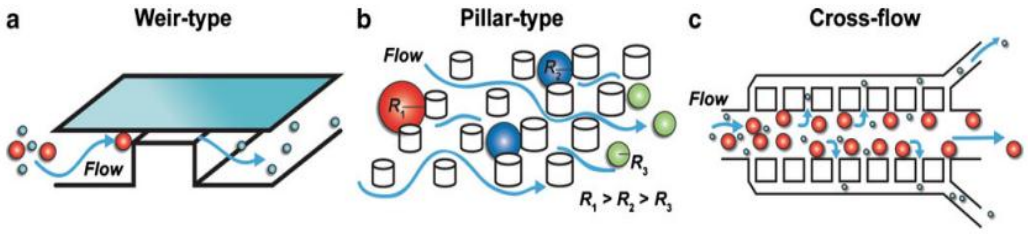

Figure 2.8 Microscale filter designs, (a) Weir-type filters size-exclude cellular (b) Pillar-type filters and (c) Cross-flow filters [15].

2.1.5 Microvortex Manipulation

Microvortex manipulation is commonly used for separating particles into multiple streams. There are three main forces that occur during manipulation process; gravitational force, buoyancy force and hydrodynamic drag force as evidenced by Figure 2.9. These forces equilibrate positions of particles. When the flow goes over the groove, vortices and a helical flow pattern are generated in the direction of the streams. The particles are forced in the vertical direction by drag, buoyant and gravitational force. As for lateral direction, the particles are forced by only drag force. As a result, the particles which are lighter than the medium will move up to the top of the channel. Whereas, the heavier particles will stay at the bottom of the channel.

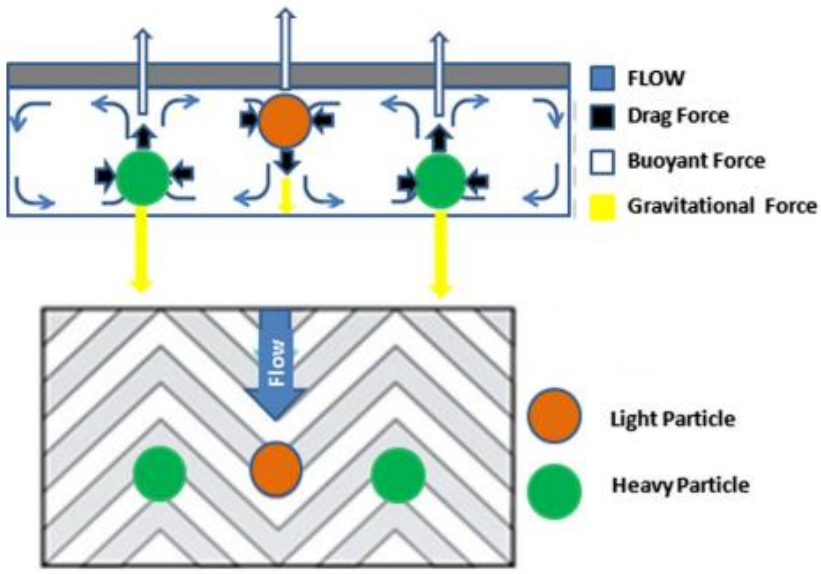

Figure 2.9 Position of the particles in micro-vortices manipulation [4].

2.1.6 Acoustophoresis

Acoustophoresis is based on particle migration in a sound field by using acoustic radiation force acting on cells. This technique is achieved in red blood cell sorting. As stated in Kumar research [6], the separation is successful within a rectangular chamber by applying both a resonant ultrasonic field and laminar flow field in orthogonal directions. This method proves that the separation capacity is high (100% efficiency and 90% purity) of 10 and 5 microspheres.

2.1.7 Dielectrophoresis

The dielectrophoresis helps polarizable particle movement in non-uniform electric field. The method is to sort cells moving into a channel. The dielectrophoresis forces manipulate cell's direction perpendicularly. This technique works very well with bacteria sorting from blood [6, 17]. Unfortunately, there are few limitations in use. First, media is suitable for living cells which are conductive. Secondly, the dielectric properties of cells may drastically depend on their stages and the environment. Thirdly, the forces of this method are usually weak compared to the hydrodynamic forces. As a result, if the forces of hydrodynamics are stronger, the time interaction between dielectrophresis forces and cells will be shorter.

2.1.8 Magnetic

This technique is one of the size-based active sorting techniques which have less effects on cell damage and time of separation. Interestingly, This technique provides several advantages in terms of specificity, high throughput and inexpensiveness. The group of Adams creates an alternative method, which combined high-gradient magnetic field along with fluorescent labeling. This combined technique is called "magnetic cell separation system" (MACS) which offers the process more efficient by purifying two types of targeted cells. The working principle of this technique is that a high-gradient magnetic field is introduced in which a column is filled with ferromagnetic stainless wool. The labeled magnetic particles will adhere to the steel wool and the non-magnetic particles will be separated from the device. When the magnetic field is removed, these magnetic particles will be separated as well.

2.1.9 Optical

This technique uses the advantage of light that produces the change in momentum of the photons produces a force. A maximum value at the center of a light beam can be explained by a Gaussian intensity profile. The working principle is that when a beam is scattered by the particles or the ratio of refractive index of the particles, the scattering force will attract the particles toward the center and move particles in the same direction of the light beam. This technique is named as "optical tweezers" because this phenomenon can be explained as a single-beam gradient force trap for dielectric particles.

As demonstrated, we can make a conclusion that the sorting techniques are categorized into two main methods— passive and active techniques. The passive techniques such as pinched flow fractionation, deterministic lateral displacement,

inertial separation, filters and microvortex manipulation are based on the size of particles. As for pinched flow fraction (PFF), this technique uses the flowing fluid— the spreading streamlines to separate particles based on their size. Similarly, inertial and Dean flow fractionation and microvortex manipulation use the idea of forces generated by the nature of physical forces— Dean Drag, lift, buoyant and gravitational forces. These methods do not require external forces leading to a complicated device structure. On the other hand, the techniques of deterministic lateral displacement and filters uses the advantages of the geometry of microfabrication— obstacles, pores and pillars. These techniques are not suitable for separating cells because a collision between cells and walls will occur during the process of separation. As a result, there will be a high risk of cell death during the process of cell separation.

According to the active sorting, this technique is based on external force fields— acoustophoresis, dielectrophoresis, magnetic and optical. These techniques are very useful for the particles which have outstanding electrical or magnetic properties. Additionally, active sorting methods do not have a strong force and depends on flow properties such as velocity and pressure because there is an external force being applied from outside the microchannel. However, active sorting techniques have a possibly effects on cell biological property. Consequently, the active sorting techniques are not considered as a good choice for cancer cell separation.

2.2 Cell and Particle Trapping

One of the ultimate goals of single cell research is to trap particles separately. The main reasons why one wants to trap a single cell is to study its motion, degree of freedom, and to investigate its affinity for other molecules that are bound or free-floating on a surface [18]. The conventional and recent trapping technology as well as the working principles and the limitations in use of each method will be discussed in this section.

2.2.1 Encaging Cell Trapping Concepts-Arrays

The advanced technological microfluidic device as encage cell trapping is to design as cages regrading the studies of single cell responses. One of this technique is known as microwells, this technique is able to trap and allow a vast number of cells to be seeded as well as settled in small well arrays in each position by using gravitational force as exhibited in Figure 2.10. Microwell array provides varying well diameters to suit various size of cells to be captured. It also shows that the efficiency of trapping is about 85% of cells in total.

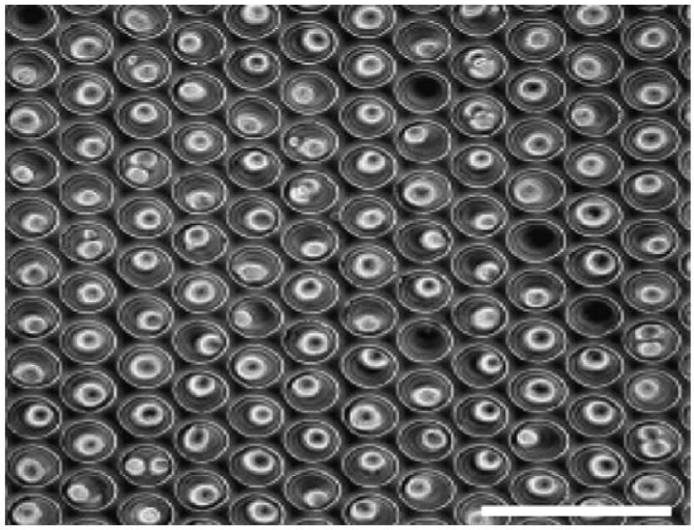

Figure 2.10 Microwell array for single cell trapping [19].

2.2.2. Hydrodynamic Cell Trapping

Hydrodynamic cell trapping is the most used approach in microfluidic technique. This technique can trap particles based on their intrinsic physical characteristics. The technique has two important keys; channel geometry and hydrodynamic forces. As a passive method, this technique does not need an external force leading to a complicated device structure. The idea is to create side channels in a main transport channel. The side main channels are able to trap cells by suction where fraction flows along the side channels. The group of Yang creates a parallel channel, which consists of two channels, which are connected via a dam structure leaving 5 micrometers opening. As a result, particles are retained along the full channel length by defining a net cross flow over the dam as presented in Figure 2.11.

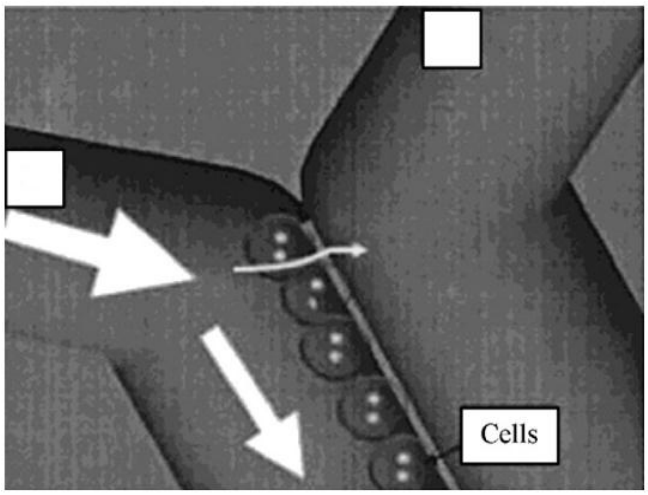

Figure 2.11 Schematic of cell trapping along dam structure [19].

2.2.3 Optical Tweezers

The principle of this technique is to use laser beam to trap and manipulate particles with high precision. A momentum is carried by laser beam and transfers to particles when the beam hits the object. Therefore, the targeted particles will be moved into the center of the beam. Therefore, the particle which is drawn in the direction of the beam will be trapped as well. The group of Arai [19] combines this technique with a thermosensitive hydrogel in a microsystem. This combination allows single yeast cells that are chosen in a microfluidic channel and transported to a hydrogel using optical tweezers. Furthermore, the group of Arai presents the high precision of using optical tweezers to tie knots on different biofilaments such as DNA or actin.

2.2.4 Dielectrophoretic Trapping

Dielectrophoresis is the method of moving dielectric objects or controlling a single particle by the means of dielectrophoresis. This force is generated by the non-uniformities of the electric fields. This method is divided into two types of dielectrophoresis; p-DEP, the dielectrophoretic force moves the object towards the higher electric field. Whereas, n-DEP, the dielectrophoretic force moves the object towards the lower electric field as exhibited in Figure 2.12. [19].

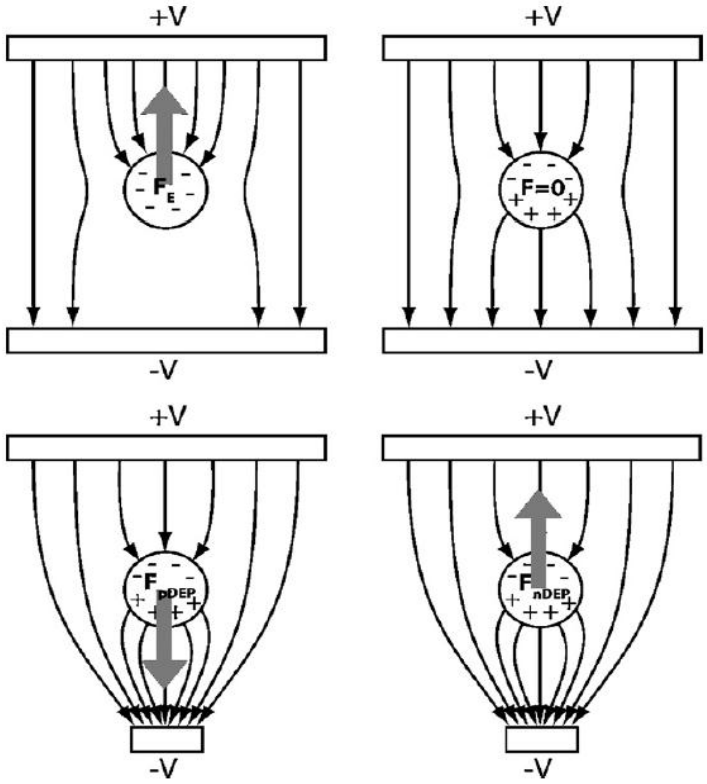

Figure 2.12 The demonstration of the movement of Electrophoresis (EP) and dielectrophoresis (p-DEP and n-DEP) [19].

2.2.5 Magnetic Trapping Technique

Magnetic trapping technique uses the ability of magnetic fields and magnetic particles of different types and sizes. This technique offers great advantages, for example, magnetite is the most used materials and it is hard to oxidize [19], the external magnet does not contact with the fluid because it is usually applied from outside the microchannel. Besides, magnetic interaction is not affected by temperature, pH, ionic concentration and surface charges [20]. This method suits the range of particle size between 5 nanometers to a couple of micrometers. After the field is removed, the large particles will maintain the degree of magnetization. As a result, it may be difficult to remove particles from traps or the cluster formed.

2.2.6 Acoustic Trapping

This technique can be used for non-contact trapping of cells by applying ultrasonic standing waves. This method is mainly used for handling of cell or bead agglomerates [19]. For this advantage, the group of Mikael represents acoustic trapping by using neural stem cells as experimental particles. The outcome is quite impressive because the experiment illustrates that neural stem cells are trapped and viable after 15 minutes. In addition, at the flow rate of 1 μm/min, yeast cells are successfully cultured for 6 hours in the acoustic trap. Thus, the non-contact method as acoustic trapping is important when studying on non-adherent cells such as stem cells, yeast cells or blood cells [21].

Like sorting technique, the trapping technique is divided into two main techniques as well—passive and active techniques. The groups of Nilsson [19] review the studies of sorting focusing on passive trapping technique. Although most passive sorting techniques have similarities, each technique has their own characteristics. For example, encaging cell trapping concepts-arrays method is suitable for trapping a large number of particles in wells, whereas the hydrodynamic cell trapping method is appropriate for retaining particles along the channel. According to active trapping technique— optical tweezers, dielectrophoretic, magnetic and acoustic trapping technique— use the external force fields to help trapping or changing the direction of particles. However, there are some limitations in use. For instance, if fluid flows particles too fast, the force fields of dielectrophoretic trapping will not be able to change the direction of particles due to the low magnitude of dielectrophoresis compared to that of Drag force. Furthermore, the external forces from electrical, magnetic and light source might affect the cell biological property as mentioned earlier. For this reason, the hydrodynamic method has a high potential to succeed for a single cell study.

2.3 Cell and Particle Releasing Technique

The releasing technique or detachment is the last technique of this study. This technique is about how to isolate a single cell from a trap by using passive or active techniques. The two most challenging parts of the releasing technique are to keep cells survival and unperturbed as well as finding the suitable strategies in order to release different kinds of particles [22]. The next section will describe the principle of each technique including its advantages and disadvantages.

2.3.1 Flowing Fluid Mediated Detachment

Flowing fluid mediated detachment is the simplest technique which generates shear stress during the process. As stated in the study of Zheng [22], it reports that the working principle of this technique is to introduce hydrodynamic forces that can overcome the cell adhesive force. The hydrodynamic forces depend on a couple of factors—flow rate, flow acceleration, and flow type in cell detachment. Technically, applying flowing fluid to attach cells by using a syringe pump to detach is not difficult. However, the most difficult part is to calculate the stresses precisely because the stresses—shear and extensional stress— may affect cell viability that can be vulnerable to cells (see in Table 2.1). For example, tumor and stem cells may be affected due to shear stress that can cause a rise in cell membrane tension. If the shear stress reaches to a critical point, the cells are more likely to be damaged and deformed. Furthermore, this technique provides low efficiency and there are still some limitations in use. However, if targeted cells sturdy enough and the shear stress is low, this technique would be the best technique because of simplicity and inexpensiveness. According to the research of Yoshinori [23], the device is fabricated as a single cell manipulation device. This device consists of two channels—main channels and buffer channels. When a single cell is trapped into a pocket, the cell is capped by the drain channel. Consequently, other cells will flow over through the channel and move to the next capture pockets. Due to releasing mode, the flow rate in the main channel is lower than the flow rate in the buffer channel. As a result, the captured cells will be released from the capture pockets and move to the main channel as demonstrated in Figure 2.13.

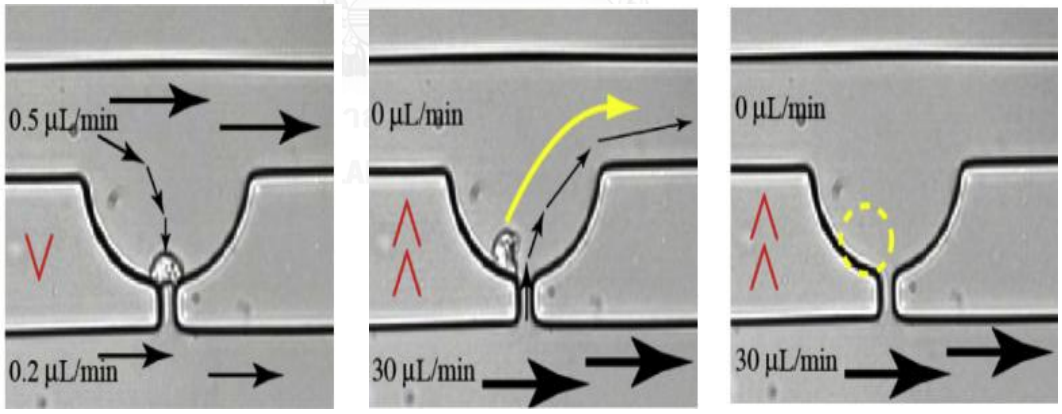

(a) (b) (c)

Figure 2.13 Releasing device using hydrodynamic detachment method (a) capturing mode (b) releasing mode and (c) the result after releasing mode [23].

2.3.2 Stimuli-Responsive Polymers Mediated Detachment

There are several of stimuli responsive polymer techniques including changes in pH, temperature, ionic strength, light, mechanical force electric and magnetic field. The idea of this technique is to use polymers to respond to external stimuli by changing their microstructures from collapsing to expanding and it can reverse their initial state as well.

2.3.2.1 Thermo-Responsive Polymers

The group of Zheng [22] states that in the field of tissue engineering, this technique is the first technique of cell sheet lift-off. The technique uses the change of temperature to attach cells and reverse cell to detach from the surface. Poly (N-isopropylacrylamide) (PNIPAAm) is the commonly used techniques for thermo-responsive polymer. Normally, cells prefer hydrophobic surface to hydrophilic ones for attachment. When the temperature decreases, cells can be lifted off from PNIPAAm. Reversely, if the temperature increases, cells will be attached to PNIPAAm.

2.3.2.2 pH-Responsive Polymer

Like Thermo-responsive polymer, pH-responsive polymer uses the change of pH—acidic or basic moieties in order for attachment and detachment. It is reported that chitosan surface will become negatively charged when medium pH is higher than 7.4. As stated by the group research of Chen [22], it shows that when pH is increased to 7.65 with >95% viability as well as over 90% **(**see in Table 2.1) of cells rapidly detaches from chitosan in 1 hour.

The group of Dirk reports the successful experiment of drug delivery by using the technique of thermo and pH responsive polymers. Their message is that the area of polymer therapeutics can be considered as a subcategory in the field of Nanomedicine, which covers the areas of analytical tools, diagnostics, imaging technique and innovative drug delivery systems. According to this review, if polymers are not drugs themselves, they can provide several advantages to help drugs more functional such as drug carriers, reducing immunogenicity, toxicity or degradation. In conclusion, both thermo and pH responsive polymers offer great advantages in drug delivery. Not only do they act passively as drug carrier but also they can respond to the environment setting [24].

In summary, Table 2.1 indicates the comparison of the cell isolation and detachment approaches which are categorized into five methods. Each method is suitable for particular conditions depending on the different types of cells, treatment conditions, releasing time, detachment rate, and cell viability.

Table 2.1 Comparison of flowing fluid and stimuli-responsive techniques [22].

Property	Cell types	Treatment conditions	Releasing-time	Detachment rate	Cell viability
Shear stress (Flowing fluid)	Various	Laminar flow with high flow rate; turbulent flow with high flow rate; flow acceleration	Few seconds	>50%	Poor
Temperature	Fibroblasts	Decreased temperature from 37 to 25 °C; at a flow rate of 560 μm s^{-1}	30 min	80%	N/A
	COScells; mesenchymal stem cells	Decreased temperature from 37 to 20 °C	10–20 min	N/A	89% and 97%
	CD4+	Decreased temperature from 37 to b32 °C facilitated by ~10 μL fluid	<10 min	59%	94%
	MCF7	Decreased temperature from 37 to 20 °C	20 min	99%	>95%
	MFC and BAEC	Decreased temperature from 37 to 20 °C,at a shear stress of 9.4 dyn cm^{-2}	~1 h	~100%	N/A
PH	HeLa	Increased pH from 6.99–7.2 to 7.65	~1 h	>90%	>95%
	Mesenchymal stem cells	Decreased pH from 7.4 to 4.0	2–3 min	N/A	>95%
Ions	C2C12 myoblast cell sheets	5 mMof ferrocyanide	<5 min	~100%	>90%
Light	Mesenchymal stem cells	UV 365 nm, 950 μW/cm2	4 min	>90%	>98%
	3 T3	He–Xe lamp, 450 W, 50 mJ cm−2 at 248 nm	<5 min	Single cell Release	>80%
	Molt-3 T-lymphocytes	UV 365 nm, 1.2 W/cm2	0.5 s	>90%	>95%
	Fibroblasts	2 WCW diode laser, 532 nm, 500–1000 mW	2–5 min	Poor	Poor
	MC3T3-E1	365 nm, 1.4 mW/cm2, total energy: 3360 mJ/cm2	20 min	>90%	>97%
	HeLa	Near infrared laser, Nd: YVO4, 1064 nm, 20 Hz, 4–6 mW	4 ns	Single cell release	Limited

As seen from the chart, the flowing fluid technique is available for many types of cells and has a quick releasing time. In addition, this technique depends on the flow rate. However, there is no data for capture efficiency. Plus, cell viability is quite low because the shear stress may affect cell viability during the process.

The methods of pH, temperature, ions and light are similar because they use the technique of changing microstructures by collapsing or expanding them. Although the detachment rate and cell viability are about 90-100 percent, they are limited under several conditions. For example, in order to activate pH stimuli-responsive polymers by using chitosan, we need to increase pH from 6.99-7.2 to 7.65. Whereas, PAH/PSS, pH needs to be decreased from 7.4 to 4.0. As for temperature stimuli-responsive polymers, they may take longer time to release cells completely. However, captured efficiency is about 90-95%.

In conclusion, cell types and treatment conditions limit the method of pH, temperature, ions and light. In contrast, the flowing fluid technique may be the best technique if the shear stress does not affect the cell viability so much [22]. For this reason, cell viability and cell degeneration are needed to be considered for using the flowing fluid technique.

2.3.3 Mechanics

One of the most interesting approaches for particle separation technique is called microbubble technique. As reported by Tan and Takeuchi [25], the experiment shows the combination of hydrodynamic and optical-based microbubble technique as a particle separation. Due to their experiment, hydrodynamics allows this technique to transport and immobilize a large number of particles. On the other hand, optical-based microbubble method gives dexterity in handling individual particles without complicated circuitry. When a trap is empty, the loop channels have higher flow resistances than the straight channels. In consequence, the particles in flow are carried by the main stream into the traps. As for optical-based microbubbles, it will be operated when particles are trapped. Aluminum patterns, as heaters are located near the traps. After that, IR laser will be focused onto the aluminum pattern. This process generates heat to create a bubble which expands a bubble and immobilize particles from traps into the main flow as seen in Figure 2.14.

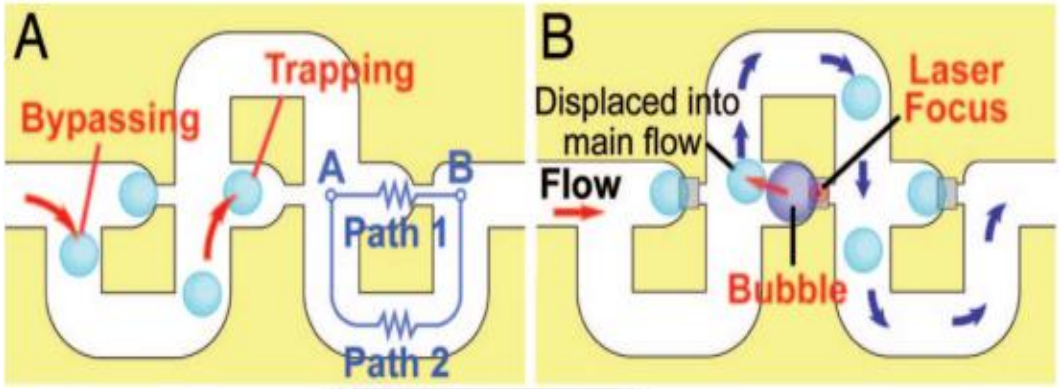

Figure 2.14 The working principle (a) trapping mode and (b) Releasing mode [25].

2.4 The Studies of Shear Stress and Extensional Stress

According to our previous experiment, it was found that cancer cells were deformed and damaged severely. Cells could survive only about 50% after passing through the setup of spiral microchannel. This brought a great attention on cell viability and cell biological property. We decided to do more research on cell viability and find the ways to reduce a risk of cell death.

2.4.1 The Studies of Shear Stress

The viability of cells is very sensitive to shear force, especially mammalian cells because they have a lack of cell wall. In order to minimize the risk of cell viability, researchers have tried to avoid shear forces as much as possible by decreasing the exposure level and duration. As reported by the experiment of Kretzmer and Schugerl, it reports that when shear stress reached to 0.16 Pa, the cells do not decrease in viability. However, it increases lactate dyhydrogenase (LDH) releasing into the medium. Furthermore, when shear stress is increased to 0.26 Pa,

there is no loss of cell viability as well. However, cell viability is decreased when the shear stress goes up to 1.5 Pa after 3 hours [26].

Furthermore, Barnes and his team illustrate the diagram and emphasizes that cells are subject to a gradient of shear stress. Using this protocol, Barnes and his team investigate the loss of cell viability by varying flow rates and duration of fluid shear stress (FSS)-exposure and testing with a needle of 30 G which human prostate cancer cell line (PC-3) is tested as experimental particles. The outcomes show that the sensitivity of cells to FSS depends on the magnitude of shear, flow rate and the exposure to FSS as illustrated in Figure 2.15a-c [27]. Similarly, the group of Mitchell and King experiment the maximum fluid shear stress that cancer cells are expelled in syringe from a syringe pump to a collector. The maximum shear stress is found about 74-650 Pa [28]. Like Barnes's study, the group of Park reports the experiment of trapping device using Human PC3 prostate cancer cells to test cell viability with various shear stresses. The device does not damage the cells during trapping process. Surprisingly, the experiment is found that shear stress above 0.2 Pa, cells started changing phenotypically. However, the shear stress reaches further to 0.5 Pa, the cells start to die [29].

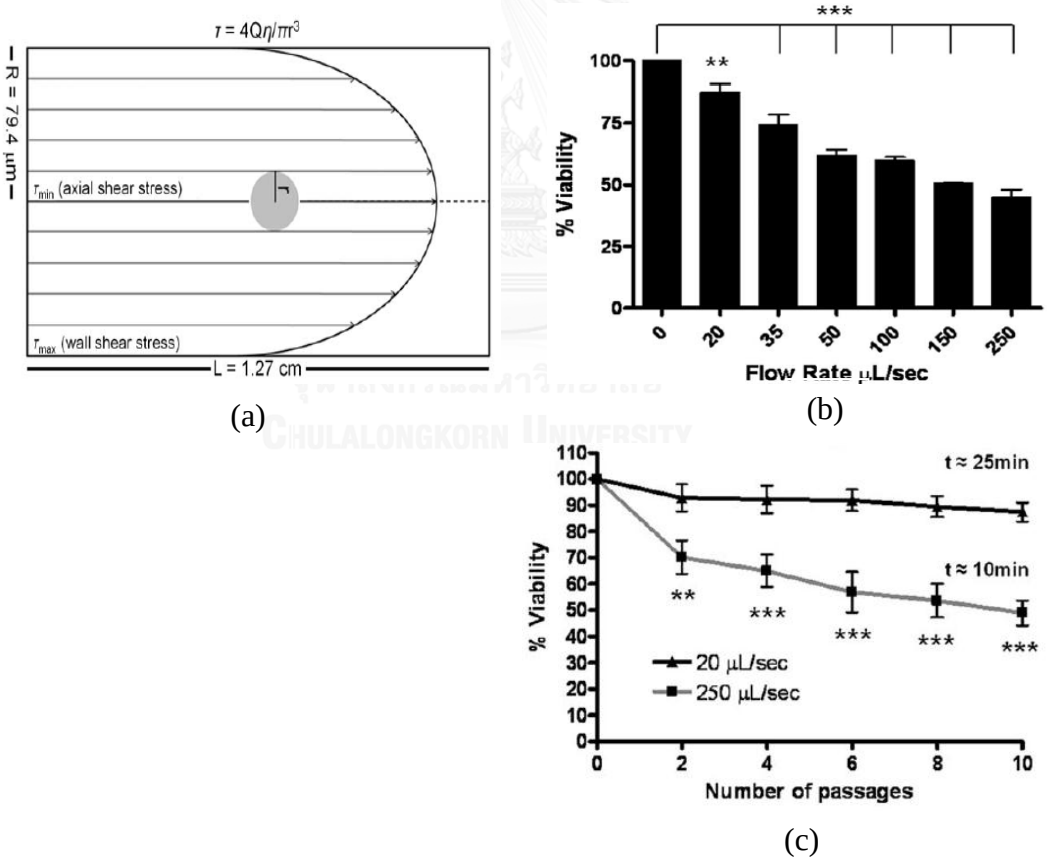

Figure 2.15 The graph shows (a) the diagram of FSS (b) the cell viability versus varying flow rates and (c) the loss of cell viability with varying flow rates and duration of FSS-exposure of 10 and 25 minutes [27].

In general, shear stress is defined as the force that generated by the flowing fluid within non-uniform velocity field. The highest shear stress occurs on the wall. For example, the wall shear stress in cylindrical tube was calculated using Poiseuille's equation as [30].

$$\tau = \frac{32Q\mu}{\pi d^3} \tag{2.10}$$

where τ is measured in pressure units, Q is the mean volumetric flow rate, μ is the dynamic viscosity of the fluid and d is the inner diameter of the cylindrical tube.

The study of Nerem also concludes the important factors that may affect cell viability. The report states that the chance of cell survival depends on the level of shear stress, the duration of exposure, the substrate on which the cells are grown and the chemical environment of the cells [31]. Over the past decades, many researchers have studied about shear stress with various types of cells. Table 2.2 presents the general summarization of shear stress studies.

Table 2.2 Magnitude of shear stress that affects various types of cell physically and biologically

Researchers (year of the study)	Types of cells	Magnitude of shear stress that does not change cells (Pa)	Magnitude of shear stress that starts to change cell biologically (Pa)	Magnitude of shear stress that starts to kill cells (Pa)
Stathopouent (1985)	Anchorage-Dependent Kidney Cells	0.26		—
Smith (1987)	Hybridoma Cells	0.16		—
Tramper and Vlak (1988)	Mammalian and Insect Cells	—	—	1.5
Manbachi (2008)	Cardiac Muscle Cell Line (HL-1)	0.2	—	—
Park (2010)	Human PC3 Prostate Cancer Cells	—	—	0.5

According to the studies of cell viability and shear stress, in mammalian cells, when the cells experience the shear stress over than 0.5 Pa, these affected cells would start to die. However, the minimum of shear stress which will not impact on biological cells is reportedly lower than 0.16-0.2 Pa [10, 26, 27, 29].

2.4.1 The Studies of Extensional Stress

In 2012, the group of Aguado [32] reports the improving viability of stem cells by using the viscosity of hydrogel cell carriers. As stated in the study, they experiment stresses with the syringe of 1 ml and the needle's number of 28-gauge and then investigates the viability of cells which one of the carriers of this experiment is PBS. The conclusion illustrates that when PBS is used as cell carrier, cell viability is about 60% as displayed in Figure 2.16. However, when the alginate hydrogel with G' (plateau storage moduli) = 29.6, the viable cells are increased drastically about 90%. Furthermore, the author concludes that there are two factors that affect cell viability (i) shearing force and (ii) stretching force. Surprisingly, stretching force is the main effect on cell viability but shearing force does not significantly impact on the viable cells.

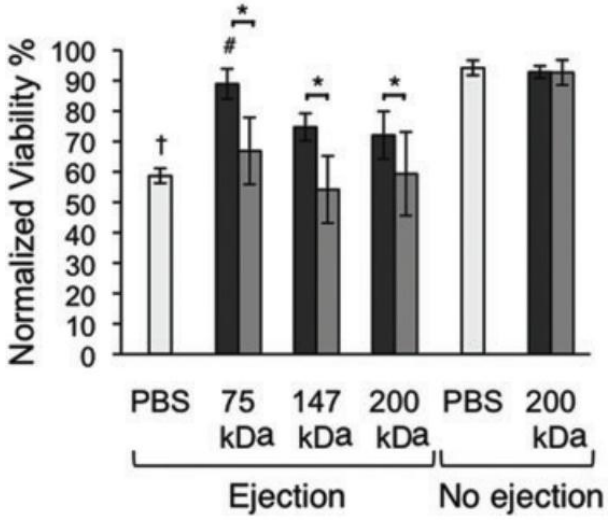

Figure 2.16 The comparison of HUVEC viability within PBS, Crosslinked and Non-crosslinked [32].

In conclusion, the main cause of cell death is the stretching force which usually occurs at the entrance of the syringe needle. The stretching force results in extensional flow occurring when there is the abrupt change in cross-sectional area which leads to the increase in linear velocity [32].

The recent research of extensional stress was published in 2015 by Bae et al. [33]. The study demonstrates the experiment of extensional stress with Chinese hamster ovary (CHO) cells. The cell is introduced at the middle of the cross-slot channel. In the middle, the cell experiences extensional stress in four directions at stagnation (the middle of cross-slot channel) as evidenced in Figure 2.17. As a results, the critical extensional stress that can damage cell mechanically is about 250 Pa.

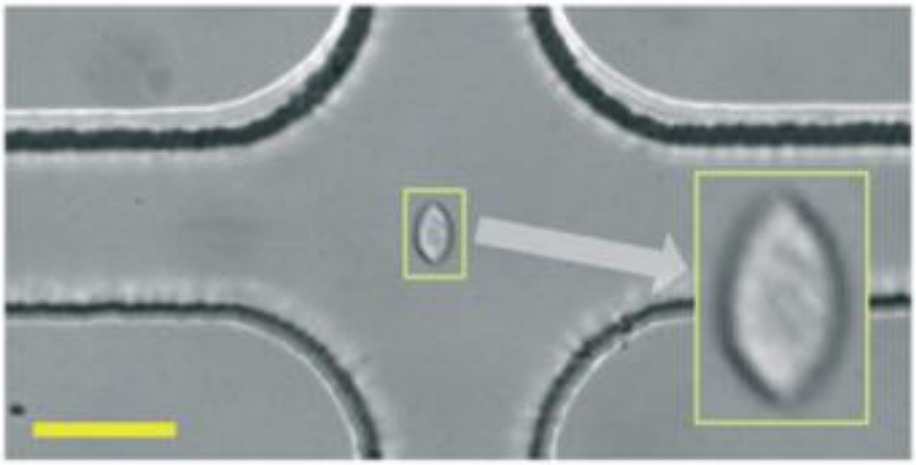

Figure 2.17 the demonstration of the particle experimented at the middle of cross-slot channel [33]

Furthermore, the study of Yen et al. [34] confirms the effects of shear and extensional stress acting as the force behind hemolysis. The study suggests that extensional stress play a significant role in cell damage rather than shear stress as the previous thought. The results indicate that the threshold value of extensional stress was 1000 Pa with the exposure time about 0.06 ms. Furthermore, computational simulation displays that high stress is usually generated at the corner and spread out from barrel to needle, especially, shear stress is extended along capillary wall. The experiment also demonstrates stress at the tapered capillary entrance. It was found that the tapered capillary can reduce both extensional and shear stress in the device. This result is exhibited as two dimensional simulation as shown in Figure 2.18. Like Yen et al., Down et al. [35] also confirms that shear stress develops at the corner of the contraction and extensional stress magnitude is highly generated at the capillary entrance. This experiment uses red blood cells (RBCs) and ovarian cells as experimental particles which each type of cell enduring different magnitude of extensional stress. However, the mechanisms of destruction on viability may affect RBCs and ovarian cells similarly including cell morphology and cell structures such as cell membrane, cytoplasm, nucleus, etc.

After reviewing, Table 2.3 shows the summarization of the studies of extensional stress affecting cell viability. As seen from the table, it is shown that extensional stress that affects cell viability is about 250 Pa. However, red blood cells tend to die when extensional stress is higher than 1,000 Pa to 3,000 Pa.

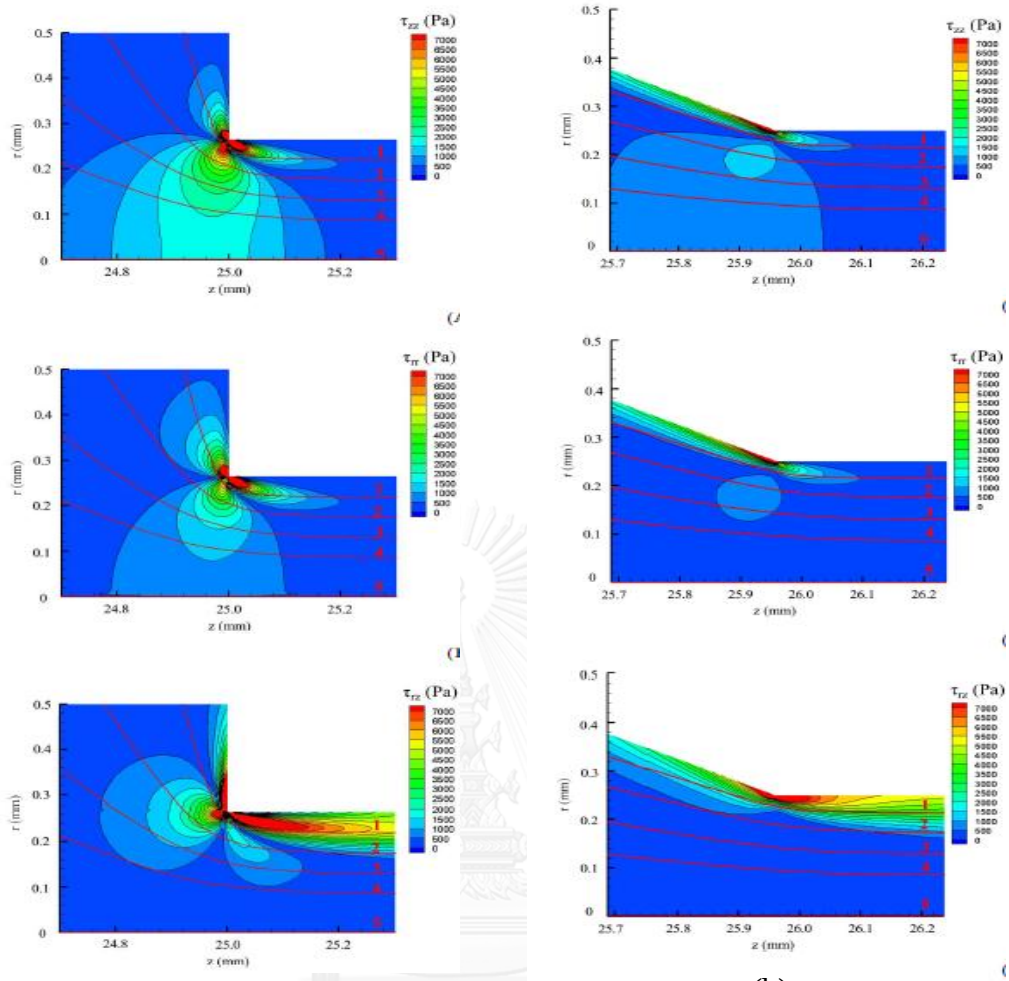

Figure 2.18 Contours displays the magnitudes of axial extensional stress, radial extensional stress and shear stress in different locations (a) corner capillary and (b) tapered capillary [34]

Table 2.3 Magnitude of extensional stress that affects various types of cell physically and biologically

Year of the studies	Type of cells	There is no change in Cells (Pa)	Cells start to change biologically (Pa)	Cells start to die (Pa)
Linden A. (2010)	Red Blood Cells	—	—	3,000
Young Bok Bae (2015)	Chinese Hamster Ovary Cells	—	—	250
Jen-Hong Yen (2015)	Red Blood Cells	—	—	1,000

Chapter 3

Current Status - Research and Development in Microfluidic Groups

Working together with doctors from The Faculty of Veterinary Science and engineers from Thailand Micro Electronics Center (TMEC), the research team of mechanical engineering at Chulalongkorn University has been researching and developing advanced Microfluidic devices over the past years in order to analyze and further understand the behavior of cancer cells. In this research, there are three activities due to three main functions of Microfluidics—sorting, trapping and releasing [36, 37] as displayed in Figure 3.1a-b.

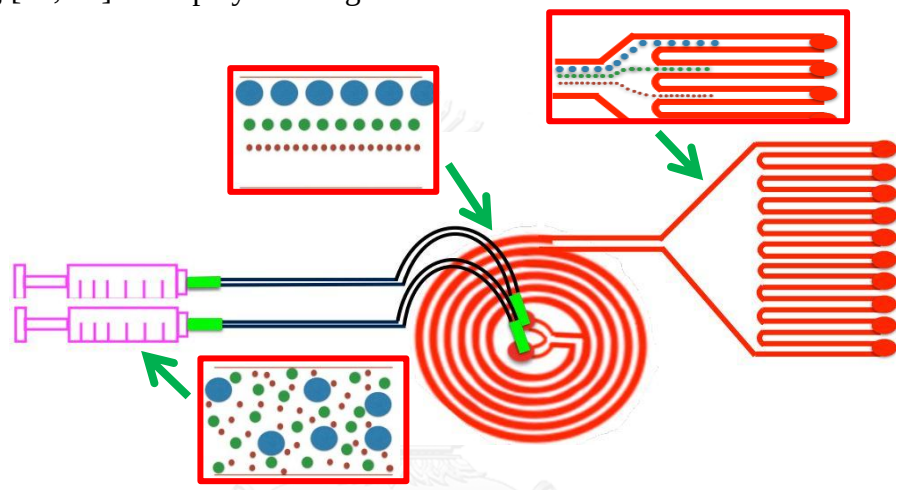

(a)

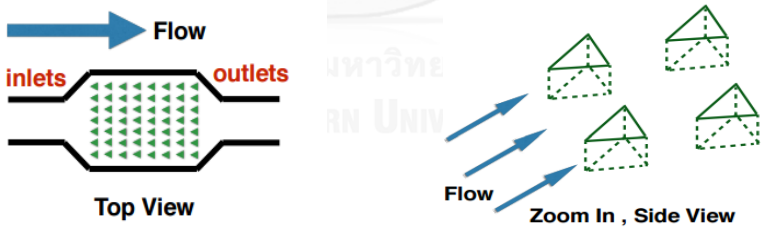

(b)

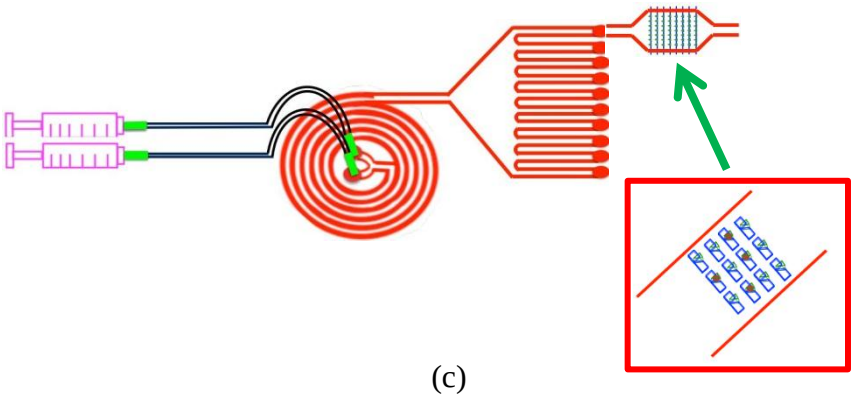

(c)

Figure 3.1 Schematic cartoon (a) Spiral chip, (b) Trapping chip and (c) Spiral microchannel and trapping method assembly

After the process of sorting technique is completed, the particles that have the exact same sizes will be moved on to the trapping device in order to separate the particles individually. This is how the sorting and trapping technique work together as displayed in Figure 3.1c.

3.1 The Sorting Chip

According to the sorting chip designing team, it is responsible for separating particle. Our research focuses on the technique of spiral microchannel. The spiral microchannel device is one of sorting techniques for a cell separation. It is a size-based passive sorting based on particle size and using geometry and hydrodynamic forces to separate particles [6, 11, 13]. The working principle of the spiral microchannel technique is that, during separation, particles are experienced by two forces in opposite directions; lift force and Dean drag force. For the lift force, it is generated due to the shear induced lift force and the wall induced lift force in a straight channel. As for Dean drag force, it is generated by the counter-rotating vortices generating due to the curvature of a spiral microchannel geometry. The magnitude of two forces are based on particle size. The bigger-size particle tends to be focused and move closer to the inner walls. [37] as shown in Figure 3.2. Furthermore, it does not require external forces that may change cell biological properties. So that, this technique would be appropriate for a cell study.

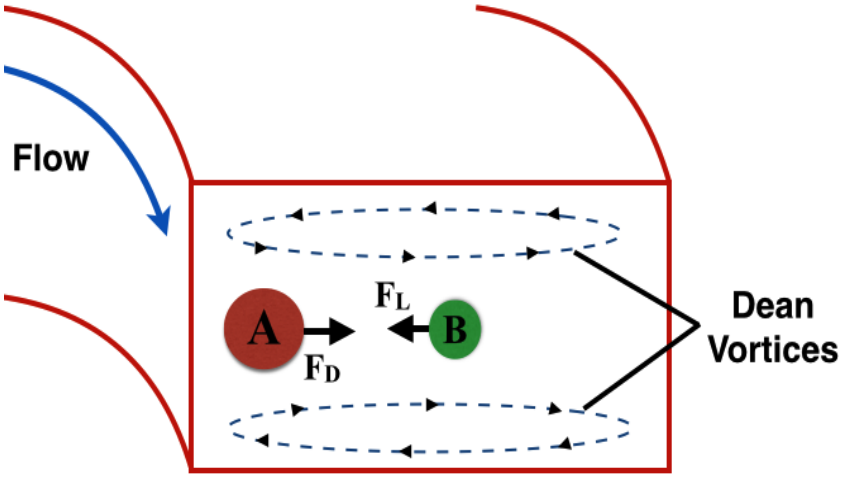

Figure 3.2 Schematic working principle of a spiral microchannel device

Additionally, this device provides several advantages such as inexpensiveness, small sample size, high throughput, portability and simplicity. Due to several advantages, the spiral microchannel device was fabricated and experimented with polystyrene beads and cancer cells in our previous study.

In the study of spirals, there are several types of spirals such as Fibonacci spiral, Fermat spiral and Archimedean spiral. As for Fibonacci spiral, it is commonly found in nature, however, it causes the drastic change in curvature which significantly leads to the reduction of Dean flows. As for Fermat spiral, the design offers weaker

downstream progression of Dean flows because the spiral runs larger in radius from inside to outside of the spiral (radius of curvature starts with larger radius and gradually decreasing in radius). Therefore, Archimedean spiral is employed in this study [36].

The main purpose of this work is to separate cells between 7-20 micrometers, find the appropriate flow rate, determine the size of the microchannels and the efficiency of the sorting device. The main advantages of this technique are: (1) external force fields are not required and (2) it has less effect on the cell property compared to other kinds of techniques. In addition, the spiral microchannel method is easy to fabricate and utilize, and provides high throughput.

3.1.1 Designing of The Sorting Chip

The setup of spiral microchannel consisted of 5 sections; syringe, silicone tube, needle, spiral microchannel, and outlets as depicted in Figure 3.3. The syringe (3ml, Nipro DISPOSABLE SYRINGE) with the length of 5.45 cm and the inner diameter of the barrel was 0.97cm mounted on the syringe pump (Chemyx Fusion Touch Series Syringe Pumps Model F200). The silicone tube with the length of 10 cm and the inner diameter of 0.05 cm were selected to transfer particles from the syringe to the spiral microchannel. The needle (20-Guage, Nipro SAFELET CATH) with the inner diameter of 0.06 cm and the length of 1.5 cm were reduced in order to connect both sides of silicone tubes. According to the spiral microchannel device, it was designed as Archimedean spiral microchannel with two inlets. The width of about 500 μm and the height of about 130 μm were fixed, the radius of curvature of about 0.75 cm and consisted of five loops. Archimedean spirals can be designed by calculating radius of curvature which is given by

$$R = r + b\theta = r + s\theta/2\pi \qquad (3.1)$$

where R is radius of curvature which is measured from the center of the channel to the inner-most wall, r is the inner-most channel radius, $b = s/2\pi$ (s is the center-to-center spacing of spiral channels), θ ($\theta=\pi/4$) is the angle between each point where radius of the loop R is calculated [36]. The device was fabricated with polydimethylsiloxane (PDMS) using the standard soft lithography method. The test was performed at the flow rate of 1 ml/min. As for the outlet, it was divided into two parts; the straight channel with the length of 10 mm with gradual expanded and the 10 outlets were designed with the width of about 200 μm and the height of about 130 μm in cross section.

The device was developed and modified the size of microchannels based on the ratio of particle size and the height of the microchannel. After many trials, the common finding is that the ratio (a_p/h) should be > 0.07 in order to separate particles more efficiently and effectively. Moreover, the cancer cells were used as experimental particles (10-12 micrometers) with about 40,000 cells/ml at the flow rate of 1.0 and 1.5 ml/min. Before the actual experiment was carried out, polystyrene was used for chip functionality test.

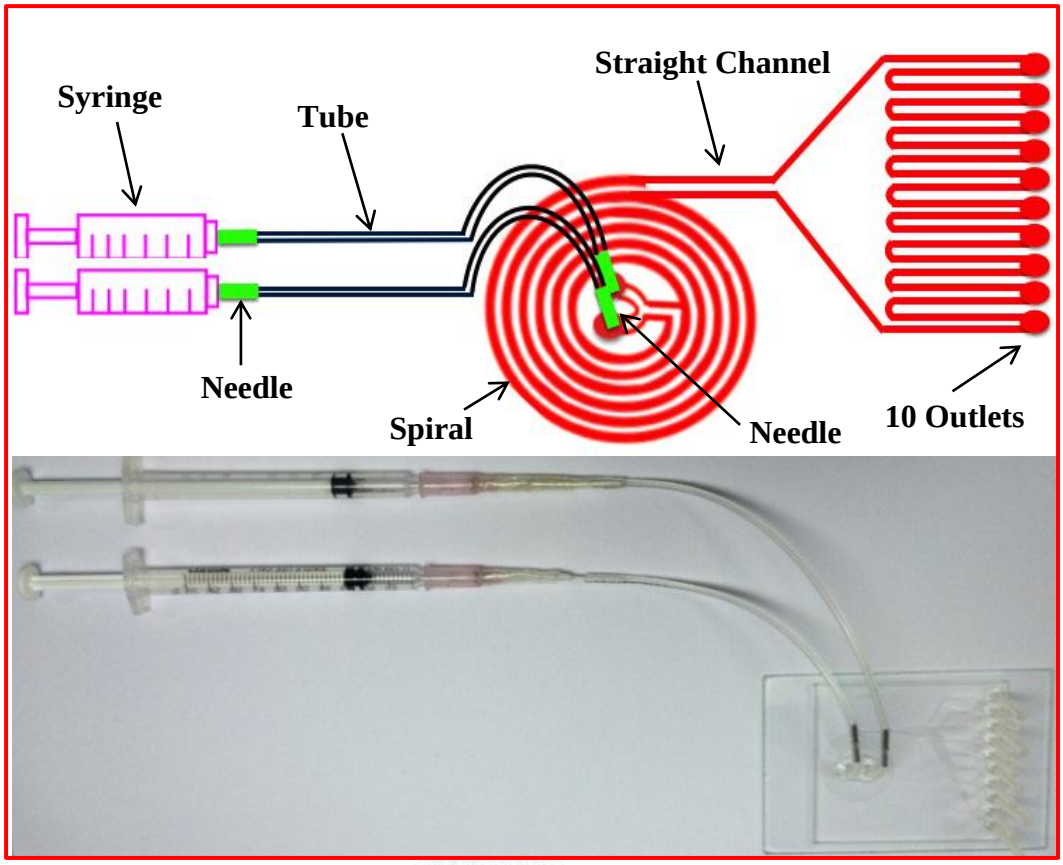

Figure 3.3 Schematic drawing and actual spiral chip image; i.e. syringe, silicone tubes, needle, spiral microchannel and outlets.

3.1.2 Outcomes of The Sorting Chip

Apparently, the device worked functionally and was able to separate different sizes of particles very well. However, some cells were deformed, torn apart and died after experimenting. It was estimated about 50% of live cells (Figure 3.4). This happened probably due to shear flow and extensional flow during the separation. Another problem was that the shearing and stretching force could not be measured directly in certain areas. Thus, the computational simulation software, COMSOL Multiphysics, was implemented to this investigation with various conditions as well. The loss of cell viability from our previous experiment encouraged us to do more researches and investigate the effects of shear and extensional stress on cell viability.

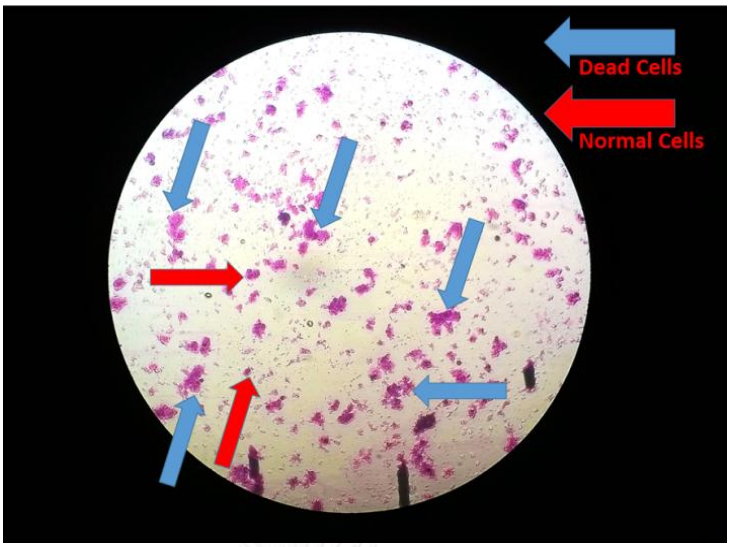

Figure 3.4 Demonstration of dead and live cells under a light microscope with Dip Quick Stain in the previous experiment[38].

3.2 The Trapping Chip

The trapping chip allows us to analyze and observe the behavior of particles. The general goal of trapping study is to immobilize particles in wells as shown in Figure 3.5 and then observe their degree of freedom and cell division. In this work, we focused on finding important parameters and the efficiency of a single cell trapping in wells. After designing and experimenting with several shapes of wells, it was found that an equilateral triangle is able to create a vortex that helps particles go down into traps easily.

3.2.1 Designing of The Trapping Chip

In the experiment, a trapping device with a length of 1,000 μm, a width of 100 μm and a height of 70 μm were fabricated. As for an triangle well, it was decided to fabricate different size of equilateral triangle well with each side was about 40 μm and another was 60 μm with varying 15, 30 and 45 μm in well's depth. Polystyrene beads and white blood cells (WBCs) were selected as experimental particles for chip functionality test. Additionally, a syringe pump was used to generate a fluid flow and a controlled flow rate of about 0.1 and 0.3 ml/hr in the main channel. It was found that the appropriate flow rate that could trap particles efficiently would be 0.1 ml/hr. The appropriate velocity to trap particles should be around 600-900 μm/s because the trapping efficiency depends on the velocity of flow.

3.2.2 Outcomes of The Trapping Chip

The consequences of this experiment indicated that the well of 40 μm with the depth of 30 μm had the highest efficiency of a single cell trapping. It was approximately 21% for polystyrene beads with the concentration of 1.8×10^5 beads/ml and 20% for WBCs with the concentration of 3×10^5 cells/ml at the flow rate of 0.1 ml/hr. As demonstrated, these numbers, the conclusion can be made that the

appropriate flow rate should be about 0.1 ml/hr and the velocity should be around 600-900 μm/s. Otherwise, the efficiency of trapping will decrease significantly because most of particles tend to float across the wells if the flow rate is too high or adhere to the channel wall if the flow rate is too low. Once the particles are trapped the next step is to release particles out of the well in order to further analyze a single cell.

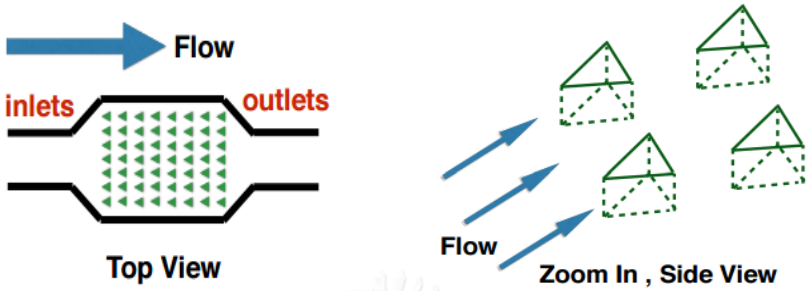

Figure 3.5 Schematic picture of trapping method

3.3 The Cell Releasing Chip

After trapping an individual particle completely, the releasing technique is used to release selected particles out of the wells. Nowadays, there are a few methods that can release cells out of wells. In this project, the releasing device needs to be designed in order to complete three main activities of our Microfluidic chip.

The releasing technique is very new designing, thus there exists little research about it. Because of this, it will be highly challenging to fabricate this device successfully. Among various techniques, flowing-fluid mediated detachment is chosen because it does not require external forces. This device mimics the nature of the mechanisms in the human body. This reason offers a great benefit to maintain cell viability and its properties.

In order to reduce a risk of failure in experiment and fabrication, computational software is needed to simulate the behavior of flow in the main and buffer channels. A computational software in which cells were modeled as solid particles, was employed in order to help examine flow behavior—streamlines, pressure, velocity distributions and total force. They were found under various flow rates. The aim of this study is to find the appropriate flow rate in the buffer channels— generating force as equal to the particle weight—as well as to examine the devices' feasibility for immobilizing and releasing. For full information of releasing device research see Chapter 6.

The above-mentioned reasons reinforce our convictions that the releasing technique will become a great discovery and help clearly analyzing cancer diseases that results in the abnormality and the change of cell biology in both animals and humans.

Chapter 4

Improving of Cell Viability

According to the previous study, it was found that the spiral setup could separate different sizes of particles successfully. However, about 50 percent of cells were dead during the process of cell separation and majority of cell death occurred in a syringe about 40%. This encouraged us to do more research and investigate cell viability and the causes of cell death. The past studies stated that stresses affect viable cells. Therefore, we focused on the studies of stresses (shear and extensional stresses) using computational software along with using different methods of experiments to test live and dead cells including Trypan Blue stain, SEM and Wright's stain.

4.1 The Studies of Shear Stress and Extensional Stress

In the past studies, shearing force emerged as a significant player in cell viability because they directly affected cell physical property. This drew a great attention of cell survival in the field of microfluidics. As our previous study, it was found that there was a possibility for cells to be damaged by shear stress in the spiral setup including syringe, needle, tube and spiral microchannel. However, recently, the study of Aguado demonstrates that extensional stress is another factor affecting viable cells beside shear stress. As reported by the study of Aguado, it suggests that extensional stress occurs when there is an abrupt change in cross section. This abrupt change from the syringe to needle causes a significantly increase in linear velocity [32]. In this conceptualization, the critical area where cells has a great potential to die is between syringe and needle as displayed in Figure 4.1. In this work, it was decided to investigate extensional and shear stress in the setup of spiral microchannel including syringe, needle, silicone tube and spiral microchannel. According to the simulation of syringe, the syringe of Hamilton Gastight High-Performance Macro Syringe with the volumes of 1, 2.5, and 5 ml were simulated to identify the critical areas inside the device where cells would be damaged due to shear and extensional stresses. For the needle and a silicone tube, it was designed as a 22G needle and a 20 cm tube with 0.02 inches in inner's diameter. For the spiral, it was simulated with the width and height of about 500 and 130μm consisting of a straight channel and 10 outltes.

As simulated from computational software, extensional and shear stress in varying syrings (1, 2.5 and 5 ml) were calculated with controlled sample and the flow rates 8 ml/min and then compared to the actual experiments with three methods—Trypan Blue, SEM and Wright's stain. These three methods allow us to observe cell viability, normal cells and degeneration and then calculate how many cells could survive after experiencing extensional stress, shear stress and exposure time in each accessory of spiral's setup. The investigation of cell viability in each accesory including syringe, needle, tube and spiral and the whole setup of spiral microchannel were examined and compared of each method as well. Summary and suggestion of how to reduce a risk of cell death and improve cell viability will be described in the last chapter.

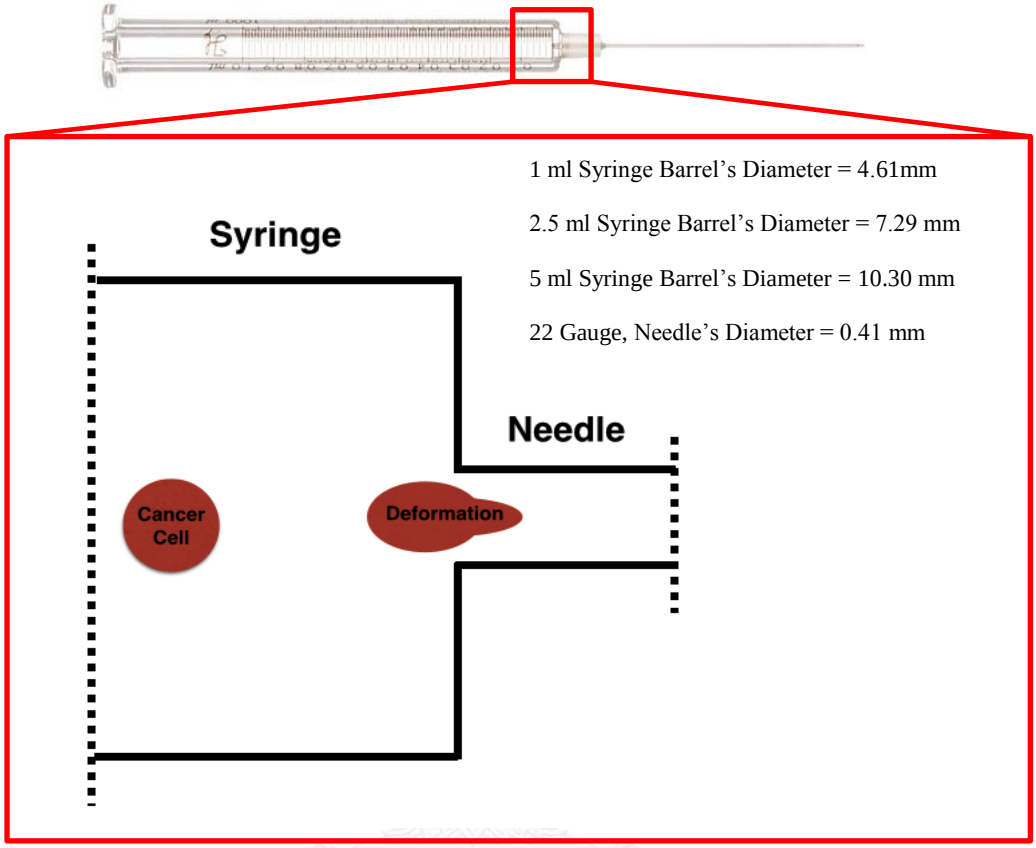

Figure 4.1 Schematic of abrupt changing in cross section between syringe's barrel and needle (not draw to actual scales)

4.2 Conditions and Properties of Simulation

4.2.1 Simulation of Flow in Syringe

4.2.1.1 Materials and Properties

This simulation particularly focused on stresses in a syringe. The medium was assumed to be PBS as it has been studied in the past with density of 998 kg/m^3 and viscosity of 0.00105 Pa•s and the flow was considered as laminar flow. Furthermore, the steady state for incompressible fluids was defined. The temperature was set at 293 K. The inlet flow was defined as a uniform flow and the pressure at the cross section of the outlet was uniform as well.

4.2.1.2 Geometry and Boundary Conditions

The glass syringe of Hamilton Gastight High-Performance with the volumes of 1, 2.5 and 5 ml were simulated from the actual syringes as shown in Table 4.1. In

addition, there is no slip boundary condition for the walls. The behavior of fluid was Newtonian fluid in which dynamic viscosity was constant at all rates of shear.

Table 4.1 Dimension of actual syringes of 1, 2.5 and 5 ml

Syringe's Volume (ml)	Barrel's Length (mm)	Barrel Inner in Diameter (mm)	Needle's Length (mm)	Needle inner in Diameter (mm)
1 ml	59.89	4.61	51	0.41
2.5 ml	59.87	7.29	51	0.41
5 ml	59.97	10.30	51	0.41

2D Axisymmetric simulation was used to reduce computational time consuming. Geometry of syringe was created as two rectangle unionized (Figure 4.2a) and used the revolving function. Furthermore, Corner Refinement and Distribution were selected to add more meshes in specific areas to provide more accurate data (Figure 4.2b). Furthermore, mesh convergence criterion independent was applied to find an optimum grid size of which the maximum and minimum element size were 10.16 and 1.016 μm as well as validating the results of force from Aguado's study [32]. The final number of meshes were about 15-20 millions.

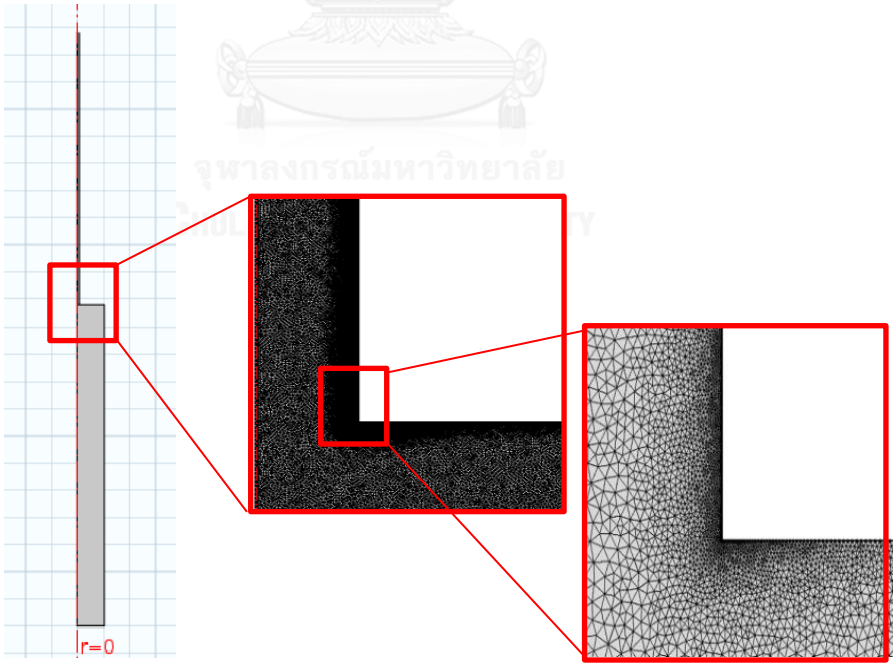

(a) (b)

Figure 4.2 The picture of (a) Geometry of syringe (b) Corner Refinement and Distribution function

4.2.1.3. The Computational Results in Syringe

The results illustrated that the maximum magnitude of extensional stress for elongating body and the minimum magnitude for shortening body of 1, 2.5 and 5 ml syringe had similar magnitude at the same flow rate of 1 ml/min. Among these conditions, the 5 ml syringe at 8 ml/min generated an extremely extensional and shear stress (Table 4.2).

Table 4.2 General summarization of the maximum and minimum of extensional and shear stress in the 1, 2.5, and 5 ml syringe

Volume of Syringe	Maximum Extensional Stress (Pa)	Minimum Extensional Stress (Pa)	Maximum Shear Stress (Pa)	Minimum Shear Stress (Pa)
1 ml at 1 ml/min	54	-2	24	0
2.5 ml at 1 ml/min	48	-2	21	0
5 ml at 1 ml/min	51	-2	25	0
5 ml at 8 ml/min	1519	-62	558	0

In addition, wall shear stress in a 20 cm silicone tube was calculated from Eq. (2.10) (Q is 1 ml/min, μ is 0.00105 Pa·s and d is 0.508 mm) that was about 1.36 Pa at the flow rate of 1 ml/min and the exposure time about 1 s (exposure time was calculated, i.e. 20 cm/0.2 m/s ≈ 1 s) and the wall shear stress significantly increased to 10.87 Pa at the flow rate of 8 ml/min increased with the exposure time of 1 s.

As the above demonstration, the extensional stress at the corner of abrupt change in cross section of 1, 2.5, 5 ml at the same flow rate of 1 ml/min displayed that they had the similar magnitude of shear and extensional stress in general as depicted in Figure 4.3 and 4.4. However, for the syringe of 5 ml, the shear and extensional stress were dramatically increased when the flow rate was increased as well. This showed that increasing flow rate by 8 times, the shear stress increased by 23 times and extensional stress increased about 30 times compared to the extensional and shear stress at flow rate of 1 ml/min. In the other words, increasing flow rate, magnitude of extensional stress was higher than the magnitude of shear stress in comparison of the same flow rate. In addition, in the case of maximum stresses, extensional stress tended to be extented inside the needle's walls whereas, shear stress tended to be expanded beside the barrel's walls as shown in Figure 4.3d and 4.4d. In conclusion, increasing flow rate had higher stresses of both extensional and shear stress rather than increasing the volume of syringe.

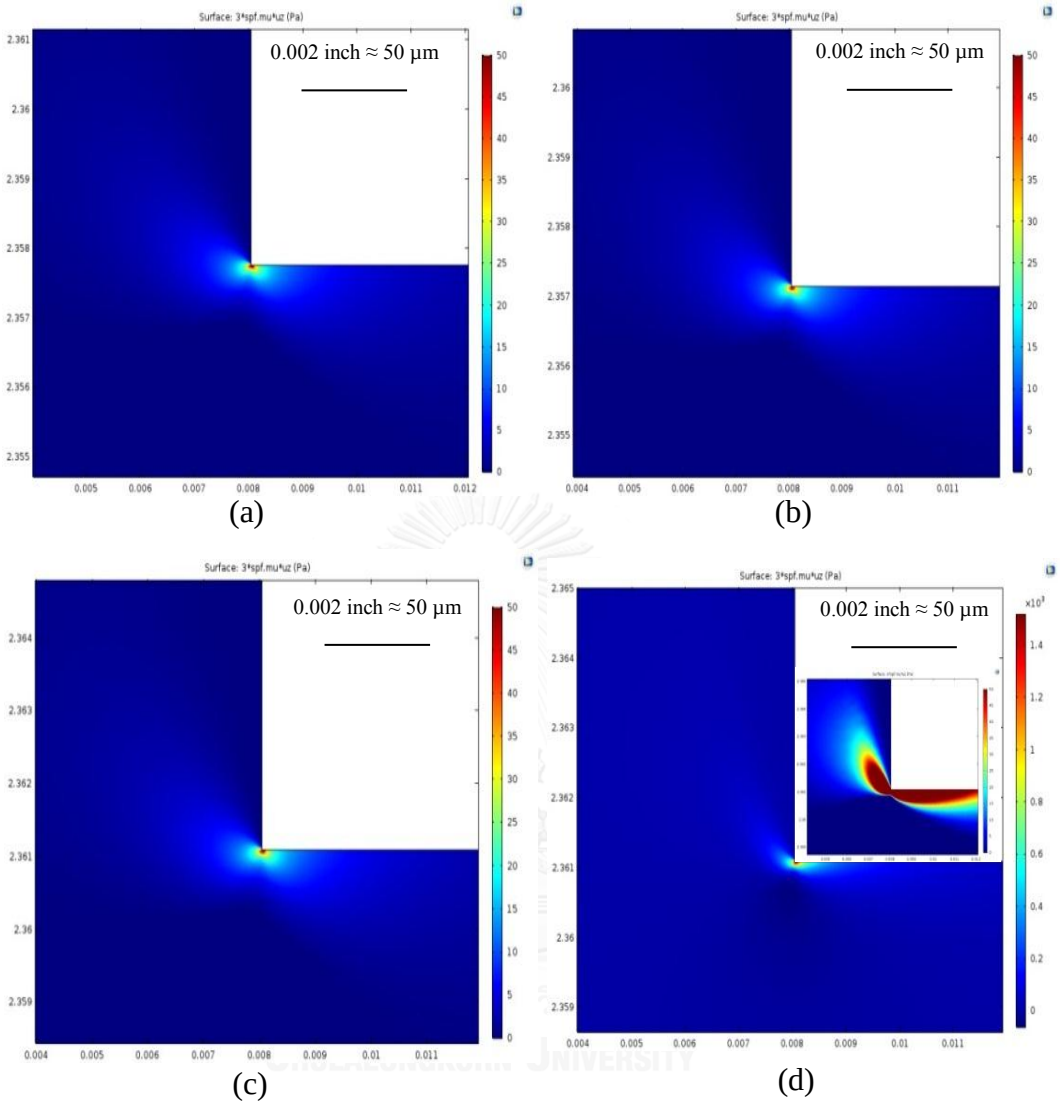

Figure 4.3 Extensional stress at the abrupt change (a)1 ml syringe, 1 ml/min (b) 2.5 ml syringe, 1 ml/min (c) 5 ml syringe, 1 ml/min and (d) 5 ml syringe, 8 ml/min

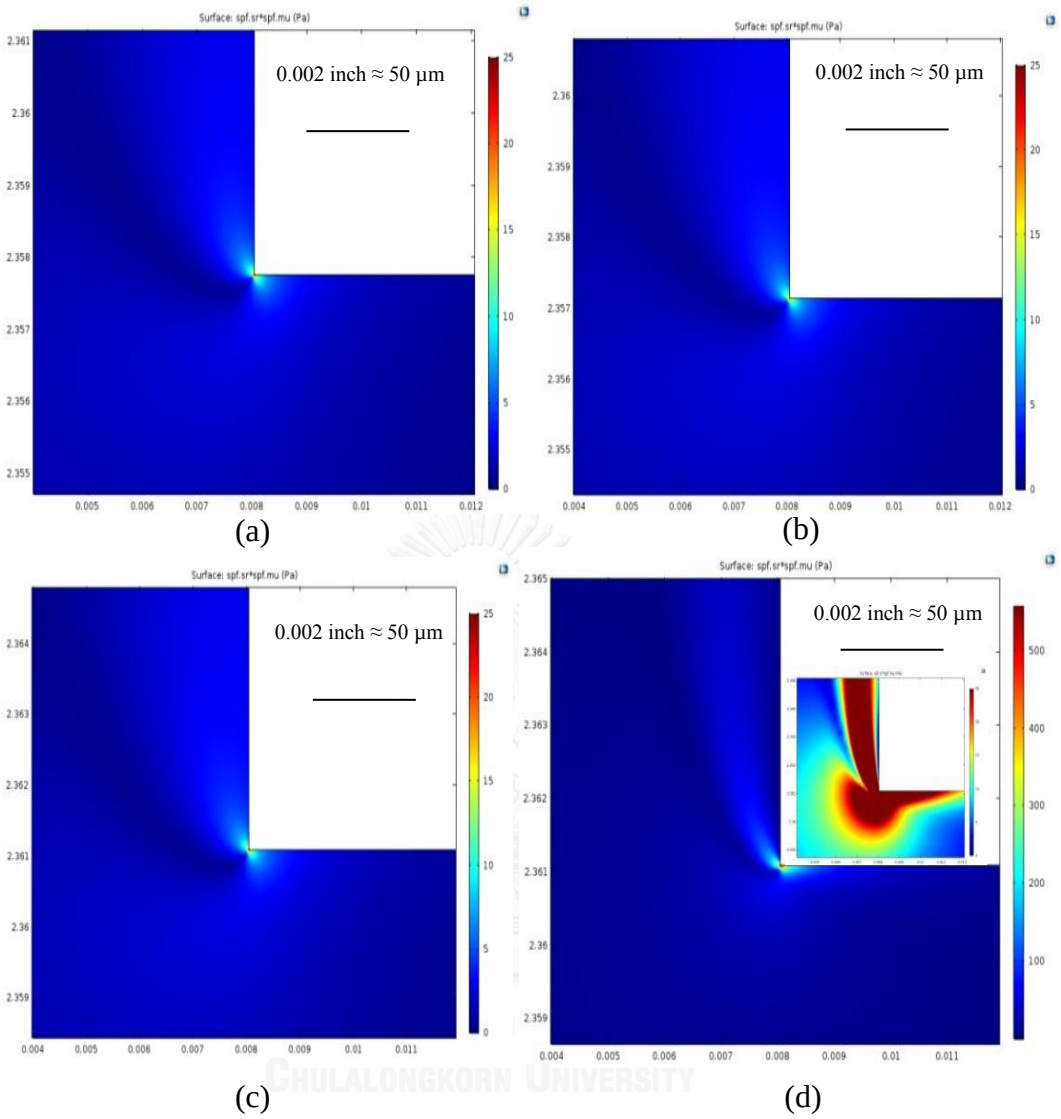

Figure 4.4 Shear stress at the abrupt change (a)1 ml syringe, 1 ml/min (b) 2.5 ml syringe, 1 ml/min (c) 5 ml syringe, 1 ml/min and (d) 5 ml syringe, 8 ml/min

4.2.2 Simulation of Flow in Microchannels

4.2.2.1 Materials and Properties

Three dimensional simulation and single-phase flow were selected. The medium was assumed as water with density of 998 kg/m^3 and viscosity of 0.00105 Pa·s. The behavior of fluid was Newtonian fluid in which dynamic viscosity was constant at all rates of shear. The steady state for incompressible fluids was defined. The temperature was set at 293 K. The inlet flow was defined as a uniform flow and the pressure at the cross section of the outlet was uniform as well.

4.2.2.2 Geometry and Boundary Conditions

The flow in the syringe's inlet was defined as a uniform flow. For the spiral microchannel, it was designed only 1 loop due to computational limitation and time consuming (Figure 4.5a). The inlet of the spiral microchannel was defined as a velocity component (normal to the inlet). The outlets were modeled into two parts; the straight channel that was designed with the length of 10 mm to allow the flow to be fully developed and the outlet that separated into 5 outlet channels which the symmetry was used to reduce computational time consuming (Figure 4.5b). The simulation was found to be grid-independent as well as controlling mesh was chosen to define more numbers of meshes in certain areas. Finally, mesh convergence criterion independent was applied to find an optimum grid size after increasing meshes. The maximum and minimum element size for spiral microchannel were 15.6 and 1.01 µm and for straight channel and outlets were 25 and 2.5 µm. The final numbers of meshes were about 3-5 millions.

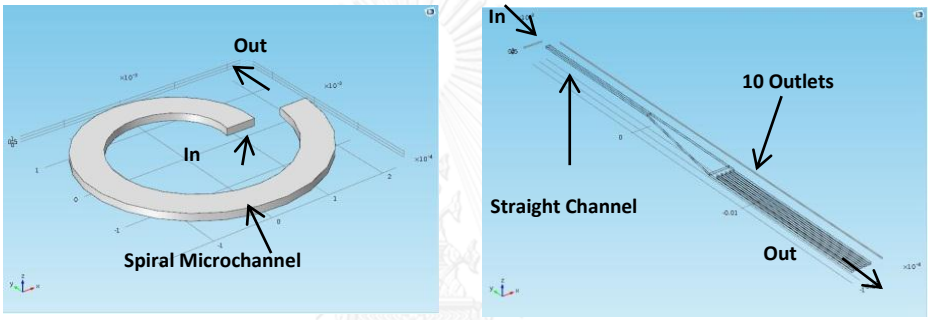

(a) (b)

Figure 4.5 Simulation domain for each component in the setup; (a) Spiral microchannel and (b) Straight channel and 10 outlets with symmetry walls.

4.2.2.3 The Computational Results in Spiral Microchannel

The simulation demonstrated that at the flow rate of 1 ml/min, the maximum shear stress of spiral, straight channel and outlets were about 15, 12 and 5 Pa, respectively, as illustrated in Table 4.3. For the average shear stress, it was evaluated that spiral microchannel, straight channel and outlets were about 6.85±3.73, 6.09±3.44 and 2.25±0.85 Pa, respectively. As evidenced, the highest shear stress occurred close to the surface of walls, especially in the spiral microchannel where the maximum shear stress was about 15 Pa and the average was 6.85 Pa as exhibited in Figure 4.6a. This showed that there was a great potential for cells to be damaged in spiral setup.

Table 4.3 General summarization of the maximum, minimum and average of shear stress in the spiral components

Components	Maximum Shear Stress (Pa)	Minimum Shear Stress (Pa)	Average Shear Stress (Pa)
Spiral	15	0	6.85±3.73
Straight Channel	12	0	6.09±3.44
Outlets	5	0	2.25±0.85

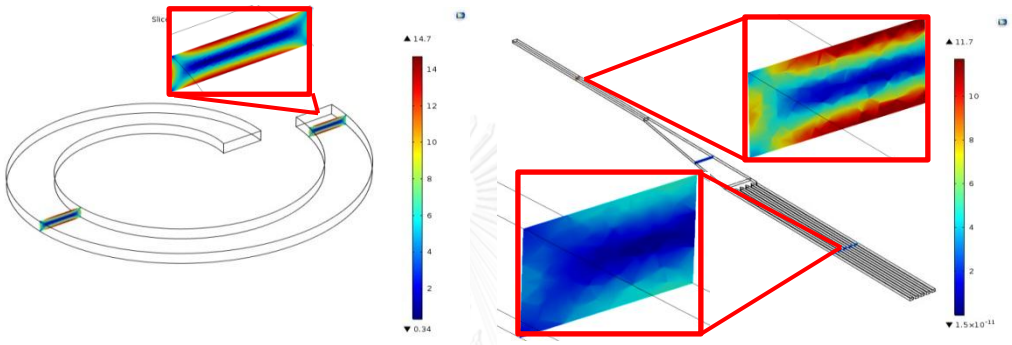

(a) (b)

Figure 4.6 Contour of wall shear stress and inside of (a) spiral mrochannel and (b) straight and 10 outlets

4.3 Experimental Conditions

We investigated the effect of extensional stress, shear stress and exposure time through each accessory in the spiral setup including the syringe, needle, silicone tube and spiral microchannel by counting viable cells on hemocytometer and then calculate the percentage of cell viability. The experiments were divided into 3 cases to test cell viability by a) increasing the volume of syringe and flow rates, b) increasing volume of syringe with connected with a 20 cm tube and c) testing cell viability with the whole setup of spiral.

Numbers of live cells were counted in controlled sample (cell suspension) right away after obtaining cell suspension. After that, we loaded cell suspension in a device and expelled the sample through the device and then took the sample from outlet to count cell viability on hemocytometer. All experiments were examined in 1-2 hours in order to reduce a risk of cell aggregation.

According to the first case a, extensional stress was examined by increasing the volume of syringes—1, 2.5 and 5 ml. Each size of syringe was examined and compared to controlled sample. For example, controlled smaple versus 1 ml syringe at 1 ml/min, controlled smaple versus 2.5 ml syringe at 1 ml/min and controlled smaple versus 5 ml syringe at 1 ml/min and 8 ml/min.

For the second case, the experiments were examined with 1, 2.5 and 5 ml syringes connected with a 20 cm silicone tube to test the impacts of extensional stress, shear stress and exposure time on cells viability in a long tube. The experiments were examined at the same flow rate of 1 ml/min.

For the final case, the whole setup of spiral was investigated in terms of cell viability. Live cells collected in the first three channels—1st, 2nd and 3rd were counted and compared to controlled sample.

In this work, unhealthy canine blood was donated from Small Animal Teaching Hospital, Faculty of Veterinary Science Chulalongkorn University and we took only white blood cells (WBCs) to examine as experimental particles. Every experiment was examined for 3 sets to ensure that we would receive accurate and precise data. The total experiments were about more than 50 sets in total as seen in Figure 4.7. In addition, we also investigated the effects of different types of suspension media—DI water was examined with Trypan Blue and SEM. For more information about results see Appendix D.

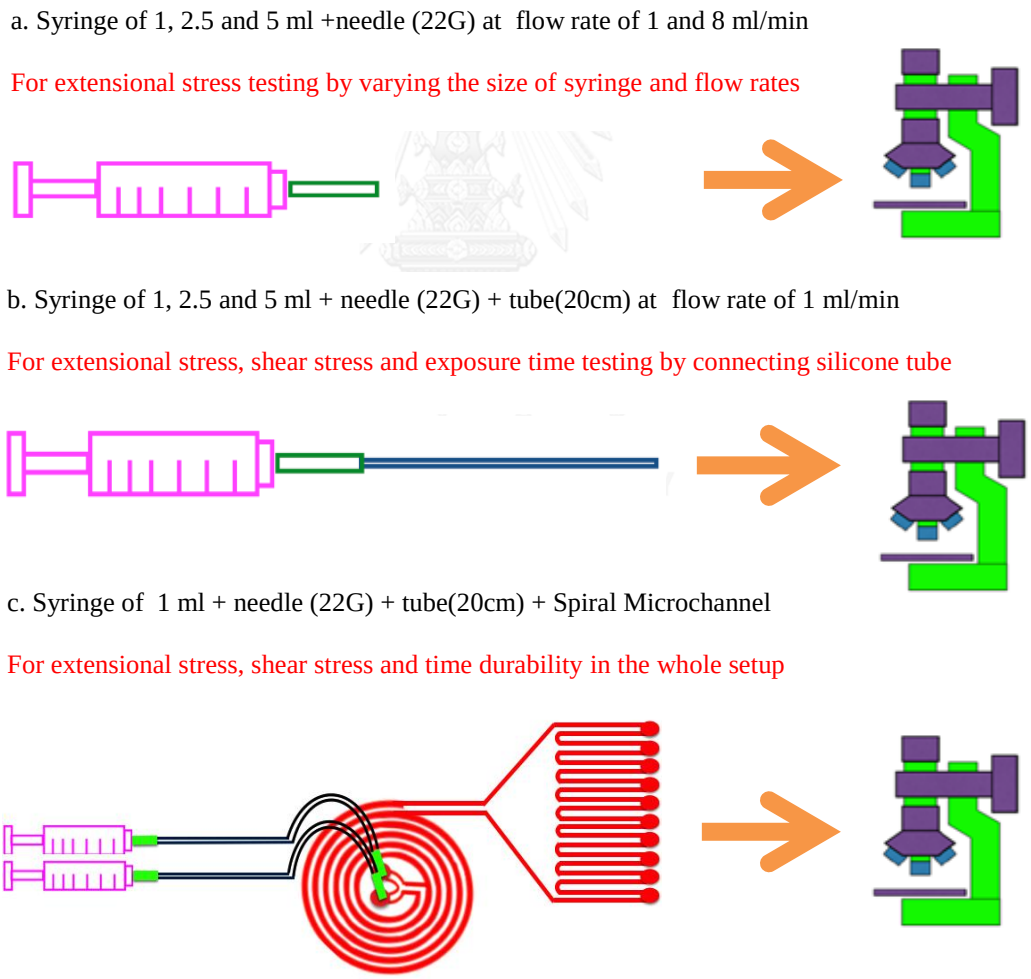

Figure 4.7 The plans of examining cell viability; (a) extensional stress testing (b) shear stress testing and (c) a whole setup of spiral microchannel

To investigate cell viability as well as normality and degeneration, three techniques including Trypan Blue stain, SEM and Wright's stain were employed. As for SEM and Wright's stain technique, only controlled sample and 5 ml syringe at the flow rate of 8 ml/min in which cells died the most were investigated in terms of normality and degeneration based on their morphology and main stuctures—nucleus, cytoplasm and cell membrane. The results of these technique will be compared each other in the last section.

4.4 Trypan Blue Stain For Cell Viability Study

The main method to test cell viability that we chose was a light microscope with Trypan Blue. In this section, we will describe the pre-preparation of cell counting by using hemocytometer, vital dye (Trypan Blue) and how to count cells on hemocytometer briefly and properly.

4.4.1 Hemocytometer

Hemocytometer (Blood Counting Chamber-Neubauer Improved and Cover glass) was used for cell enumeration. Hemocytometer and coverglass had to be cleaned up with DI water and alcohol before performing the experiments every time as displayed in Figure 4.8. After cleaning up the hemocytometer and coverglass, a sterile wiper was needed to dry up both of them. For full information for cell enumeration protocols, see Appendix B.

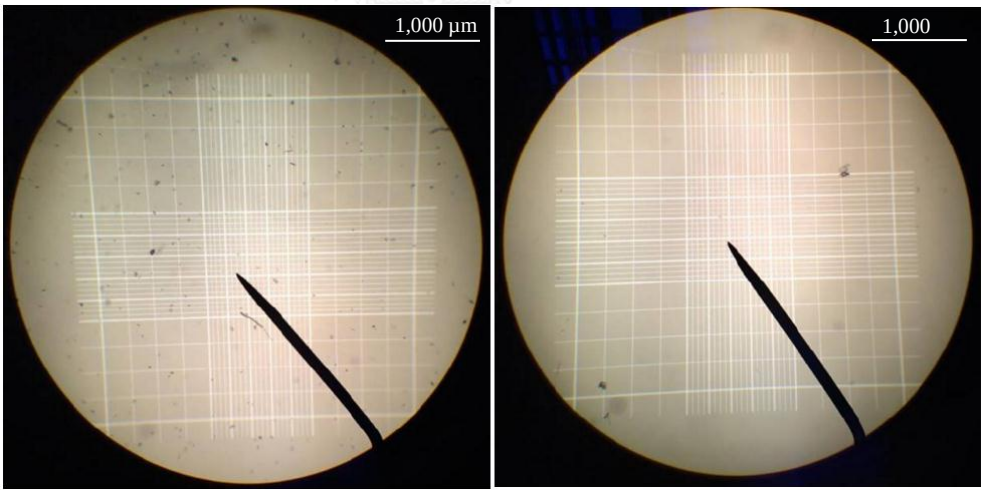

Figure 4.8 Hemocytometer (a) cleaning up with a regular towel and (b) cleaning up by a sterile wiper with DI water and alcohol.

4.4.2 Vital Stain

Trypan Blue (TB) assay was performed as a vital stain to check dead cells and viable cells. In this experiment, the initiated concentration of our trials were about 1×10^6 cells/ml. For full information for cell suspension protocols see, Appendix A. In the experiments, Trypan Blue was diluted by PBS in the ratio of 1:10 in order to see particles and grids more clearly on hemocytometer.

4.4.3 Protocols of Cell Enumeration

The cell suspension was drew up by a pipette (100/1000 µm) and dispensed liquid between hemocytometer and coverglass for 10 µl on both sides of hemocytometer. The images were viewed under the microscope at 40x magnification.

As demonstrated from the microscope, live cells were appeared as bright feature in circle, whereas dead cells were appeared as a blue feature in circle. This because dead cells absorbed Trypan Blue but live cells did not as shown in Figure 4.9.

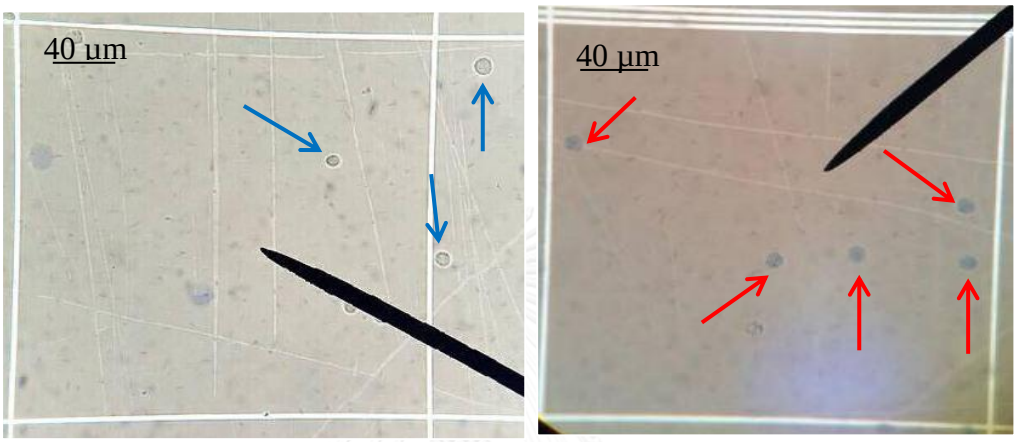

(a) (b)

Figure 4.9 Cell features were observed under a light microscope (a) live cells and (b) dead cells

4.4.4 Determine the number of cells

A hand tally counter was used for counting numbers of live and dead cells. After we obtained the numbers of live and dead cells, we was able to estimate how much cells were survive in terms of the percentage of cell viability (viable cells×100 divided by total cells in 4 main areas—each area consists of 16 small areas). For more information for cell enumeration and formula, see in Appendix B. In this experiment, cell suspension was counted repeatedly for 3 sets and the initiated concentration was about 1×10^{6} cells/ml. In every experiment of using Trypan Blue, all samples and Trypan blue were mix together in the same among of volume for 5 minutes to allow dead cells to appear as a blue circle more clearly.

4.5 Experimental Results

The experiment got started with the technique of Trypan Blue. Cell viability was counted by a light microscope with Trypan Blue at the room temperature of 25 degree Celsius. Moreover, Scanning Electron Microscopy (SEM) investigated the samples in terms of cell morphology. This technique allowed us to observe cell's surface as normal cells or degenerated cells. Finally, Wright's stain also investigated cell's structures including cell membrane, cytoplasm, nucleus and etc. In order to reduce a risk of confusion, normal cells would be defined as a circle shape and

consisting of three main structures—cell membrane, cytoplasm and nucleus. Whereas, cell degeneration would be defined as cell missing one of three main structures or being deformed severely.

4.5.1 Experimental Results by Trypan Blue

Before counting cells on hemocytometer, Trypan Blue and cell suspension were withdrawn 0.5 ml each and were mixed well into a 2 ml centrifuge tube by a bioshaker for 5 minutes in order to allow Trypan Blue to appear more clearly in dead cells. After that, cell suspension (controlled sample) was counted on hemocytometer. The reason why we counted cell viability in the controlled sample first because we could count cell viability in the controlled sample and checked initiated concentration at the same time. The next step was to load cell suspension into a syringe and then counted cell viability after the sample passing through the syringe and mixed with Trypan Blue for 5 minutes. In this experiment 1, 2.5 and 5 ml syringe were examined and compared to each controlled sample at the flow rate of 1 and 8 ml/min.

As can be seen from the data in Table 4.10-4.12, it presented that increasing the volume of syringes—1, 2.5 and 5 ml—or increasing flow rate from 1 to 8 ml/min had no effects on cell viability. Due to the data from simulation illustrated that the syringe of 1, 2.5 and 5 ml with increasing flow rates from 1 to 8 ml/min, extensional stress and shear stress increasing from 50 to 1,500 Pa and 25 to 550 Pa and exposure time was about 0.04 ms (exposure time was calculated, i.e. 4×10^{-6}m/0.1 m/s $\approx$ 0.04 ms). The percentage of cell viability showed that numbers of live cells in each case was about 90-99% compared to their controlled samples

For the second case, syringe of 1, 2.5 and 5ml connected with a 20 cm tube at the same flow rate of 1 ml/min were investigated. The experiment started with counting cell viability in controlled sample first and then loaded cell suspension in syringe 1 ml and counted cell viability after the sample passing through the syringe of 1 ml and then examined with 2.5 and 5 ml syringe, respectively

The results of the percentage of cell viability with varying volumes of syringes 1, 2.5 and 5 ml had the similar numbers. They were approximately 90-99% at the same flow rate of 1 ml/min as shown in Figure 4.13. Due to the data from simulation showed that the syringe of 1, 2.5 and 5 ml generated maximum extensional stress about 50 Pa, shear stress about 0 and exposure time about 0.04 ms (exposure time was calculated, i.e. 4×10^{-6}m/0.1 m/s $\approx$ 0.04 ms). For shear stress in the tube, it was calculated that maximum shear stress occurred close to the tube's wall about 1.36 Pa with exposure time about 1 s (exposure time was calculated, i.e. 20 cm/0.2 m/s $\approx$ 1 s). The results showed that increasing volume of syringes by connected with a tube in the second case (Figure 4.13) or disconnected with a tube in the first case (Figure 4.10-4.12), they had no effect on cell viability as well.

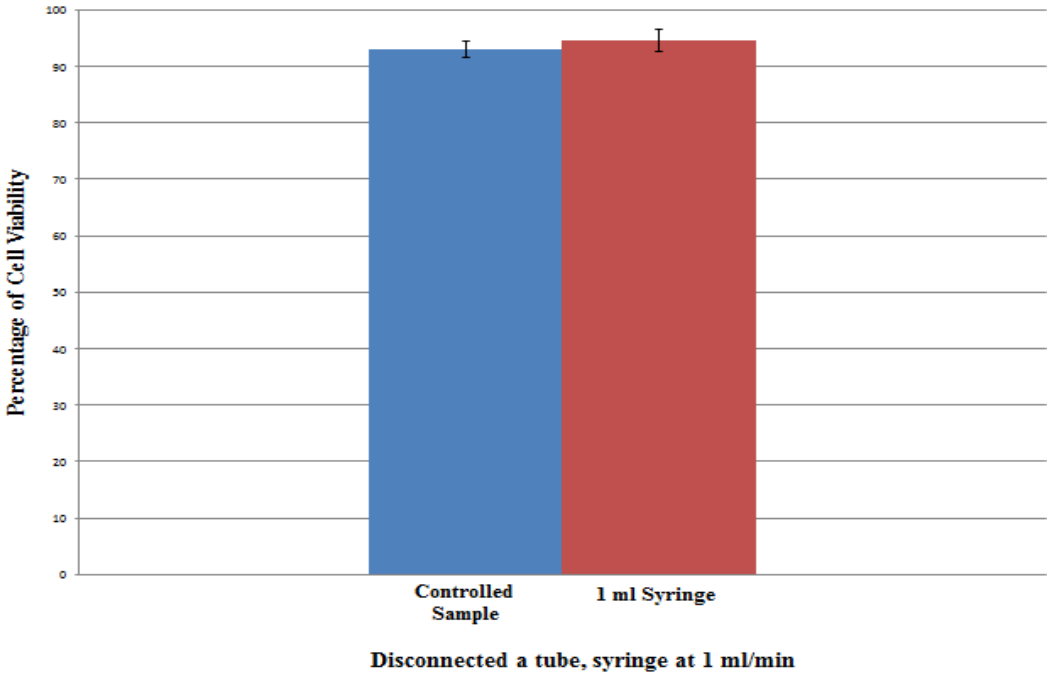

Figure 4.10. Percentage of cell viability of controlled sample compared to 1 ml syringe at 1 ml/min

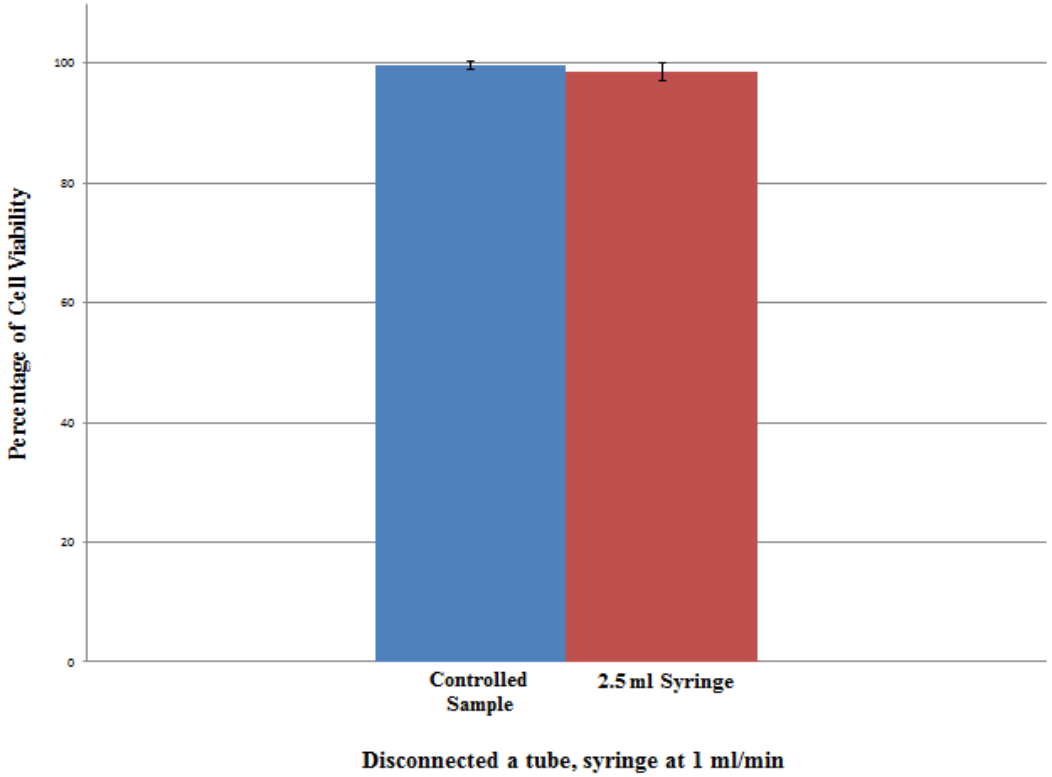

Figure 4.11 Percentage of cell viability of controlled sample compared to 2.5 ml syringe at 1 ml/min

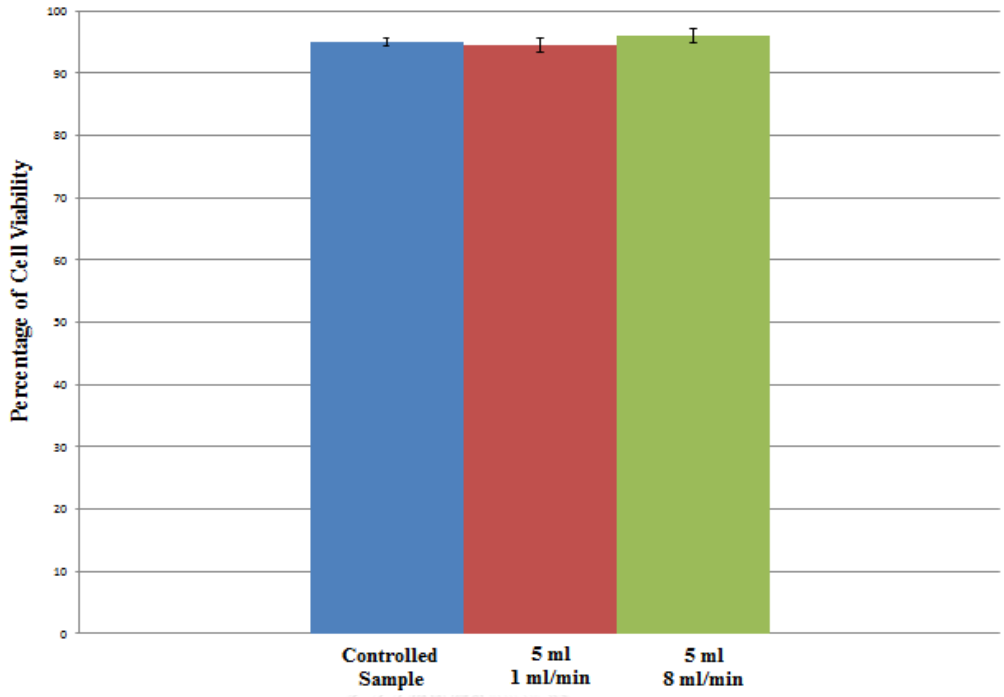

Figure 4.12 Percentage of cell viability of controlled sample compared to 5 ml syringe at 1 and 8 ml/min

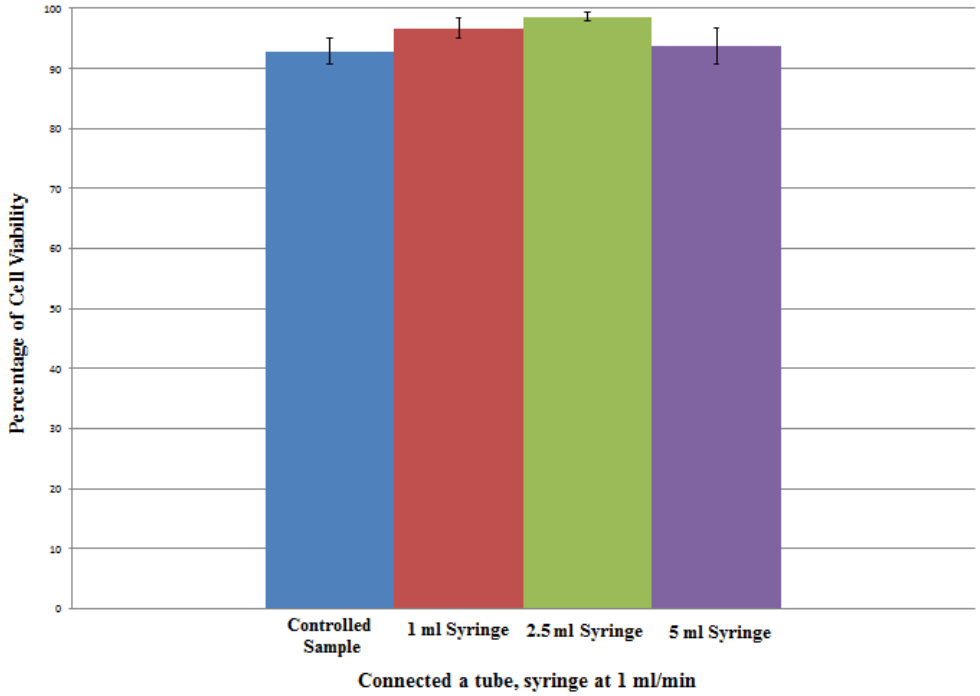

Figure 4.13 Percentage of cell viability of controlled sample compared to 1, 2.5 and 5 ml syringe at 1 ml/min and connected with a 20 cm tube

4.5.2 Experimental Results by Scanning Electron Microscopy

After testing viable cells with Trypan Blue, it was found that percentage of viable cells was about 90-99% under a light microscope with Trypan Blue. However, Scanning Electron Microscopy allowed us to observe 3D images of the samples by scanning with beam of electrons. For full information about sample preparation protocols, see in Appendix A. In this work, normal cells and degenerated cells were examined by scanning electron microscopy for two cases—using 5 ml syringe at the flow rate of 8 ml/min compared to controlled sample. In this experiment, normal cells were considered as a circle shape (Figure 4.14) whereas, cell degeneration was considered as severe body deformity (Figure 4.15).

The experiments of SEM started with collecting both of samples—the controlled sample and the sample of 5 ml syringe at the flow rate of 8 ml/min—for 0.5 ml into a 2 ml centrifuge tube and then dropped the sample on the specimen stub and fixed both of samples by fixative (For more information about fixation, see Appendix A). After that, the SEM protocols including—drying, coating and image processing—took about a couple of days to finish. In this experiment, 20 images were taken for 2 sets and counted the numbers of normal cells and degenerated cells by observation and then calculated the percentage of each case. The results presented that in the case of controlled sample, there was normal cells about 86% while 5 ml syringe at the flow rate of 8 ml/min, normal cells were reduced slightly to 76% as shown in Figure 4.16. Therefore, the case of maximum stress which generate maximum extensional and shear stress about 1519 and 558 Pa with exposure time about 0.04 ms, normal cells was decreased about 11.62% by scanning electron microscopy.

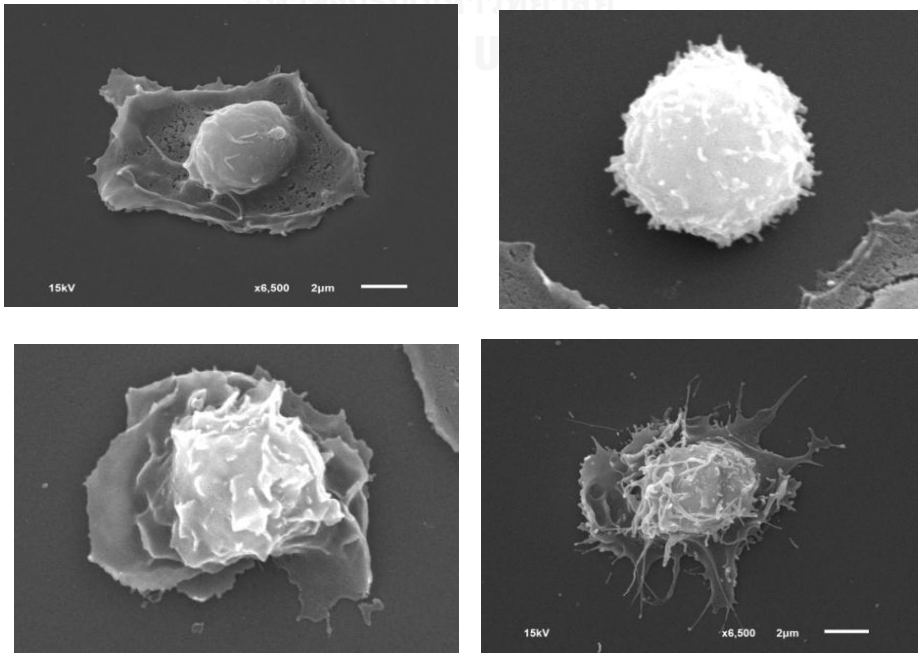

Figure 4.14 Normal cells observed using SEM

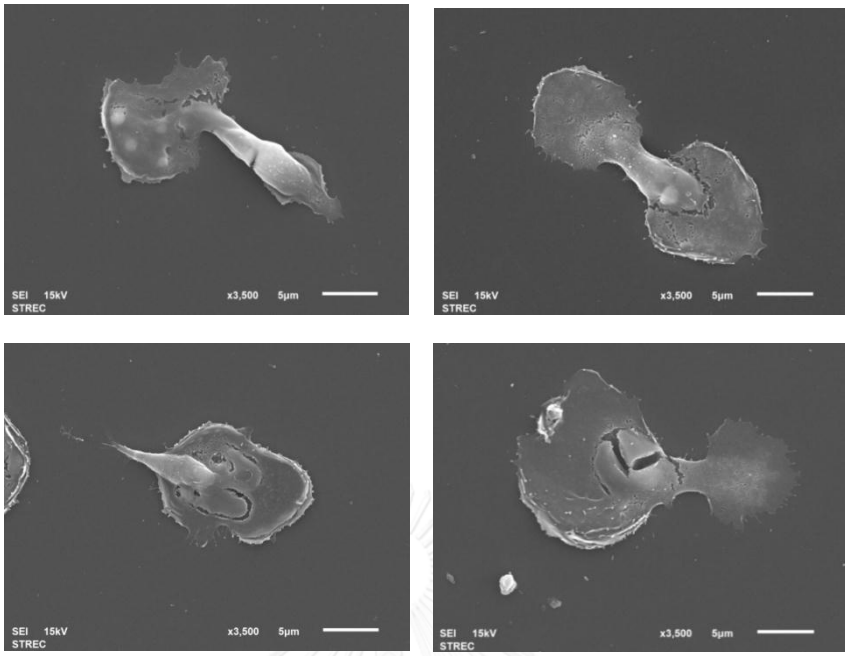

Figure 4.15 Degeneration of cells observed using SEM

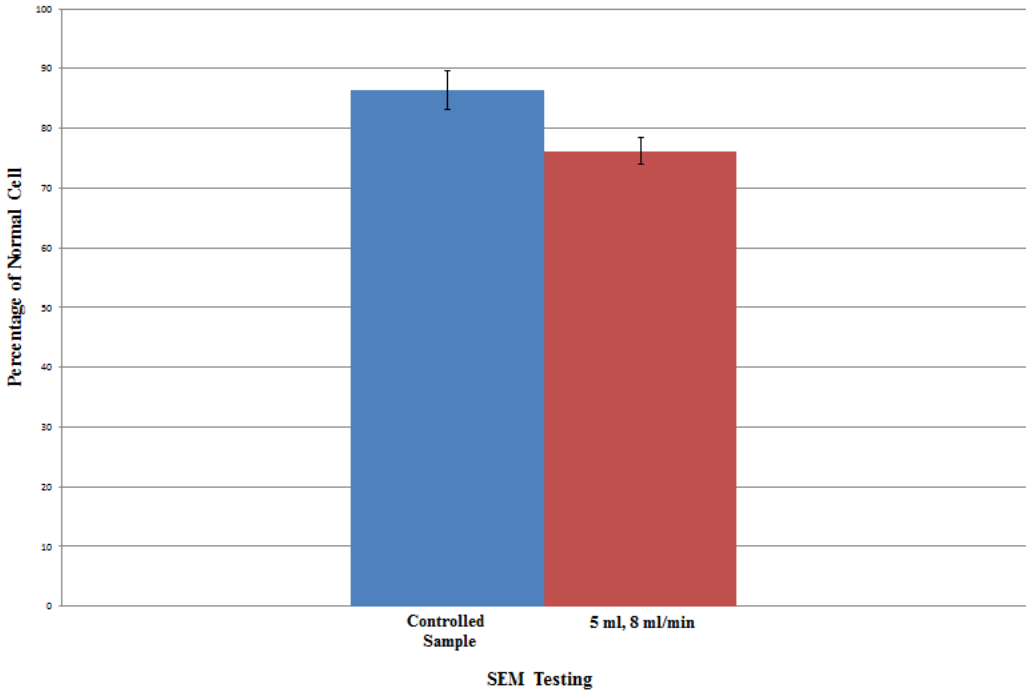

Figure 4.16 Comparison of normal cells in controlled sample and 5 ml syringe at 8 ml/min

4.5.3 Experimental Results by Wright's stain

Wright's stain was another common method to be used primarily to stain peripheral blood smears under a light microscope. The Wright's stain provided blue or purple color which allowed us to see nucleus inside cells clearly.

The experiment of wright's stain started with the technique of smear with the controlled sample and then smear again with the sample of 5 ml syringe at 8 ml/min. Leaving these two samples until they were dried completely. After that, both controlled sample and the sample of 5 ml at 8ml/min were put into fixative for 2 minutes and dyed with wright's stain afterward. (For full information for specimen preparation see, Appendix A).

This experiment was examined 1 time with 10 images were taken at the same locations and estimated normal cells and degenerated cells by the color of wright's stain. For normal cells, they were appeared as blue color consisting of three main structures—cell membrane, cytoplasm and nucleus as displayed in Figure 4.17. As for degeneration, they were appeared as a circle with no color inside as shown in Figure 4.18. The outcomes illustrated that there were about 86% of normal cells in the controlled sample. However, after the sample passing through the 5 ml syringe at 8 ml/min, normal cells were reduced to 72% as illustrated in Figure 4.19.

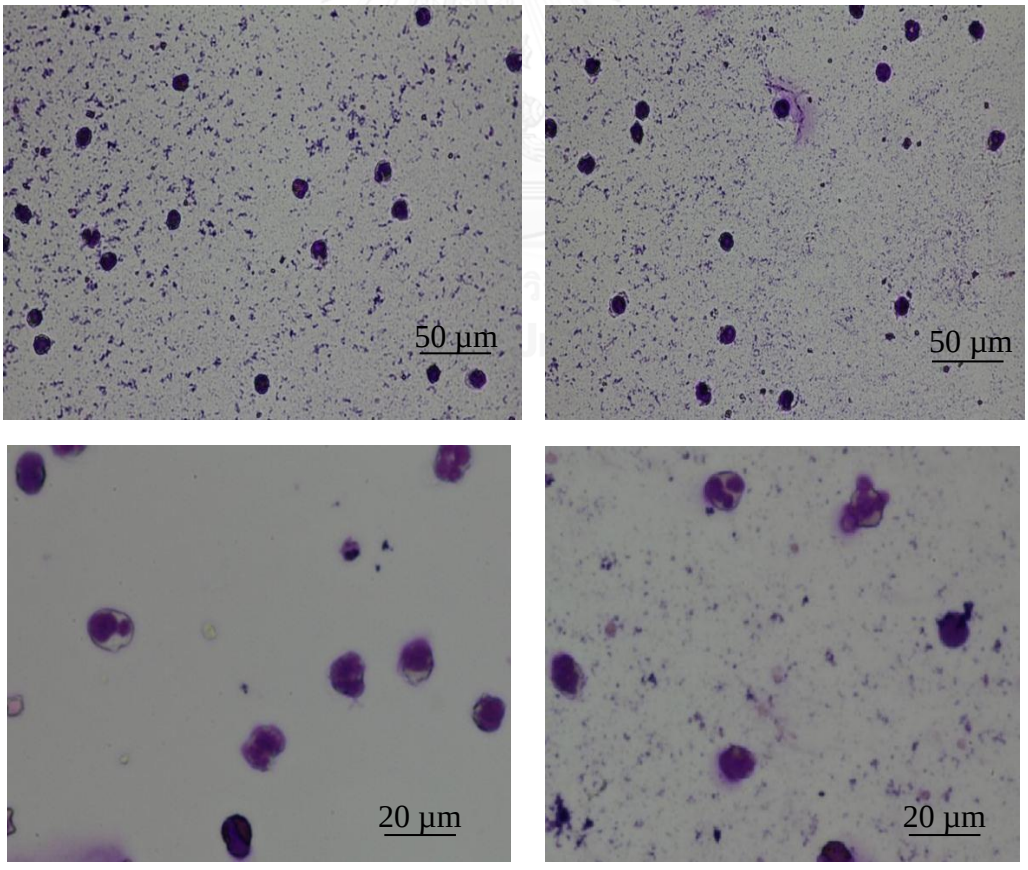

Figure 4.17 Normal cells observed using Wright's stain

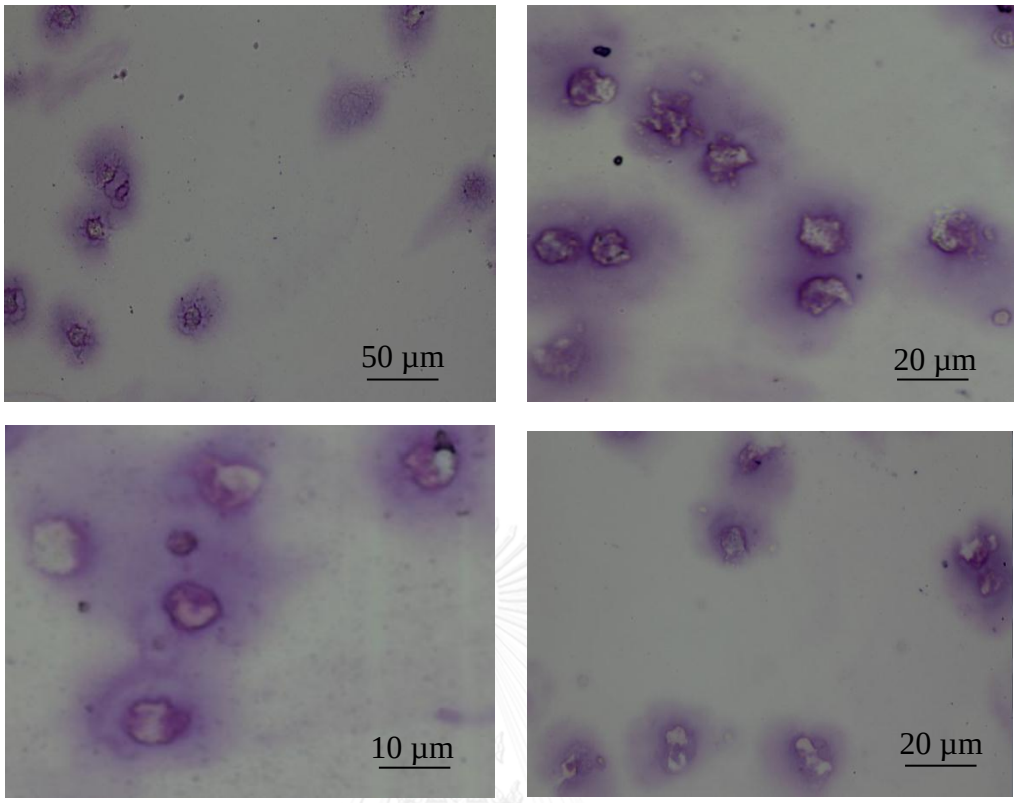

Figure 4.18 Degeneration observed using SEM

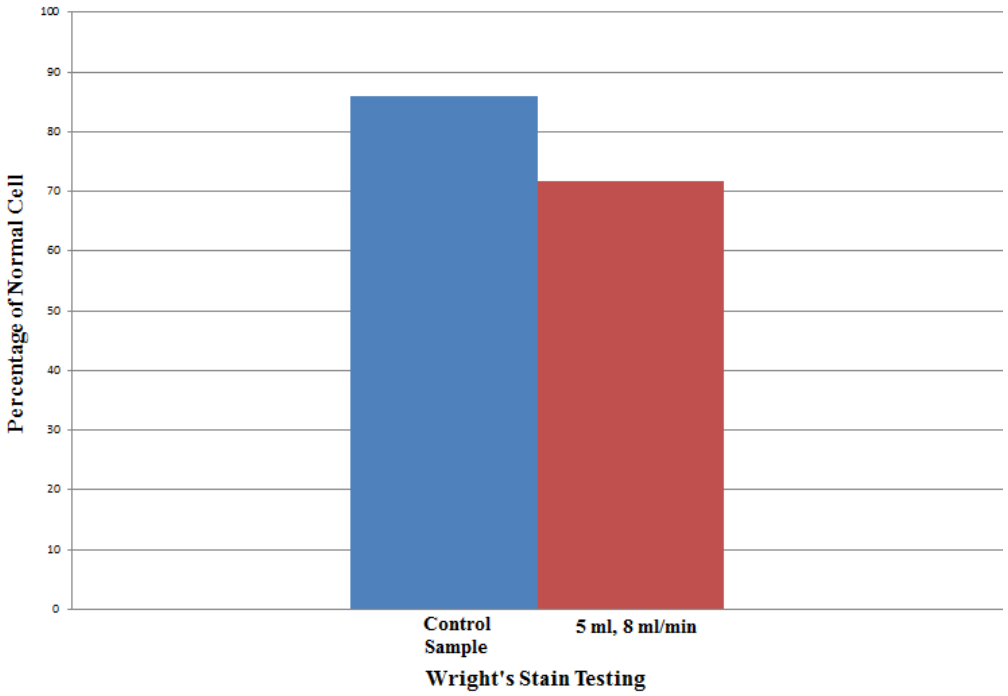

Figure 4.19 Comparison of the percentage of normal cells in controlled sample and 5 ml syringe at 8 ml/min under a light microscope with wright's stain

4.6 The Summarized Results of All Techniques

All three techniques demonstrated the percentage of live and normal cells in both cases –controlled sample and 5 ml syringe at flow rate of 8 ml/min as shown in Figure 4.20. According to the technique of Trypan Blue, it provided high percentage of live cells which showed that extensional stress, shear stress or exposure time in the case of maximum stress, had no effects on cell viability. However, among of these live cells would be deformed physically and some live cells would be damaged internally such as cell membrane, cytoplasm and nucleus etc. Obviously, this external and internal damage slightly affect on normal cells. It was evaluated that cell degeneration was increased about 10-15% after testing with the case of maximum stress in our study. To sum up, there was a great possibility for cells to be damaged externally and internally and then become cell degeneration but still survival with very high percent of 90-99% after experiencing extensional stress, shear stress and exposure time in the setup.

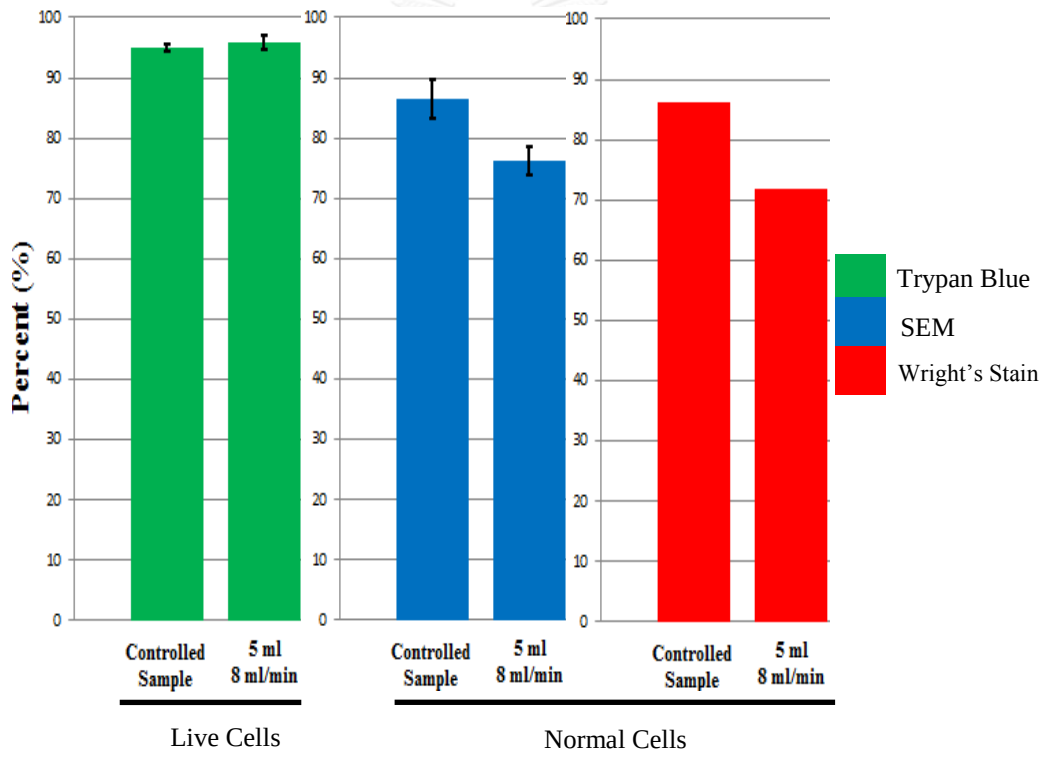

Figure 4.20 Percentage of live and normal cells with different methods and conditions.

4.7 The Setup of Spiral's Results

The last experiment, cell viability in the setup of spiral microchannel were investigated by a light microscope with Trypan Blue. The results indicated the viability of cells in 3 channels including 1st, 2nd and 3rd most likely exited to the first 3 channels. The data confirmed that the minority of cells exited to the first and second channel but the majority of cells exited to the third channel. The viable cells at the

outlet of the third channel were evaluated about 69.23%. Unfortunately, due to low numbers of cells exiting in channel 1st and 2nd and the experiment was examined only one time, we were not be able to determine the exact percentage of cell viability as proved in Table 4.3 and Figure 4.22.

Table 4.4 The percentage of cell viability in each channel; 1st, 2nd and 3rd

	Live Cells		Dead Cells		% Cell Viability Average
Controlled Sample	1	139	1	3	96.46%
	2	153	2	7	
	3	163	3	7	
Channel 1	1	3	1	0	77.78%
	2	5	2	0	
	3	1	3	2	
Channel 2	1	82	1	17	75.26%
	2	79	2	6	
	3	18	3	18	
Channel 3	1	296	1	81	69.23%
	2	256	2	118	
	3	238	3	154	

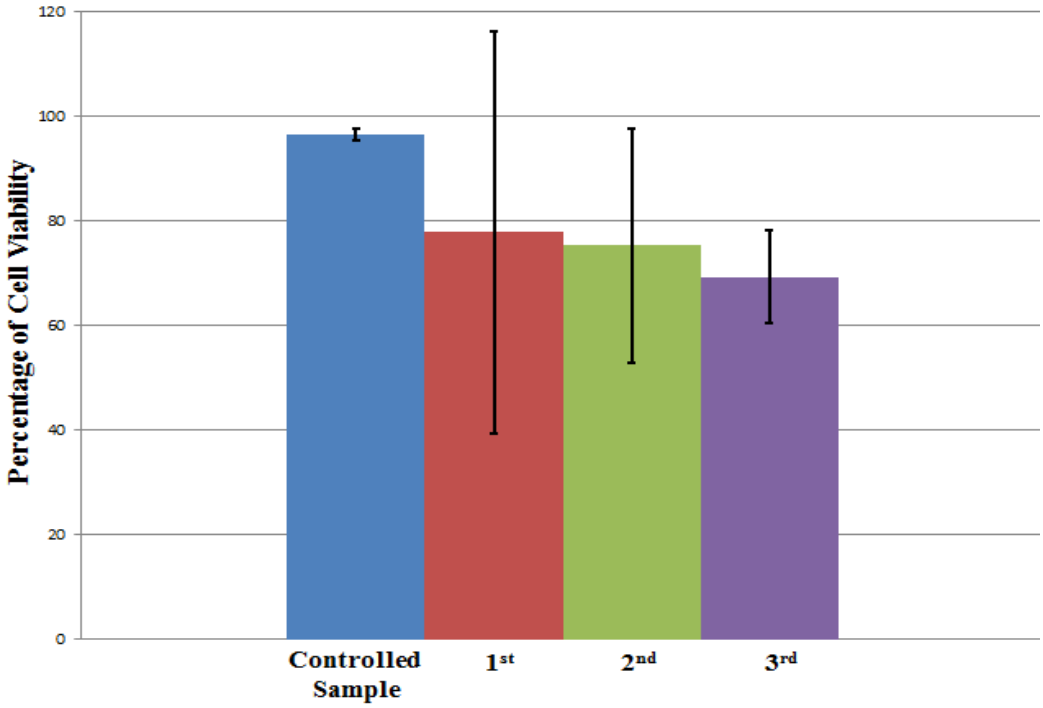

Figure 4.21 Percentage of cell viability in each channel of spiral microchannel

Interestingly, the images from Figure 4.22 showed that the majority of cells tend to exit the third channel. Whereas, small numbers of cells would go out from first and second channel. Figure 4.22a-c depicted the cell distribution observed from the experiments. Additionally, the images of cells in channel 1st, 2nd and 3rd demonstrated that the population of cells in channel 3rd agreed with the previous experiment as illustrated in Figure 4.22d. This is the fact that WBCs have an average size around 10 µm.

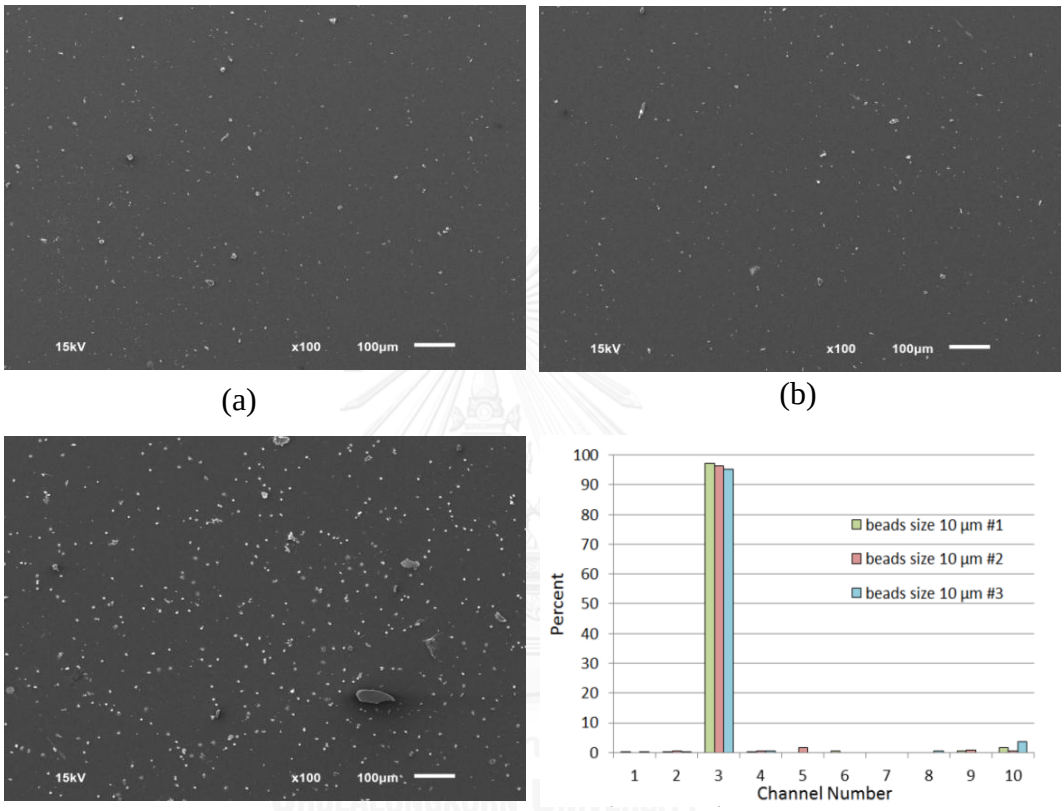

Figure 4.22 Population of cells in (a) 1st (b) 2nd and (c) 3rd channel and (d) the data of population of poly styrene beads in each channel from the previous study [39]

4.8 Conclusion

The aim of this work was to find the way to reduce a risk of cell death in the setup of spiral microchannel. It was found that extensional and shear stress played an important role in cell viability, deformity and structures during the process of cell separation. Recently, our protocols of cell preparation showed cell viability was about 90-99 percent of controlled sample. Furthermore, we decided to investigate cell viability in accessories including syringe, needle, silicone tube and spiral microchannel by a light microscope with Trypan Blue. In this work, Trypan Blue was

used to test cell viability in each accessory for 3 cases. Moreover, we also investigated cell morphology and cell structures in both cases; the best case (controlled sample) and the case of maximum stress (5ml syringe at 8 ml/min) with two more methods; SEM and Wright's stain to examine the numbers of normal cells and degenerated cells after the sample passing through the syringe.

For the experiment of Trypan Blue, we compared cell viability in the controlled sample and the syringes of each volume—1, 2.5 and 5 ml. The results demonstrated that each case showed high percent of cell viability. The majority of viable cells would survive about 90-99%. Furthermore, in the case of increasing flow rate from 1 to 8 ml/min with the syringe of 5 ml, the percentage of cell viability was about 94-96% compared to the percentage of controlled sample around 90-99%. The second case showed that even through a syringe connected with a 20 cm tube which the extensional and shear stress in syringe were 1519 and 558 Pa for 0.04 ms and the wall shear stress in 20 cm silicone tube was evaluated about ~11 Pa with exposure time around 1 s had not significant effects on cell viability as well. Therefore, extensional and shear stress in syringe within the range of investigation, has no impact on cell viability.

For the experiment of SEM, we examined the controlled sample and the case of maximum stress. The results indicated that normal cells were evaluated about 86% in the controlled sample and decreased to 76% after passing through the 5 ml syringe at the flow rate of 8 ml/min. Therefore, normal cells decreased about 11.62% by extensional and shear stress in the syringe.

Moreover, the data of Wright's stain also depicted that there were normal cells about 86% in controlled sample and reduced to 72% after passing through the syringe of 5 ml at the highest flow rate of 8 ml/min. This showed that extensional and shear stress in syringe had effects on cell structures either cell membrane, cytoplasm or nucleus.

Finally, the experiment of the whole setup of spiral showed that after the sample passing through the syringe of 1 ml at the flow rate of 1 ml/min under a light microscope with Trypan Blue, live cell were decreased from 95% to 69%. This indicated that the majority of cell death occurred in the spiral microchannel with the maximum shear stress about 15 Pa and exposure time about 2 second (exposure time was calculated, i.e. 40 cm/0.2 m/s ≈ 2 s).

In conclusion, the above data showed that stresses in syringe may not affect cell viability in the range of 50-1500 Pa for extensional stress and 20-560 Pa for shear stress with exposure time of 0.04 ms. The effects of cell viability from wall shear stress and exposure time were not found either in connected or disconnected with a 20 cm tube. However, it could potentially cause cell deformity and destruction of cell

structures when examining the case of maximum stresses with SEM and Wright's stain. According to the experiment of SEM and Wright's stain, there was a great possibility that degeneration would become dead cells afterward due to the severe deformity and destruction of cells. As for, the spiral microchannel, although it created moderate magnitude of shear stress only 15 Pa in the channel, viable cells must take some time to flow along with wall's channel around 2 seconds. This may suggest that stresses and exposure time in spiral may had enough effects on cell viability that caused a huge number of cells to die about 26% during separation.

Chapter 5

Releasing Device.

This chapter presents a computational simulation to design a microfluidic device that combines two main functions together—immobilizing and releasing for a single cell study. According to the previous study, we has accomplished both sorting and trapping device. In order to complete Lab-on-a Chip, releasing device is needed to assemble sorting and trapping device together.

5.1 The Studies of Releasing Device

As reported by the group of Yamaguchi, the experiment focused on a single cell manipulation and injection by fabricating two main parallel channels which were connected by a drain channel in the middle of device. These parallel channels allowed a cell suspension and flow to inject the cell separately [23]. Similarly, the group of Chanasakulniyom presented cell proliferation and migration by designing and fabricating perpendicular channels. The device had two main channels as well. However, these two channels were perpendicular to the horizontal axis. The second channel and the well were designed in one piece without having a drain channel linking the first and second channel [40].

Both designs greatly inspired our idea in this releasing project. We decided to use the concepts of injection and the design of Chanasakulniyom et al. [40] combined together. This technique will become our next challenge and a new discovery. Dealing with the challenge, a risk of cell viability and its property are taken into our considerations. Consequently, flowing fluid mediated detachment was chosen as the releasing method because there is no external forces which affect the cell biological and physical properties. In addition, our device will be able to immobilize the cell by keeping the cell floating in the middle of the well in order to avoid a wall effect that might change cell's biological and physical properties. Moreover, this microfluidic technique is inexpensive due to the simplicity of the design and no need of external equipments.

5.2 Design and Plans

The idea is that the releasing device is designed as the main channel located over the wells and the second channels (buffer channels) located at the bottom of the wells as presented in Figure 5.1a. During immobilization, the fluid in the main channel flows over the wells, while the fluid from buffer channels will be slowly injected in to keep the cell floating as exhibited in Figure 5.1d. As for the releasing process, the fluid flow in the main channel will be slow down; instead, the stronger fluid flow will be released from the buffer channels in order to push cells out of the wells as demonstrated in Figure 5.1e. Using computational software, in which cell is modeled as a solid particle, is employed in order to help examine flow behavior. From the study, the appropriate flow rate in both channels is found in order to immobilize the cells and then release the cells out of the wells. Obviously, this technique has a great potential to succeed. The device can be fabricated successfully and that the

particles will be safely released out of the wells. It will help researchers further analyze and understand cancer cell's behavior by taking a single cell from the device to test their biology such as PCR test, DNA test, Tissue Microarray, gene and protein expression.

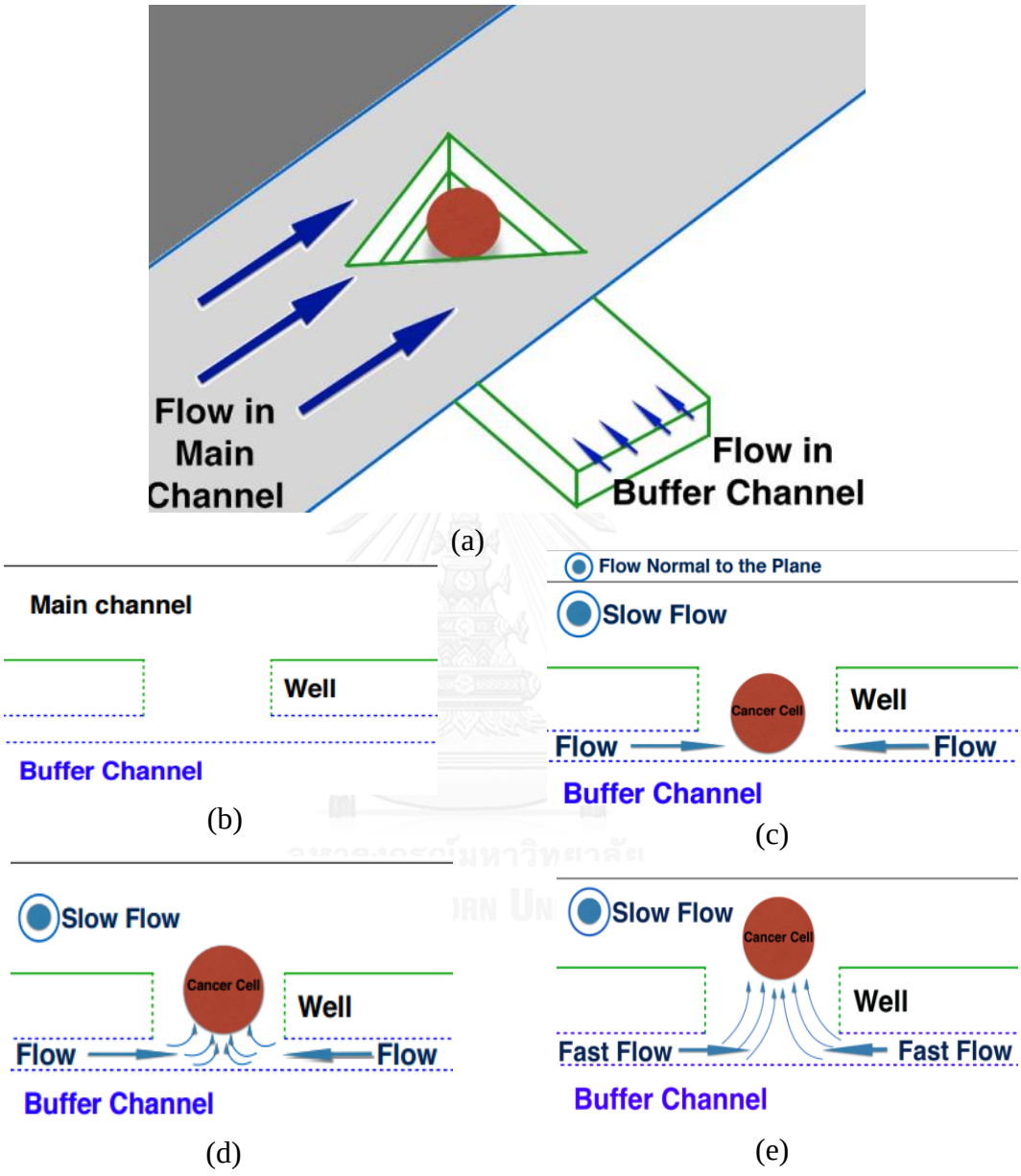

Figure 5.1 Working principle of immobilizing and releasing device; (a) schematic picture of the device and flow direction of both main and buffer channels (b) vacancy well, (c) trapping, (d) immobilizing, (e) releasing.

As stated in the previous data of trapping device, the appropriate flow rate was fixed at 0.1 ml/hr which this flow rate will be employed in the main channel in this study. The next step was to employ a solid particle with different sizes in the middle of the well. In this case, the flow rates in the buffer channels were varied into several cases. After that, total forces were evaluated over a surface of the solid particle at different flow rates in the buffer channels. If these total forces were generated equivalent to the polystyrene beads' weight—10, 15 and 20 μm, the beads would be floating in the middle of the wells. For the releasing, the flow rate in the buffer channel will be increased beyond the flow rate during the immobilization in order to release the particle out of the well.

5.3 Simulation

5.3.1 Materials and Properties

In computational simulation, 3D simulation and single-phase flow were selected. The medium was assumed to be water as it has been studied in the past with density of 998.2 kg/m^3 and viscosity of 0.00105 Pa•s and the flow was considered as laminar flow.

5.3.2 Geometry and Boundary Conditions

In order to avoid computational time consuming, a computational domain was modeled with a length of 1,200 μm, a width of 80 μm and a height of 160 μm. The well size was modeled as a triangle shape with each side of 40 μm and a depth of 15 μm as the main channel where was located over the wells. As for the buffer channel, it was modeled with a length of 40 μm and a height of 5 μm which was located at the bottom of the well. Furthermore, no slip boundary condition for the walls and the stead-state Navier-Stokes equation for incompressible fluids which is defined as

$$\rho(u\cdot\nabla)u = \nabla\cdot[p+\mu(\nabla u+(\nabla u)^T]+F=0 \quad (5.1)$$

where u is the fluid velocity, p is the fluid pressure, ρ is the fluid density, and μ is the fluid dynamic viscosity, F is the external forces applied to the fluid [41].

After finishing modeling geometry and defined the conditions, meshing was the next step of this process. The program provides nine built-in size parameter set [42]. Distribution of meshing was selected and separated into three domains—the solid particle**,** the well and the edges of the well. The number of meshes in these three domains was increased until the results were stable. A grid independence tests were done with the maximum and minimum element size were 9.92 and 1.87 μm. The final number of meashes was 4.4 millions.

5.3.3 The Computational Results

The results were focused on total forces over the surface. The total hydrodynamic forces on the surface of the sphere were able to be evaluated by the sum of integral of pressure distribution and viscous stress is defined as

$$F_{hydro}=F_{pressure}+F_{viscous} \quad (5.2)$$

5.4 Results

5.4.1 Immobilizing Process

To improve the results of simulation, the technique of the grid independence was implemented by using smaller size of meshes for calculation. After the data of the grid independence were stable, the next step was to find the appropriate flow rate and total force in the vertical direction. In this case, density or weight of a solid particle was referred from polystyrene beads used as a replica model of a cancer cell in different diameters—10, 15 and 20 μm. The net force from a gravitational effect of the different size of polystyrene beads were calculated which was written as

$$F_{net} = mg\text{-}\rho V_{disp} g \qquad (5.3)$$

where F_{net} is a net force (N) due to gravitational effect, m is a mass of the object (kg), ρ is a density of the fluid (kg/m^3), $V_{disp}$is the volume of the displaced body of liquid (m^3) and g is the acceleration due to gravity 9.807 (m/s^2).

Additionally, as demonstrated in Figures 5.2a-c, what we found was that the streamlines passed over the solid particle of 15 and 20 μm smoothly. However, recirculation behind the particle occurred for the solid particle of 10 μm. For this reason, the larger size of particles relative to the size of micro-well could reduce recirculation and may be able to stabilize the floating of particle in the well.

According to the data in Table 5.1, the data indicated that increasing flow rates in the range of 0-1.87 nl/hr resulted in an increasing of the total hydrodynamic force. The magnitude of the hydrodynamic force also depended on a particle size. For instance, at the flow rate of 1.87 nl/hr, the hydrodynamic force exerting on a particle with the size of 10, 15 and 20 μm was equal to 0.45, 1.39 and 4.26 pN, respectively.

Table 5.2 represented the flow rate in buffer channels where the net force due to gravitational effect equal to hydrodynamic force of each size of solid particles. It was found that the flow rate in buffer channels should be equal to 1.07 nl/hr, 1.18 nl/hr and 0.92 nl/hr in order to immobilize the solid particle of 10, 15 and 20 μm, respectively. The results suggested that the flow rate in buffer channels should be precisely controlled in order to achieve the floating of cells.

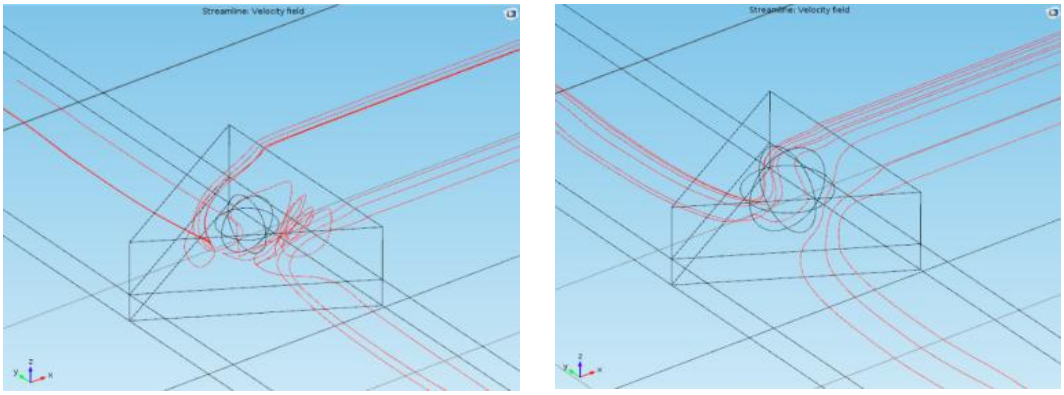

(a) (b)

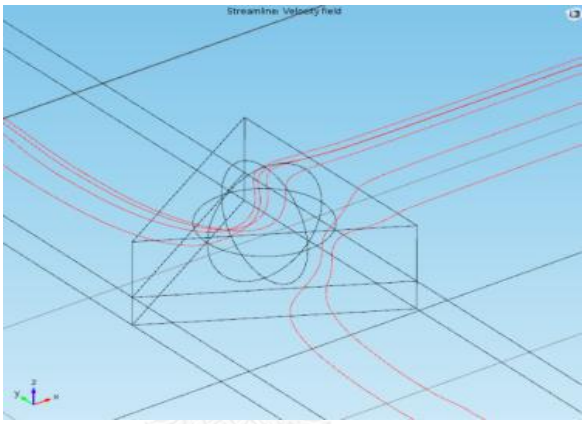

(c)

Figure 5.2 Streamlines from computational results at the flow rate of 1 nl/hr in buffer channels for different sizes of particle; (a) 10 µm, (b) 15 µm, (c) 20 µm.

Table 5.1 Comparison of total hydrodynamic forces in a vertical direction with different diameters of a solid at various flow rates in buffer channels

Flow rate in buffer channels (nl/hr)	Total hydrodynamic force (pN)		
	10 µm	15 µm	20 µm
0	0	0	0
0.62	0.15	0.46	1.42
1.25	0.30	0.91	2.85
1.87	0.45	1.39	4.26

Table 5.2. Flow rates in buffer channels when the floating of cells occurs.

Diameters (µm)	Flow rate (nl/hr)	$F_{net} = F_{hydro}$ (pN)
10	1.07	0.26
15	1.18	0.87
20	0.92	2.05

The conclusion was made that the flow rate which could keep the particles floating in the well for 10, 15 and 20 µm should be in an order of magnitude of 1 nl/hr. Figure 5.3 demonstrated the linear increment of hydrodynamic force due to the change of flow rate in buffer channels as well as the appropriate flow rates that should be for floating the cells in micro-wells when the flow rate in the main channel is fixed at 0.1 ml/hr.

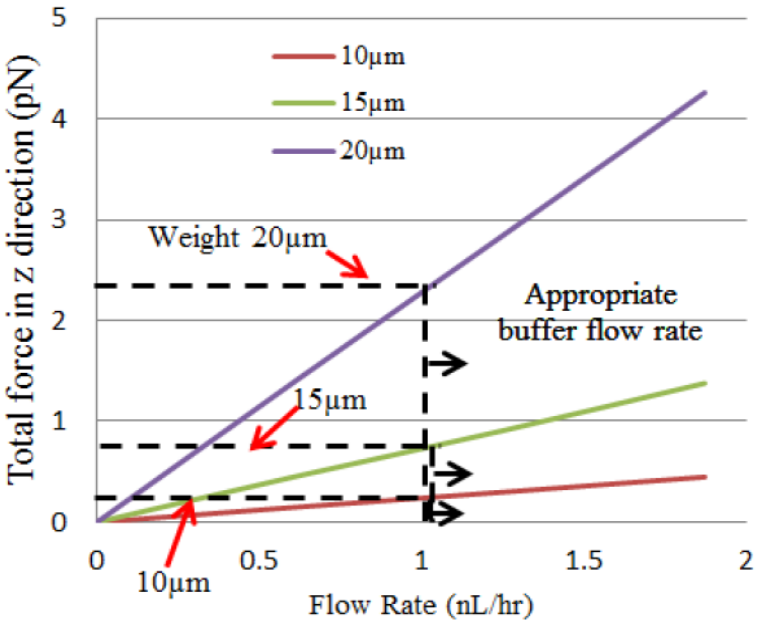

Figure 5.3 Vertical hydrodynamic forces versus flow rates for 10, 15 and 20 µm particles.

5.4.2 Releasing Process

In the releasing process, the fluid flow in the main channel was slowed down. Meanwhile, the stronger fluid flow is released from the buffer channels in order to push the cells out of the wells. This purpose of this process was to find the appropriate flow rate in the buffer channel to release particles out of the wells. Due to the data from the immobilization process, the consequences demonstrated that the particle of 10, 15 and 20 µm would be able to be released out of micro-wells with the flow rates in buffer channels higher than 1.07, 1.18 and 0.92 nl/hr, respectively.

Another interesting issue is the appropriate flow rate in buffer channels that could float a particle. A simulation of particles with a diameter between 5 to 20 µm was performed further in order to investigate an effect of the particle size on this flow rate where the net force due to the gravitational effect equal to hydrodynamic force. The data is shown in Figure 5.4 comparing between two cases, i.e. with and without micro-well. With the well, when the size was increased, the required flow rate was increased as well until the particle size of around 14 µm. At this size, the required flow rate was around 1.2 nl/hr for the proposed microchannel size. Beyond this particle size, the required flow rate reduced.

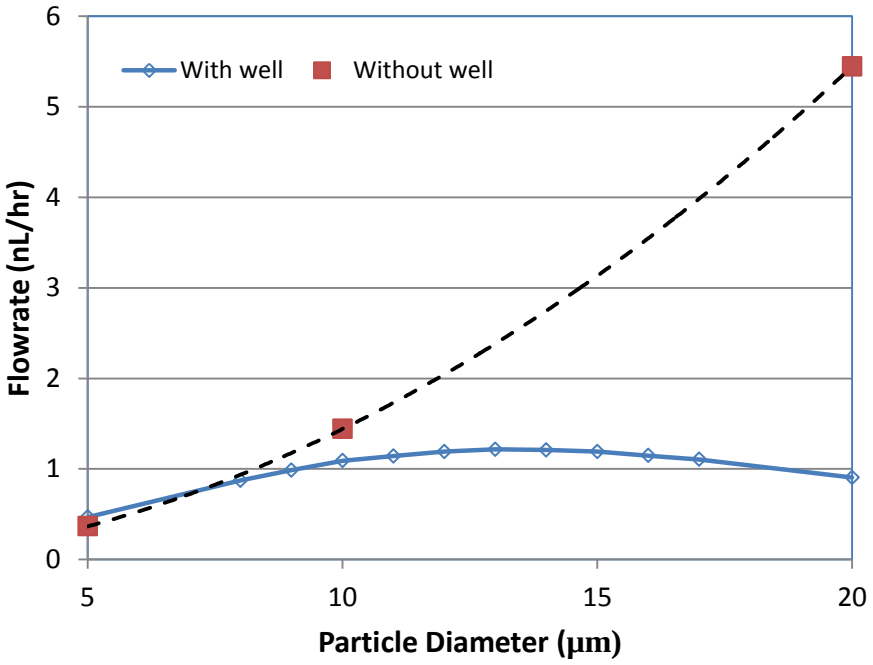

Figure 5.4 Flow rate in buffer channels when hydrodynamic force equal to the net force due to a gravitational effect for different particle sizes ranging from 5-20 µm.

5.5 Conclusion

The goal of this project is to design the releasing device which consists of two functions—immobilizing and releasing process. In order to do so, the design of releasing device—main channel, triangle wells and buffer channels were modeled based on the data from previous experiments on a trapping device. Furthermore, the appropriate flow rates in the buffer channels were found in order to immobilize (generating force equivalent to the particle weight) various sizes of the particle and release (increasing force over the particle weight). From simulation results, it suggested that for different sizes of particles on 10, 15 and 20 µm, the critical flow rates in buffer channels for the fixed flow rate in the main channel of 0.1 ml/hr should be 1.07, 1.18 and 0.92 nl/hr, respectively.

Chapter 6

Summary and Suggestion

This chapter presents summary and suggestions of this work. The first section presents how to improve cell viability in the setup of spiral microchannel from computational simulation and actual experiments. In the second section demonstrates the phenomenon of required flow rate reduced in the releasing device from the simulation.

6.1 Summary and Suggestion on Investigation of Stresses

According to 2D-Axisymmetric simulation, it demonstrated the magnitude of stresses including syringe, needle and silicone tube. As you can see from the simulation in the case of maximum stresses, extensional and shear stress were generated over 1,000 and 500 Pa at the corner of abrupt change in cross section between the barrel and needle. As reported by Young Bok Bae [33] and Jen-Hong Yen [34], they stated that extensional stress about 1,000 to 250 Pa could damage cell viability. However, the extent of high-stress area (higher than 1,000 Pa), it was estimated about 4 micrometers in length and 1 micrometers in width compared to the size of WBCs about 10 to 15 micrometers in diameter. Because of a small high-stress area in syringe, it may not have effects on cell viability. Moreover, the higher flow rate allowed the extent of high-stress to exposure viable cells more quickly. As it measured, exposure time in the 5 ml syringe allowed viable cells to pass the high-stress area just about 0.04 ms. For this reason, it could be predicted that there may be less likely for cells to be damaged by stresses in the syringe due to the small extent of high-stress and the short exposure time. Although extensional and shear stress in a syringe may not affect cell viability, it could possibly cause deformity and the destruction of cell structures. After examining cell viability in a syringe with various conditions, we also examined cell viability in the whole setup of spiral microchannel. According to the results, about 26% of cells were death in spiral microchannel with shear stress about 15 Pa and exposure time about 2 seconds. This showed that a long exposure time and only moderate magnitude of stresses could cause cells to die.

Furthermore, the results suggested that a feeding system from a syringe to a silicone tube had no effect on cell viability but the spiral microchannel caused cell death during the process of separation. For a feeding system, there was no need to fix or modify to improve cell viability because the small extent of high-stress and the short exposure time could not cause cell death due to the results of Trypan Blue stain examination. Despite of that, some of viable cells may be deformed in a syringe because some of cells experienced high extensional and shear stress from changing cross section at the corners between the barrel and the needle before entering the spiral channel. However, the ultimate goal of our studies is to not only obtain cells which are survival but also are normal after passing through a sorting, trapping and releasing device. In order to reduce extensional stress in syringe that causes cell deformity and the destruction of cell structures, the low flow rate should be applied as low as possible in the first place as well as the size of syringe should be small.

Moreover, the area of changing in cross section should be inclined as a taper with a small angle (Figure 6.1b). This method could help reducing extensional stress dramatically from ~1500 to ~20 Pa. Every corner in syringe should be rounded with a large radius. Although decreasing more stresses was not found in this strategy, it could reduce more extent of stresses at the entrance between taper and needle as illustrated in Figure 6.1b-c.

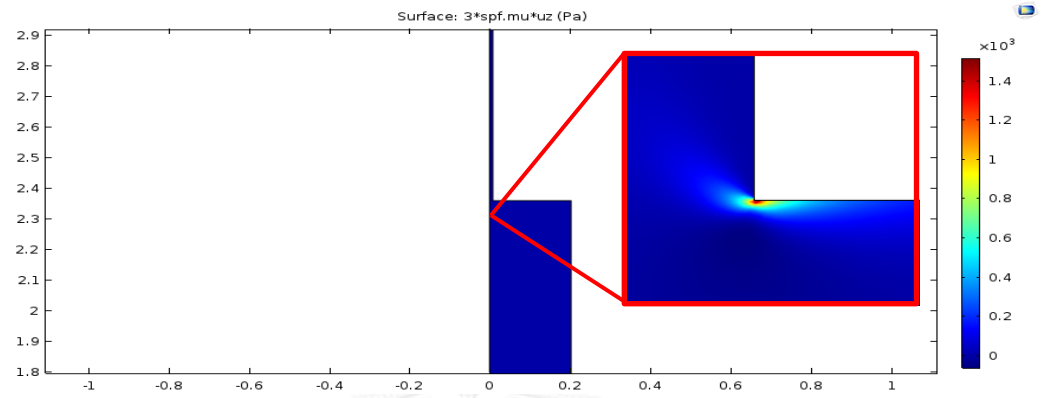

(a)

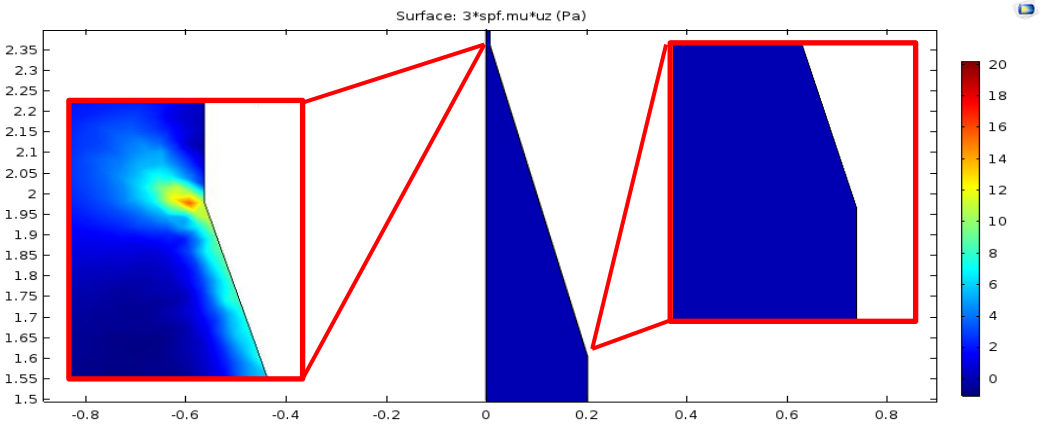

(b)

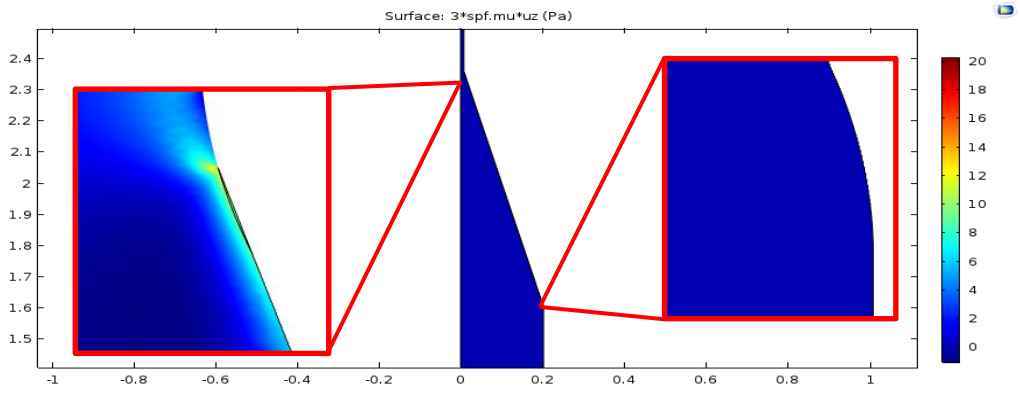

(c)

Figure 6.1 Magnitude and extent of extensional stress in a syringe (a) with the abrupt change in cross section (b) with incline wall and sharp corners and (c) with incline wall with rounded corners.

Additionally, we should use silicone tubes as big as possible to reduce wall shear stress as suggested from Eq (2.10). As for spiral microchannel, in order to improve cell viability, the value of radius of curvature (r) should be low. In this way, it allows streamline focusing to get to the equilibrium position more quickly with a short distance (more information about radius of cuvature, see in Appendix C). Therefore, it could reduce exposure time from the length of channel. According to the studies of Nivedita et al. [36] and Xiang et al. [9], they stated that the appropriate length of the channel should be around 3-4 loops not 5 loops as we fabricated. Furthermore, the cross sectional area should be larger including increasing channel width, channel height or decreasing spacing between channels to reduce wall-shear stress in the channel. Finally, required flow rate to separate different size of particles should be low but still under good separation conditions and the lowest flow rate used was 1 ml/min.

Lastly and importantly, uncertainty of measurement from the experiment of Trypan Blue, SEM and Wright's stain may occur in the percentage of cell viability. For example, donated Canine blood from the hospital was unhealthy blood. These unhealthy cells may result in the weakness and loss of cell easily during the experiments. For cell counting with Trypan Blue, the controlled sample and the case of syringes should have examined at the same time but we decided to count the controlled sample before examining the experiment of syringe because we were able to determine cell viability in controlled sample and concentration of cell suspension at the same time and reduce a risk of being aggregated in cell suspension. However, this may not have a huge effect on cell viability due to high percentage of cell viability around 90-99% in both cases. For uncertainty of SEM's results, 20 images were taken for 2 samples. Due to unclear images of cell morphology, some cells could not be identified the exact types of white blood cells. This probably causes uncertain results of SEM. For Wright's stain results, we took 10 images of both controlled sample and the case of syringe that examined only one sample, it may need to examine repeatedly in order to reduce the uncertainty of the experiment.

6.2 Summary and Suggestion on Releasing Device

Computational simulation helped designing the releasing device by creating a solid particle in the middle of the well and investigating the appropriate flow rates that keep the solid particle floating in the well. Technically, there are two working principles of the releasing device—immobilizing and releasing mode. The general idea is that the releasing device will be fabricated as the main channel located over the wells and the second channels (buffer channels) located at the bottom of the wells. During immobilization, the fluid in the main channel will flow over the wells, while the fluid from buffer channels will slowly be injected to keep the cells floating. In the releasing process, the fluid flow in the main channel will be slowed down. Meanwhile, the stronger fluid flow is released from the buffer channels to push the cells out of the wells. A computational software, in which cells were modeled as solid particles, was employed to help examine flow behavior. From the study, the appropriate flow rate—generating force equivalent to the particle weight of various sizes of the particle— in buffer channel would be found in order to immobilize the cells and then release the cells out of the wells.

According to the data of appropriate flow rates, the flow rate that could float a particle was around 0.1 nL/hr and the flow rates tended to increase when the solid particle's size increasing as well because the magnitude of the hydrodynamic force depended on a particle size. However, it was found that when the particle was increased to 14 μm in diameter, the appropriate flow rates started gradually decreasing.

According to the simulation, we found that when the flow was injected from the buffer channel and passing through the solid particle in the middle of the well, the solid particle tended to create recirculation on the side of particle. Surprisingly, the fluid flow went through more smoothly when the particle was increased. This showed that increasing size of the solid particle can affect the flowing streamline in the well.

According to the case when the particle floating in a non-confined space, the flow rate required for the floating increased with the increasing of particle size. This suggested the strong effect of the ratio of particle and the micro-well dimensions. When the particle size is still small comparing to the micro-well, two cases showed a similar trend. However, when the particle size became larger, e.g. 10 μm, the difference of the required flow rate between two cases was observed.

These might be an effect of flow phenomena that was different between the two cases, and the reason that caused the reducing of required flow rate for large particle must be investigated further.

REFERENCES

[1] T. Khuhaprema, "Current Cancer Situation in Thailand " *Thai J Toxicology,* vol. 23, pp. 60-61, 2008.

[2] (2015, October 27). *Cancer*. Available: http://www.who.int/mediacentre/factsheets/fs297/en/

[3] H. Yin and D. Marshall, "Microfluidics for single cell analysis," *Curr Opin Biotechnol,* vol. 23, pp. 110-9, Feb 2012.

[4] P. Sajeesh and A. K. Sen, "Particle separation and sorting in microfluidic devices: a review," *Microfluidics and Nanofluidics,* vol. 17, pp. 1-52, 2013.

[5] M. Kuschel and "Lab-on-aChip Technology—Applications for Life Sciences," *Pharmaceutical Technology Europe,* 2001.

[6] J. Autebert, B. Coudert, F. C. Bidard, J. Y. Pierga, S. Descroix, L. Malaquin, *et al.*, "Microfluidic: an innovative tool for efficient cell sorting," *Methods,* vol. 57, pp. 297-307, Jul 2012.

[7] N. Xiang, K. Chen, D. Sun, S. Wang, H. Yi, and Z. Ni, "Quantitative characterization of the focusing process and dynamic behavior of differently sized microparticles in a spiral microchannel," *Microfluidics and Nanofluidics,* vol. 14, pp. 89-99, 2012.

[8] I. D. Johnston, M. B. McDonnell, C. K. L. Tan, D. K. McCluskey, M. J. Davies, and M. C. Tracey, "Dean flow focusing and separation of small microspheres within a narrow size range," *Microfluidics and Nanofluidics,* vol. 17, pp. 509-518, 2014.

[9] N. Xiang, K. Chen, Q. Dai, D. Jiang, D. Sun, and Z. Ni, "Inertia-induced focusing dynamics of microparticles throughout a curved microfluidic channel," *Microfluidics and Nanofluidics,* vol. 18, pp. 29-39, 2014.

[10] A. E. Hasni, K. Göbbels, A. L. Thiebes, P. Bräunig, W. Mokwa, and U. Schnakenberg, "Focusing and Sorting of Particles in Spiral Microfluidic Channels," *Procedia Engineering,* vol. 25, pp. 1197-1200, 2011.

[11] A. A. Bhagat, S. S. Kuntaegowdanahalli, and I. Papautsky, "Continuous particle separation in spiral microchannels using Dean flows and differential migration," *Lab Chip,* vol. 8, pp. 1906-14, Nov 2008.

[12] S. S. Kuntaegowdanahalli, A. A. Bhagat, G. Kumar, and I. Papautsky, "Inertial microfluidics for continuous particle separation in spiral microchannels," *Lab Chip,* vol. 9, pp. 2973-80, Oct 21 2009.

[13] J. Zhang, S. Yan, R. Sluyter, W. Li, G. Alici, and N. T. Nguyen, "Inertial particle separation by differential equilibrium positions in a symmetrical serpentine micro-channel," *Sci Rep,* vol. 4, p. 4527, 2014.

[14] M. G. Lee, S. Choi, and J. K. Park, "Inertial separation in a contraction-expansion array microchannel," *J Chromatogr A,* vol. 1218, pp. 4138-43, Jul 8 2011.

[15] D. R. Gossett, W. M. Weaver, A. J. Mach, S. C. Hur, H. T. Tse, W. Lee, *et al.*, "Label-free cell separation and sorting in microfluidic systems," *Anal Bioanal Chem,* vol. 397, pp. 3249-67, Aug 2010.

[16] A. A. S. Bhagat, S. S. Kuntaegowdanahalli, and I. Papautsky, "Inertial microfluidics for continuous particle filtration and extraction," *Microfluidics and Nanofluidics,* vol. 7, pp. 217-226, 2008.

[17] R. S. Kuczenski, H. C. Chang, and A. Revzin, "Dielectrophoretic microfluidic device for the continuous sorting of Escherichia coli from blood cells," *Biomicrofluidics,* vol. 5, pp. 32005-3200515, Sep 2011.
[18] K. Dholakia, A. E. Cohen, W. E. Moerner, and G. C. Spalding, "An all-glass microfluidic cell for the ABEL trap: fabrication and modeling," vol. 5930, pp. 59300S-59300S-8, 2005.
[19] J. Nilsson, M. Evander, B. Hammarstrom, and T. Laurell, "Review of cell and particle trapping in microfluidic systems," *Anal Chim Acta,* vol. 649, pp. 141-57, Sep 7 2009.
[20] N. Pamme, "Magnetism and microfluidics," *Lab Chip,* vol. 6, pp. 24-38, Jan 2006.
[21] M. Evander, L. Johansson, T. Lilliehorn, J. Piskur, M. Lindvall, S. Johansson, *et al.*, "Noninvasive Acoustic Cell Trapping in a Microfluidic Perfusion System for Online Bioassays," *Analytical Chemistry,* vol. 79, pp. 2984-2991, 2007.
[22] Q. Zheng, S. M. Iqbal, and Y. Wan, "Cell detachment: post-isolation challenges," *Biotechnol Adv,* vol. 31, pp. 1664-75, Dec 2013.
[23] Y. Yamaguchi, T. Arakawa, N. Takeda, Y. Edagawa, and S. Shoji, "Development of a poly-dimethylsiloxane microfluidic device for single cell isolation and incubation," *Sensors and Actuators B: Chemical,* vol. 136, pp. 555-561, 2009.
[24] D. Schmaljohann, "Thermo- and pH-responsive polymers in drug delivery," *Adv Drug Deliv Rev,* vol. 58, pp. 1655-70, Dec 30 2006.
[25] W. H. Tan and S. Takeuchi, "A trap-and-release integrated microfluidic system for dynamic microarray applications," *Proc Natl Acad Sci U S A,* vol. 104, pp. 1146-51, Jan 23 2007.
[26] G. Kretzmer and K. Schiigerl, "Response of mammalian cells to shear stress," *Appl Microbiol Biotechnol,* vol. 34, pp. 613-616, 1991.
[27] J. M. Barnes, J. T. Nauseef, and M. D. Henry, "Resistance to fluid shear stress is a conserved biophysical property of malignant cells," *PLoS One,* vol. 7, p. e50973, 2012.
[28] M. J. Mitchell and M. R. King, "Computational and experimental models of cancer cell response to fluid shear stress," *Front Oncol,* vol. 3, p. 44, 2013.
[29] J. Y. Park, M. Morgan, A. N. Sachs, J. Samorezov, R. Teller, Y. Shen, *et al.*, "Single cell trapping in larger microwells capable of supporting cell spreading and proliferation," *Microfluid Nanofluidics,* vol. 8, pp. 263-268, Feb 1 2010.
[30] T. G. Papaioannou and C. Stefnadis, "Vascular Wall Shear Stress: Basic Principles and Methods," *Hellenic J Cardiol,* vol. 46, pp. 9-15, 2005.
[31] R. M. Nerem, "Shear Force and Its Effect on Cell Structure and Function," *ASGSB Bulletin,* vol. 4, 1991.
[32] B. A. Aguado, W. Mulyasasmita, J. Su, K. J. Lampe, and S. C. Heilshorn, "Improving viability of stem cells during syringe needle flow through the design of hydrogel cell carriers," *Tissue Eng Part A,* vol. 18, pp. 806-15, Apr 2012.
[33] Y. B. Bae, H. K. Jang, T. H. Shin, G. Phukan, T. T. Tran, G. Lee, *et al.*, "Microfluidic assessment of mechanical cell damage by extensional stress," *Lab Chip,* vol. 16, pp. 96-103, Dec 15 2015.

[34] J.-H. Yen, S.-F. Chen, M.-K. Chern, and P.-C. Lu, "The Effects of Extensional Stress on Red Blood Cell Hemolysis," *Biomedical Engineering: Applications, Basis and Communications,* vol. 27, p. 1550042, 2015.
[35] L. A. Down, D. V. Papavassiliou, and E. A. O'Rear, "Significance of extensional stresses to red blood cell lysis in a shearing flow," *Ann Biomed Eng,* vol. 39, pp. 1632-42, Jun 2011.
[36] N. Nivedita and I. Papautsky, "Continuous separation of blood cells in spiral microfluidic devices," *Biomicrofluidics,* vol. 7, p. 54101, 2013.
[37] N. Nivedita and I. Papautsky, "Sorting of blood in spiral microchannels," *Miniaturized Systems for Chemistry and Life Sciences,* 2012.
[38] T. Suwannaphan, "Investigation of shear stress and cell survival in a microfluidic chip for a single cell study," 2015.
[39] A. Thanormsridetchai, "SIZE-BASED CELL SORTING USING SPIRAL MICROCHANNELS," Year 2014.
[40] M. Chanasakulniyom, A. Glidle, and J. M. Cooper, "Cell proliferation and migration inside single cell arrays," *Lab On Chip,* vol. 15, pp. 208–21, 2014.
[41] (2015, October 27). *Navier-Stokes Equations*. Available: http://www.comsol.com/multiphysics/navier-stokes-equations
[42] A. Griesmer. (2014, October 27). *Size Parameters for Free Tetrahedral Meshing in COMSOL Multiphysics*. Available: https://www.comsol.com/blogs/size-parameters-free-tetrahedral-meshing-comsol-multiphysics/
[43] J. M. Martel and M. Toner, "Particle Focusing in Curved Microfluidic Channels," *Scientific Reports,* vol. 3, 2013.

APPENDIX

Appendix A

Solution Preparation

RBC Lysing Solutions (10X concentration)

RBC Lysing Solutions (10X concentration) consists of :

1.NH4Cl (ammonium chloride) 8.02gm

2.NaHCO3 (sodium bicarbonate) 0.84gm

3.EDTA (disodium) 0.37gm

Storing RBC Lysing Solutions (10X concentration) at 4°C

RBC Lysing Solutions (1X concentration) Procedure

Red blood cell (RBC) lysing solution is a buffer supplied as a 10X solution and should be diluted to 1X in DI- water. In this experiment, Red blood cell (RBC) lysing solution (10x concentration) 40 ml is diluted with 400 ml DI water in 500 ml beaker.

WBCs Preparation of Cell Suspension

The preparation protocols of cell suspension get started with collecting Canine blood using the pipette of 100/1000 and taking the blood into a 50 ml plastic centrifuge tube (Figure A.1). RBC lysing solution was performed under the recommended protocols previously which the appropriate amount of Canine blood should be about 3 mL and add sufficient quantity of DI water to 45 ml into a 50 ml plastic centrifuge tube as shown in Figure A.2. If Canine blood is more than 3 mL, Red blood cells (RBCs) will not be able to be lysed completely. For this, the RBCs need to be lysed repeatedly until it is completely disappeared. After that, the solution of Canine blood and RBC lysing solution are mixed together using biomixer (shaker) for 15 minutes (Figure A.3) and then using centrifugation (Figure A.4) at 4 degree Celsius and 3000 rpm for 20 minutes to allow WBCs to sediment at the bottom of the tube (Figure A.5). After the process of centrifugation is done, the next step is to take out the RBC lysing solution from the sample (Figure A.6). In the meanwhile, using a filter to ensure that there is no debris and contaminations in phosphate buffered solution, PBS (Figure A.7) and rinses RBC remains by mixing with PBS and centrifuge repeatedly. In order to keep cell alive as many as possible, we have developed the protocols of preparation process. As previous experiment, we took RBCs out of the WBC sediment by mixing PBS and then centrifuged the sample to

obtain the cell suspension. This process usually repeated about 4-5 times until the red color from RBCs disappeared. However, the new protocols allow us to use the process of centrifugation only one time. Therefore, the new protocols could reduce a risk of cell death effectively. Here is our techniques, using a pipette containing PBS and rinsing the sediment of WBCs inside the plastic centrifuge tube slowly and carefully until the red color from blood is almost disappeared (Figure A.8) and mixing PBS to 45 mL and then centrifuge again. However, this technique might lose some WBCs from rinsing but it is significantly useful to keep the majority of cells to survive. After obtaining cell suspension, putting PBS into the cell suspension until we have the right concentration. Finally, mixing cell suspension well with Biomixer for 5 minutes again (Figure A.9). Additionally, cell suspension should be swirled and flasked to ensure that the cell suspension is distributed well. Ethylenediaminetetraacetic acid, EDTA could be another option that helps cell suspension distributed evenly. Furthermore, cell-strainer (40 µm) and filter are needed to separate debris and contamination from cell suspension before performing the experiment (Figure A.10).

Figure A.1 Collecting Canine blood for 3 ml into a 50 ml plastic centrifuge tube

Figure A.2 Putting 3 ml of Canine blood with RBC lysing solution together into a 50 ml plastic centrifuge tube

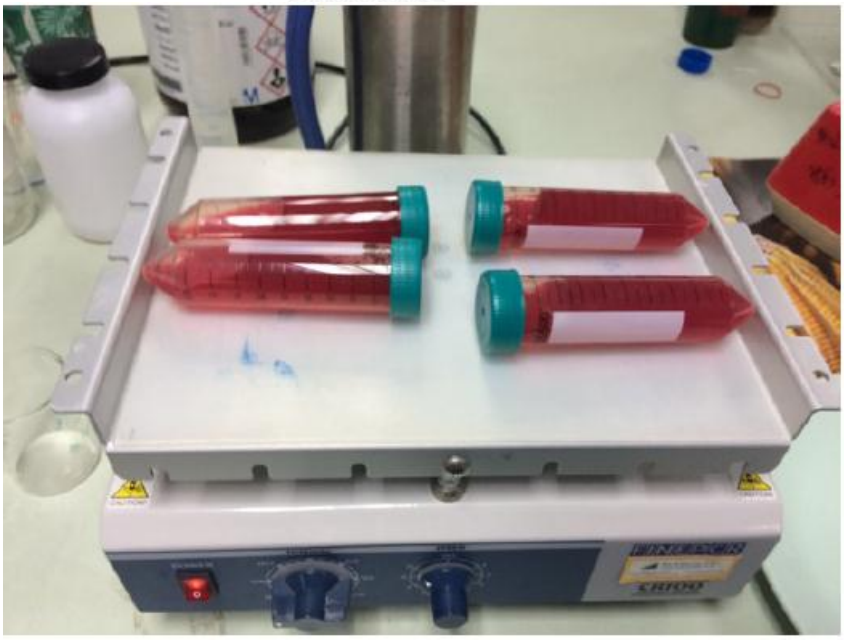

Figure A.3 Mixing Canine blood and RBC lysing solution with the biomixer.

Figure A.4 Centrifugation at 4 degree Celsius and 3000 rpm for 20 minutes

Figure A.5 The solution after being centrifuged for 20 minutes

Figure A.6 WBCs’sediment at the bottom of a 50 centrifuge tube

Figure A.7 Filter for PBS buffered solution

Figure A.8 WBC's sediment after rinsing manually in a centrifuge tube a) after being centrifuged, b) being rinsed first time, c) being rinsed second time and d) being rinsed third time.

Figure A.9 The final process of cell suspension a) after adding PBS and b) cell suspension.

Figure A.10 Cell-Strainer (40 μm)

Biological Specimen Preparation for SEM

1. Place 1 drop of WBC suspension on a cover slip. Make sure the suspension is all over the plate.
2. Fix specimens with 2.5% glutaraldehyde in 0.1 M phosphate buffer pH 7.2 for 1 hour.
3. Wash specimens twice with phosphate buffer to remove glutaraldehyde and then once with distilled water for 5 min/each.
4. Dehydrate specimen with a graded series of ethanol (30%, 50%, 70%, 95% 5 min/each and 100% 3 times, 5 min/time, respectively).
5. Remove fluid from specimens by evaporating with high-pressure heating to the critical point dry (critical point dryer, Quorum model K850, UK).
6. Mount the specimen onto stubs with conductive tape and coat with gold (sputter coater, Balzers model SCD 040, Germany).
7. Observe by means under a SEM (JEOL, model JSM 6610LV, JAPAN).

Blood Smear

1. Picking up a coverglass (make sure the coversglass is clean prior) with your thumb and index finger on adjacent corners.
2. Drop a specimen (40 μl) and touch the specimen with the coverglass at an angle. By using capillary attraction, the sample should be all over the coverglass.
3. Dry the specimen with air completely.

Biological Specimen Preparation of Wright's Stain

1. Fix specimens with methanol for 2 minutes
2. Place the Wright Stain Solution upon a coverglass for 3 minutes
3. Add Buffer pH 7 upon the coverglass (the same volume of Wright Stain Solution) by using a wash bottle (make sure Wright Stain Solution and buffer mixed well together for 15 minutes).
4. Rinse off the coverglass with tap water.
5. Dry the coverglass thoroughly with air or bibulous paper.

Appendix B

Cell Enumeration

Cell Enumeration Protocols for Hemocytometer

1. Use a pipette, withdraw 0.5 ml of cell suspension and 0.5 ml of Trypan Blue and put in a 2 ml eppendorf and then mixes together with bio-shaker for 5 minutes. After that, withdrawing 10 µL of solution from the eppendorf and apply to the hemocytometer with both sides of chambers.
2. Try to find the grid lines by using a light microscope and focus with magnification of 10x, 20x and 40x, respectively.
3. Use a hand tally counter to count live cells and dead cells. Live cells are appeared as bright feature in circle, whereas the dead cells are appeared as a blue feature in circle.
4. When counting cells, our method is to count 4 main areas (1 main area contains 16 small square areas). Cells are counted only in square areas and within on the right-hand or bottom boundary line.

Cell Concentration Formula

Cell concentration can be calculated from this following formula:

$$\text{Cells/ml} = \frac{\text{Total cells counted} \times \text{dilution factor} \times 10^4}{\text{numbers of squares}}$$

Example: In this experiment, total cells in 4 main areas are 200 cells. If you dilute cell suspension with Trypan Blue 1:1. The concentration (Cells/ml) will be:

$$\text{Cell concentration} = \frac{200 \times 2 \times 10^4}{4} = 10^6 \text{Cells/ml}$$

Percentage of Cell Viability Formula

Percentage of cell Viability can be calculated from this following formula:

$$Percentage\ of Cell\ viability = \frac{(Live\ cells) \times 100}{(\text{Live cells} + \text{Dead cells})}$$

Example: In this experiment, live cells are 180 cells and dead cells are 20 cells. Percentage of cell viability will be:

$$\text{Percentage of Cell viability} = \frac{(180) \times 100}{(180 + 20)} = 90\%$$

PS.You can apply this Formula to find the percentage of cell death also.

Appendix C

The Studies of Spiral Microchannel

Important Parameters of Spiral Microchannel

As stated by the group of Martel and Toner, their work present the effects of Reynold number, curvature ratio and particle confinement ratio on particle migration. The particles can move away from or towards the center of microchannel migrating across streamlines. These particles are aligned and located at the equilibrium positions within the flow. The experiment demonstrates that the inertial focusing in the straight channel depends on Reynolds number which is defined as

$$Re_c = \frac{\rho U_{max} D_h}{\mu} \quad (1)$$

Where ρ is the fluid density, μ is the fluid viscosity, $U_{max} \cong \frac{3}{2} U_{avg}$ is the maximum velocity of the fluid and D_h is the hydraulic diameter which is defined as $D_h = \frac{2hw}{h+w}$ where h is height and w is width of the channel. It has researched that inertial focusing occurs when $\lambda > 0.07$ and $Re_p \gg 1$ where λ is the particle confinement ratio and Re_p is the particle Reynolds number.

Theoretically, increasing or decreasing Reynolds number and the dimension of the channel, particle migration can be moved towards or away from the centerline of microchannel. Furthermore, using curved channel can control particles moving to the equilibrium position more quickly. So that, the radius of curvature and the dimension of the channel are used to explain the behavior of inertial focusing which is defined as a dimensionless as

$$\delta = \frac{D_h}{2r} \quad (2)$$

where δ is curvature ratio, D_h is the hydraulic diameter and r is the radius of curvature. The particles with the diameters of 4.4 μm, 9.9 μm and 15 μm are used as the experimental replica. They decide to vary the radius of curvature and observe inertial focusing on the spiral channel.

The results demonstrate that when it comes to the larger particles, the increase of curvature ratio is needed in order to create inertial focusing on the channel. In addition, increase of curvature ratio tends to move inertial focusing towards the inner walls as seen in Figure C.1.

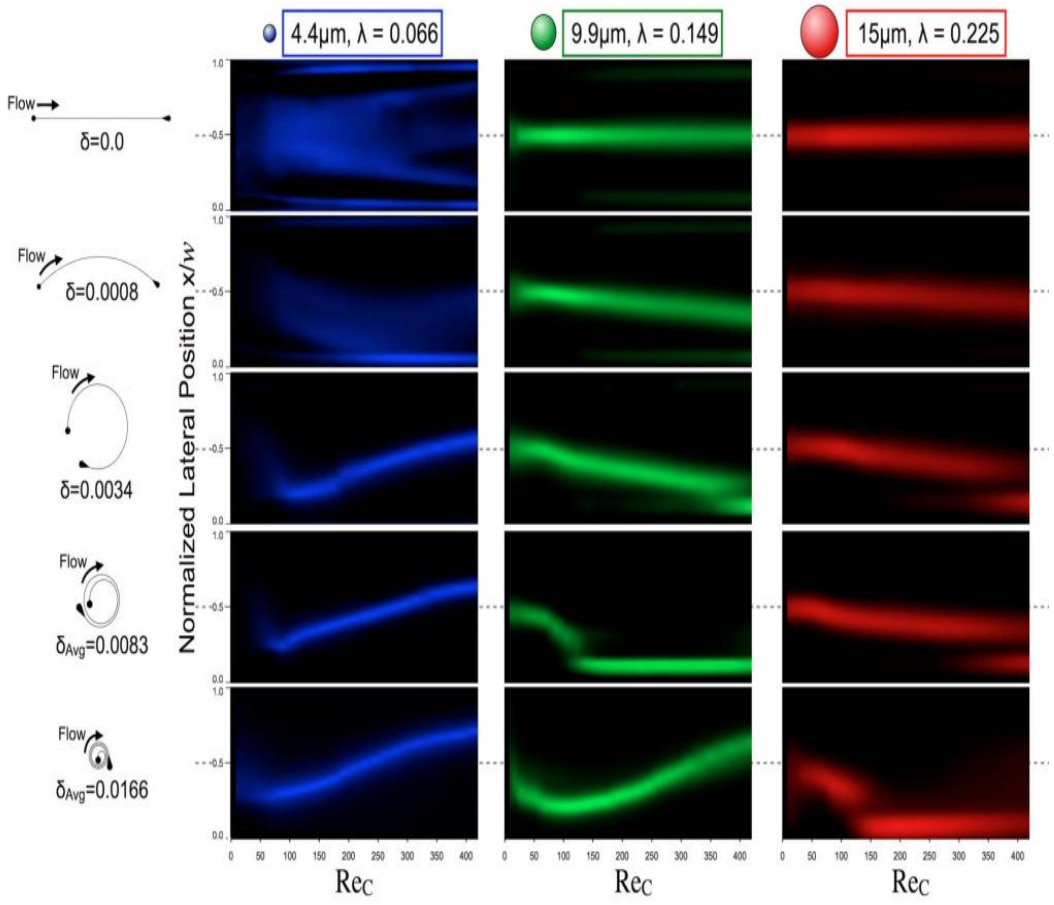

Figure C.1 The comparison of curvature and particle confinement (increasing from top to bottom and from left column to right) [43]

According to the results, it illustrates that the smallest particle will be aligned along the streamline with δ is 0.0008 and Re > 229. However, if δ is increased further and Re is fixed, the streamline seems to move from the inner walls to outer walls. As for the middle size of the particle, single point focusing occurs when δ is 0.0083 with Re is about 157-382. Similar to the first case, the trend will move away from the inner wall, if δ is increased further. As for the largest particle, single point focusing occurs clearly at Re is about 150 with δ is 0.0166 as depicted in Figure C.2.

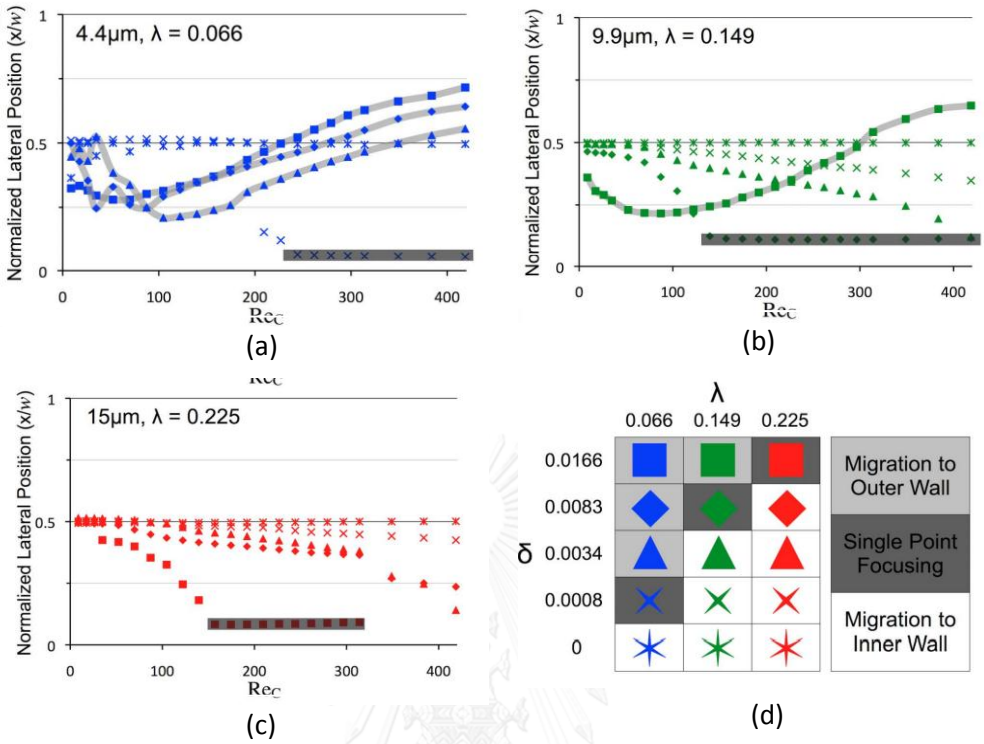

Figure C.2 Position data for particles of (a) 4.4, (b) 9.9 and (c) 15 μm with varying Re_c,(d) the table displays the particle confinement ratio,(λ) and curvature ratio, (δ) which are categorized into 3 regions; migration to the outer wall, single point focusing and migration to the inner wall (asterix = straight, x = 0.0008, triangles = 0.0034, diamonds = 0.0083 and squares = 0.0166) [43]

After knowing all parameters and the inertial focusing behavior, the experimental mixture particles are tested—4.4μm (λ=0.066), 9.9 μm λ=0.149) and 15 μm (λ=0.225). The outcomes demonstrate that the best separation occurs when the λ is 0.0116 and the Re should be about 200 to separate the mixture particles of 4.4, 9.9 and 15 μm efficiently. [43]. For this, Reynolds number, particle size, hydraulic diameters (width and height) and radius of curvature are fundamental factors that help migrate particle to the equilibrium position.

Similarly, the group of Kuntaegowdanahalli reports the technique of separation using inertial focusing in spiral microchannels. As reported by their study, the Archimedean spiral microchannel is designed with 5 loops, the length of 500 μm, the height of 130 μm and the radius of curvature of 1 cm. In order to have an improved understanding of the effects of inertial lift force and Dean drag force on an equilibrium position, all parameters such as lift force, Dean drag force, size of particle, flow rate and the dimensions of channel are taken into their considerations. In the study, the confinement ratio should be equal to or greater than 0.07 ($\frac{a_p}{D_h} \geq 0.07$, where a_p is a particle diameter D_h is the hydraulic diameter) to help

particles move to the equilibrium position as a streamline. As for the net lift force—the sum of shear and wall induced lift forces—acting on the particles in the channel, this is given by

$$F_L=\rho G^2 C_L a_p^4 \quad (3)$$

where ρ is density of fluid, G is the shear rate of fluid which is defined as $G=U_{max}/D_h$, U_{max} is the maximum fluid velocity, C_L is the lift co-efficient—estimated an average value of $C_L \sim 0.5$ [7] — which is related to Reynolds number and a_p is a particle diameter. As for Dean drag number, this number is increased by the increasing cross sectional area or flow rate. These factors result in a strong Dean drag force which is given by

$$F_D=3\pi\mu U_{Dean} a_p=5.4\times10^{-4}\pi\mu De^{1.63} a_p \quad (4)$$

where $U_{Dean}$is the average Dean velocity which is given by $U_{Dean}=1.8\times10^{-4}De^{1.63}$ and De is dean number which is defined as

$$De = \frac{\rho U_f D_h}{\mu}\sqrt{\frac{D_h}{2R}} = Re\sqrt{\frac{D_h}{2R}} \quad (5)$$

Where U_f is the average fluid velocity (ms^{-1}) and μ is the fluid viscosity ($kg\ m^{-3}$)

As stated in the experiment of Kuntaegowdanahalli, the consequences demonstrate that when De is increased, the well-focused stream tends to move away from the inner walls. These results are different from the study of Xiang who found that if the flow rate is increased, the focusing degree moves towards the inner wall [7]. This may be explained by the experiment of Martel and Toner (Figure C.2). In the meanwhile, Dean drag force dominantly control the lift force when De is increased further. In addition, as seen from the equation of (3) and (4)— $F_L \propto U_f^2$ and $F_D \propto U_f^{1.63}$, this illustrates that increasing flow rate would increase F_L rather than increasing F_D. However, the particles tending to move away from the inner walls can be explained by the decrease of lift co-efficient [12]. When the Reynolds number is increased by increasing flow velocity, the lift co-efficient tends to be decreased. In addition, the equilibrium position can move away or toward the inner wall by changing Dean number and the dimension of channel—width or height. The group of Kuntaegowdanahalli experimented further the equilibrium positions with the mixture particle of 10, 15 and 20 μm by varying Dean number and the height of the channel. The results demonstrate that the equilibrium position of particles of 10, 15 and 20 μm depending on the height of channel and the size of particles when dean number is increased. As is evident from the graph, the appropriate height of channel to separate the mixture particles of 10, 15 and 20 should be about 130 to 140 μm. In contrast, the particle of 20 μm tends to be overlapped with the height of 90 and 110 μm. The equilibrium positions of particles of 10, 15 and 20 μm seem to be separated widely at a high flow rate. However, a high flow rate has a high potential to damage cell viability due to a high shear stress and extensional stress. In conclusion, the spiral microchannel works quite well with a high flow rates. It has a great potential to separate different sizes of particles of 10, 15 and 20 depending on the particle's size,

flow rate and the height of microchannel. Additionally, using the wider channel could increase spacing particle streams due to the increase of dean numbers. The consequeces of using polystyrene beads as experimental particles can exhibit 90% separation efficiency. As for neuroblastoma and glioma cells, the efficiency of separation is 80% and the cell viability is greater than 90% [12].

As can be seen from the above two experiments, they demonstrates the spiral technique employing the particle of 5 to 20 μm. Normally, the Dean flow-based has been reported using the particle 5 or above. However, the most recent experiment of Johnston presents unprecedented spiral microchannel technique that experiments the particle focusing of 1, 2.1 and 3.5 μm. The spiral is designed with the 20 μm wide and 20 μm deep in cross-section, the radius of curvature is 2.12 mm and the total length of the channel is 82 mm. The outlet diverges at 30 degrees in angle until the width of the channel becomes 550 mm. The results indicate that at a low flow rates at 1 μl/min, the particle of 1 μm can be unfocused due to the high pressure associated with the focusing conditions. However, the particle of 2.1 and 3.2 are able to focus at the flow rate of 5 and 10 μl/min. In addition, increasing flow rates further would increase the efficiency of focusing (for 2.1 and 3.2 μm) as well. In summary, in order to increase the efficiency of particle streamline, Dean number is needed to increase as well [8].

The above studies, Dean number depends on 4 main factors, as stated by the equation; channel width, channel height, radius of curvature and Reynolds number (flow rates) [8, 11, 12].The recent studies have proved that beside 4 main factors, there are a few more factors that can improve the particle focusing— the channel length and the concentration of samples. As reported by the group of Bhagat, the experiment illustrates the achievement of spiral microchannel separation of 1.9 and 7.32 μm particles by determining the channel length for the particles of 1.9 μm migrating to the outer half of the channel and particles of 7.32 μm to focus close to the inner wall. Using Asomolov's lift force equation and assuming Stokes drag, we can determine the particle lateral migration velocity (U_L).

$$U_L = \frac{\rho U_{max}^2 a^3 C_L}{3\pi\mu D_h^2} \tag{6}$$

the channel length for the particle to focus an equilibrium position is given by

$$L_I = \frac{U_f}{U_L} \times L_M \tag{7}$$

where L_I is the channel length, U_f is the average velocity and L_M is the migration length (m). Likewise, the channel length required for Dean migration (L_D) which is given by

$$L_D = \frac{U_f}{U_{Dean}} \times L_M \tag{8}$$

As a result, the appropriate length of the channel in this work is about 13 cm at De = 0.47 to separate particles of 1.9 and 7.32 μm. Similarly, the group of the Xiang, demonstrates the effects of the channel length on particle focusing in each loop of spiral microchannel. It is stated that the increase of migration length affects the particle focusing position by the decrease of Dean drag force with increasing in loops [7].

Another experiment of Xiang provides more details of the relationship between a stream focusing and migration lengths using the experimental particle of 5 and 10 µm. The outcomes demonstrate that at the Reynolds number of 75, the particle streams are well-focused from the position of P1-L3 (position 1-loop 3) to P3-L5 (position 3-loop 5). Surprisingly, when the length of the channel is increased further, the particle streams tend to be overlapped or unstable during separation as evidenced in Figure C.3 [9]. The reason why the length of the channel has an effect on streamlines focusing because spiral has a continuous change in radius of curvature. This results in the decrease of Dean number which leads to the overlapping streamlines.

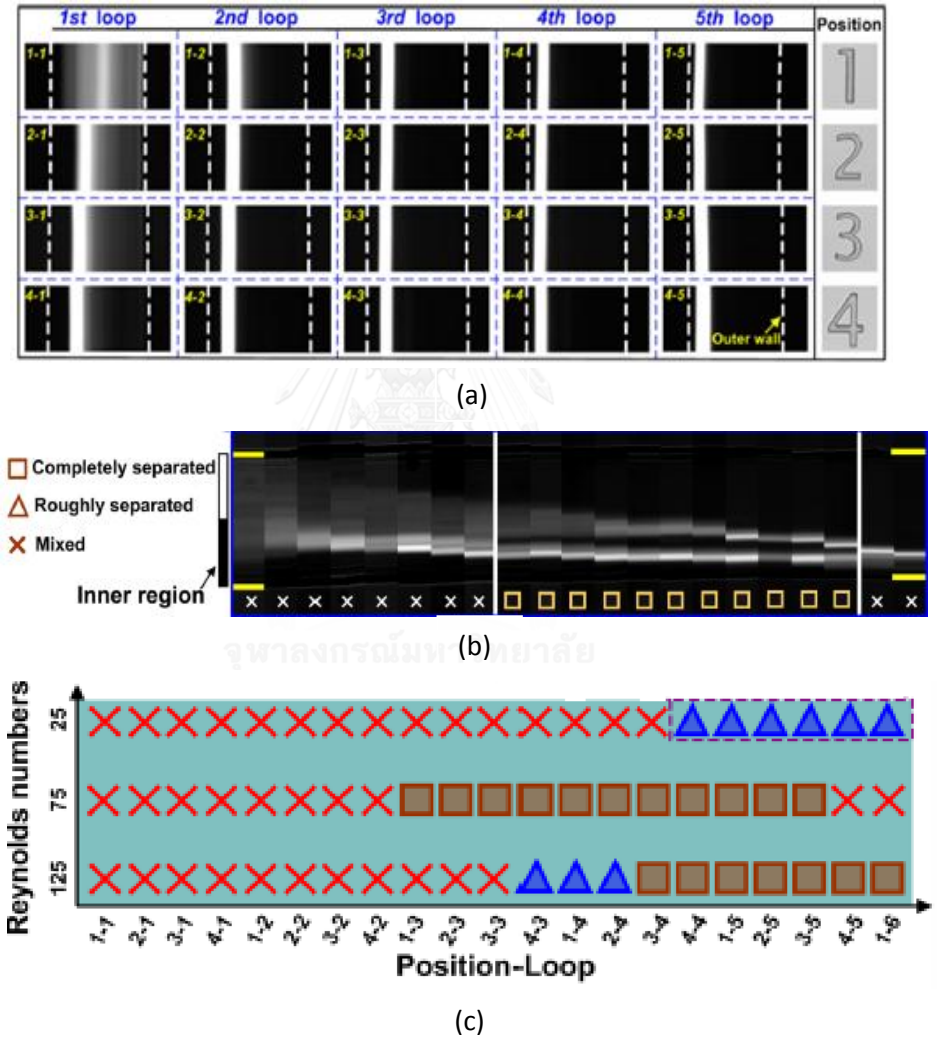

Figure C.3 The position of streamline (a) the different positions of particle streamline in each loop at Re = 66.67, (b) positions of 5 and 10 µm particles at the flow rate of Rec = 75 (the square shape is completely separated, the triangle shape is roughly separated and X is mixed particle streamline) and (c) the comparison of different Reynolds numbers and position of loop [9].

Furthermore, the experiment of Nivedita and Papautsky also confirms that the polystyrene beads of 20 µm are focused almost a single-particle stream by the time when the particles reach to loop 4th according to the spiral microchannel design of 500 µm × 100 µm in width and height at the flow rate of 900 µm/min as shown in Figure C.4 [36]. Moreover, Nivedita and Papautsky present the equation of downstream length. This focusing length can be calculated by adjusting the optimized Dean number. This equation is defined as

$$De_{op} = 3.5 \frac{L_m}{D_h} x^{\frac{D_h}{L_m}} \quad (9)$$

where De_{op} is the optimized, L_m is the Dean migration length (L_m = W+H+3/4W, where W is the channel width and H is the channel height) and x is the downstream length of spiral requiring to focus cells/particles.

For this, the channel length is one of the significant factors that should be considered in terms of increasing particle focusing efficiency [36].

Furthermore, Nivedita and Papautsky state that the spacing between channels is another factor that affect the radius and length of the channel as well. These results in the efficiency of cell separation. The increase of spacing between channels decreases the Dean number, therefore, the increase of channel length is needed to allow particles to move further to focus in the equilibrium position. The best way to prevent the decrease of Dean number is to keep spacing between channels as narrow as possible. However, the spacing of 500 µm between the loops is more commonly used to fabricate because it is more convenient for soft-lithography process [36].

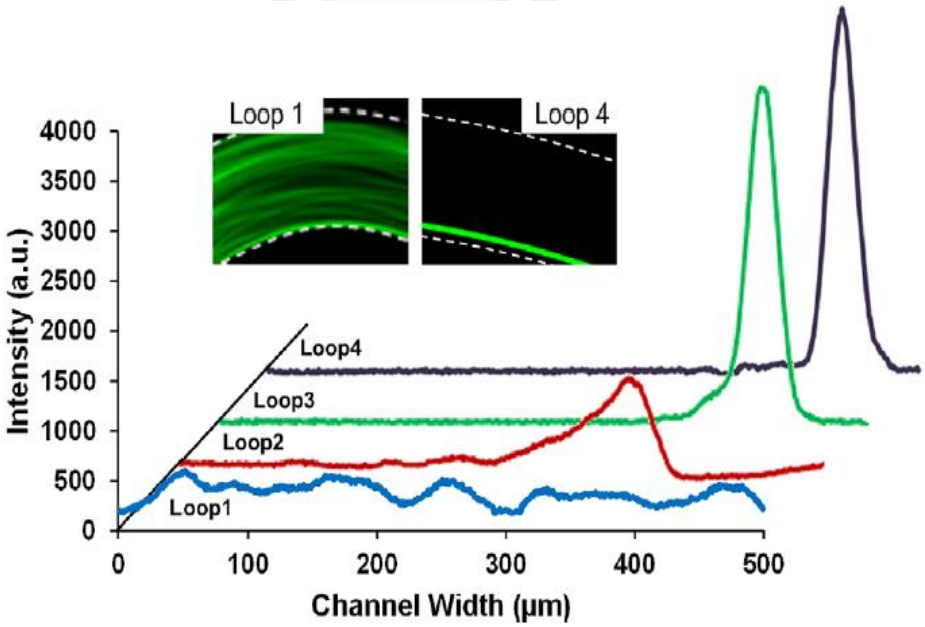

Figure C.4 Intensity versus the width of the channel at the end of each loop in the spiral using polystyrene of 20 µm in diameter—loop 1 being the inner-most loop and loop 4 being the outer-most [36].

Recently, concentration of sample is a new factor that is able to increase the efficiency of streamline focusing. The experiment of Johnston and his group shows the increasing microsphere concentration by increasing the width of the channel. The results demonstrate that the particle streamline of 2.1 µm tends to degrade the flow focusing when the concentration is increased [8] as proved in Figure C.5. Like Johnston, Nivedita and Papautsky confirm that higher dilution provides a better focusing of cell separation. As reported by their experiment, it is found that cells tend to bounce off of each other with a high concentration. The interaction between cells (cell to cell interaction) poses a significant contention to the ability of sorting device as presented in Figure C.6 [36].

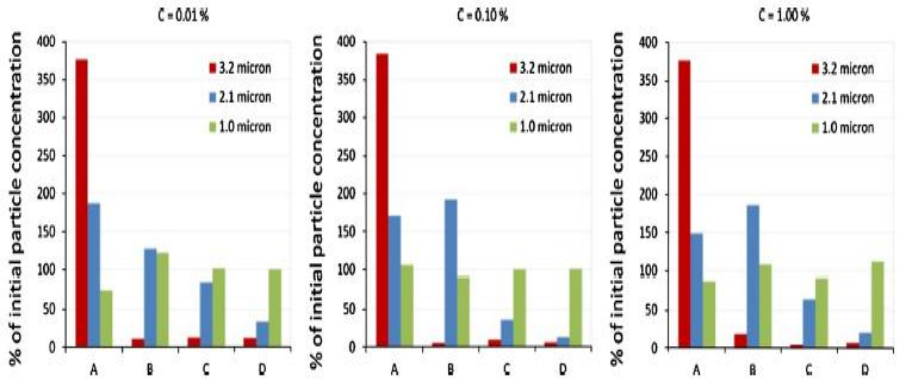

Figure C.5 Particle count data displaying different concentrations (0.01, 0.1 and 1%) of 1.0 µm (green), 2.1 µm (blue) and 3.2 µm (red) microspheres at sample outputs [8]

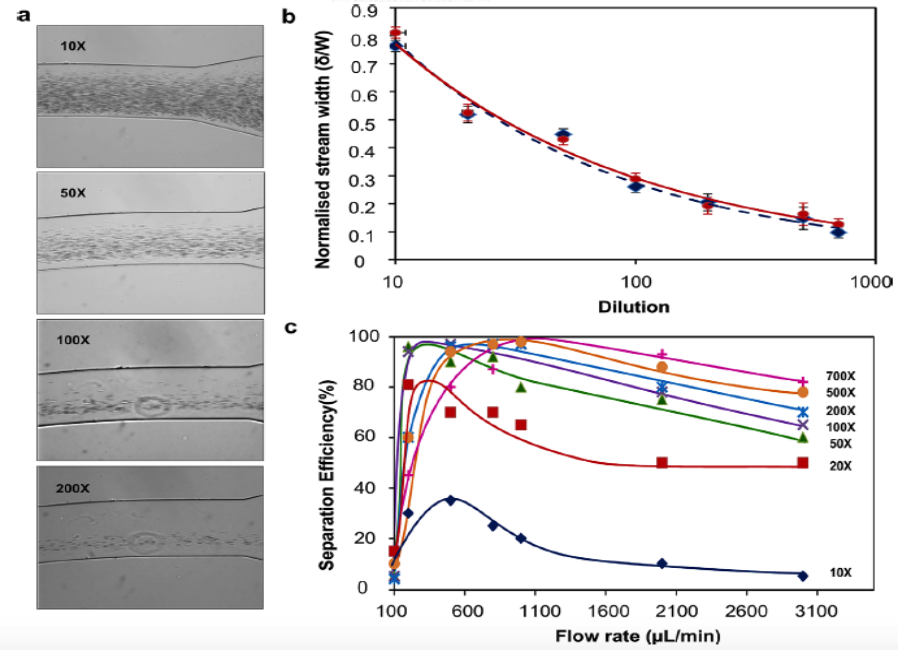

Figure C.6 (a) whole blood cells focused in the outermost loop with the dilution of 10x, 50x, 100x and 200x, (b) graph of normalized stream width versus various dilutions from 10 to 1000 and (c) the separation efficiency versus flow rate with varying dilutions from 10x to 700x [36].

In addition to increase the efficiency of separation, sorting multiple cell types (more than two types of cells) causes the reduction of efficiency of separation and throughput [36].

The studies of the spiral microchannel reinforced our personal convictions that the efficiency of particle separation depending on 8 parameters. These parameters can be categorized into two main parts. The first part is spiral geometry and another is particle by itself and flow properties. As for the part of spiral geometry, there are 5 parameters; channel width, channel height, channel length, radius of curvature and spacing between channels. As for the particle and flow properties, there are 3 parameters; particle size, concentration, and flow rates. However, it is quite difficult to vary the geometry and dimensions of the channel such as width, height, length and radius of curvature while varying flow rate and concentration are easier and more practical compared to varying other parameters.

Appendix D

The Investigation of Cell Viability in Different Suspension Media

Experimental Results with Trypan Blue

In this case, cell suspension was counted after the sediment of WBCs and suspension media mixed together well by a bioshaker for 5 minutes. The outcomes of the this case presented that cell viability was reduced to 8% as shown in Figure D.1. when using DI water compared to 95% of using PBS as suspension media. As can be seen from Figure D.2., cells were obviously swelling in 5 minutes after DI water with the sediment of WBCs were mixed.

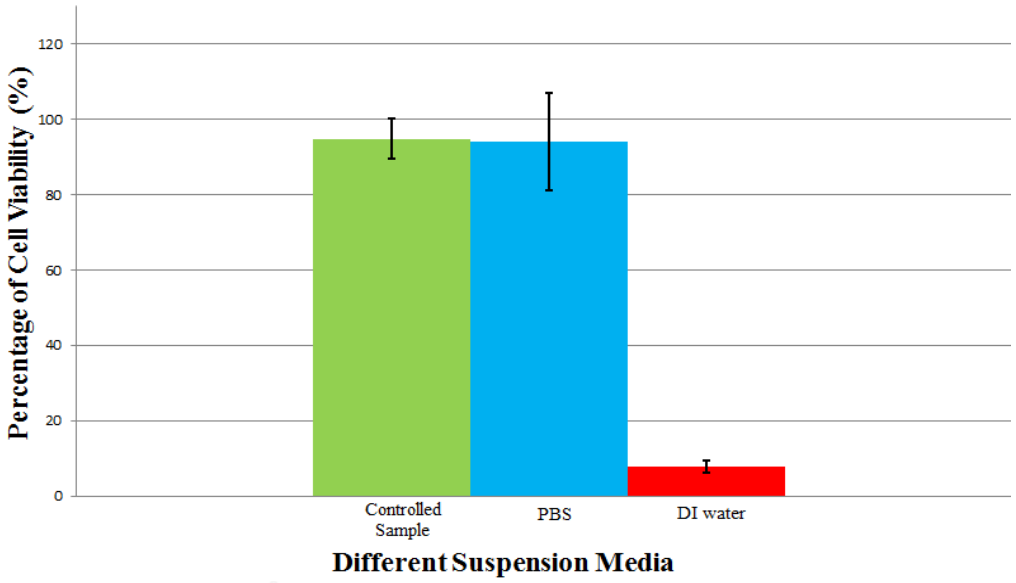

Figure D.1 Comparison of percentage of cell viability in different suspension media

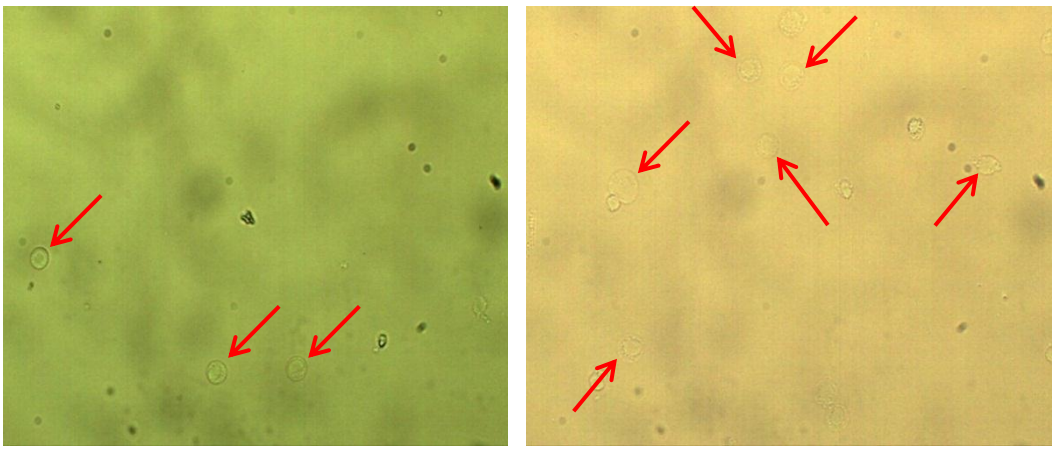

(a) (b)

Figure D.2 Morphology of cells (a) using PBS and (b) using DI water as suspension media.

Experimental Results with SEM

Experimental Results by Scanning Electron Microscopy

Beside investigating Trypan Blue, we investigated morphlogy of cell by observation of SEM. Normal cells and cell degeneration were examined using different suspension media; DI water and PBS. In this case, using DI water as cell suspension media, the images showed that all cells were dead with cytoplasm lysed. This because WBCs swell and eventually expand until they broke open in 1 hour. In order to observe morphology of cells more clearly, the Figure D.3 showed more details of WBC morphology when using different suspension media.

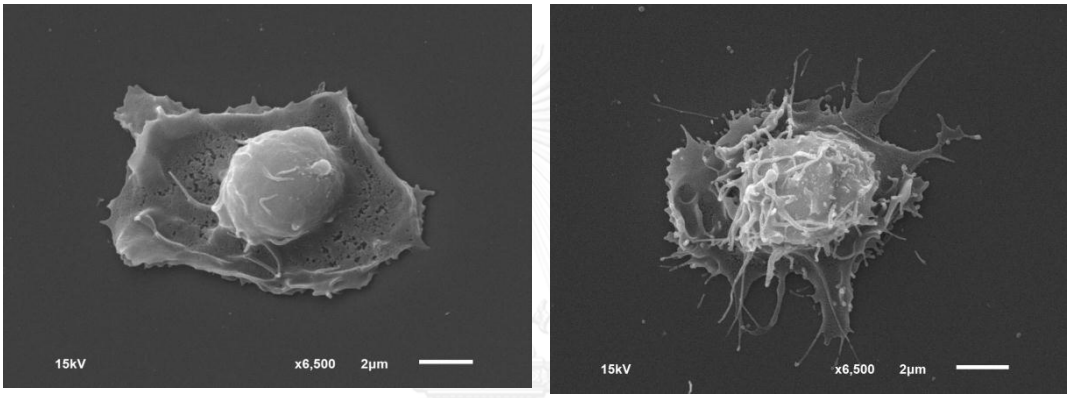

(a)

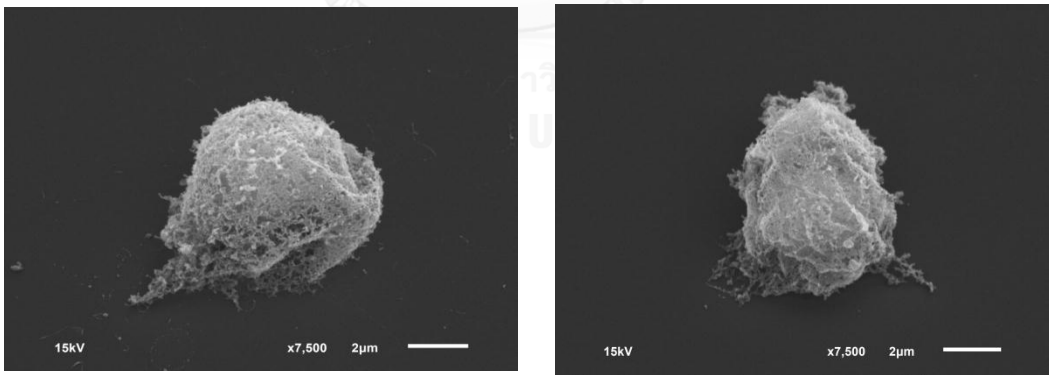

(b)

Figure D.3 Morphology of WBCs in (a) PBS (x3,500 magnification) and (b) DI water (x7,500 magnification)

VITA

Thammawit Suwannaphan was born on October 19th, 1987 in Phitsanulok as the only child in his family. He attended at Sriayudhya School as a junior high student and graduated with a vocational certificate at King Mongkut's Institute of Technology North Bangkok and then obtained Bachelor of Mechanical and Aerospace Engineering in March 2010 from Faculty of Engineering, King Mongkut's University of Technology North Bangkok and graduated a Master's degree in Mechanical Engineering from Faculty of Engineering at Chulalongkorn University, July 2016.